APPENDICES

APPENDIX A

Geometry of RF-Gun

Table A1: Geometry of half (left) and full (right) cell for the optimized RF-gun

segment (units mm)	x	y	segment (units mm)	x	y
origin	0.00	0.00	origin	0.00	5.20
line to	0.00	41.90	line to	4.35	5.20
line to	5.00	41.90	arc,-90°,r=5.00 mm to	9.35	10.20
arc,90°,r=24.64 mm to	29.64	17.26	line to	9.35	10.50
line to	29.64	15.00	arc,-90°,r=2.50 mm to	6.85	13.00
arc,90°,r=2.00 mm to	27.64	13.00	line to	4.46	13.00
line to	26.50	13.00	arc,0°,r=2.00 mm to	2.46	15.00
arc,90°,r=2.50 mm to	24.00	10.50	line to	2.46	17.26
line to	24.00	10.20	arc,180°,r=24.64 mm to	51.74	17.26
arc,90°,r=5.00 mm to	29.00	5.20	line to	51.74	15.00
line to	32.10	5.20	arc,90°,r=2.00 mm to	49.71	13.00
			line to	47.35	13.00
			arc,-90°,r=2.50 mm to	44.85	10.50
			line to	44.85	10.20
			arc,-90°,r=5.00 mm to	49.85	5.20
			line to	58.00	5.20

Table A2: Geometry of half (left) and full (right) cell for the actual SURIYA RF-gun

segment (units mm)	x	y		segment (units mm)	x	y
origin	0.00	0.00		origin	0.00	5.20
line to	0.00	41.90		line to	3.57	5.20
line to	4.51	41.90		arc,-90°,r=5.00 mm to	8.57	10.20
arc,90°,r=24.64 mm to	29.15	17.26		line to	8.57	10.50
line to	29.15	15.00		arc,-90°,r=2.50 mm to	6.07	13.00
arc,90°,r=2.00 mm to	27.15	13.00		line to	4.46	13.00
line to	26.36	13.00		arc,0°,r=2.00 mm to	2.46	15.00
arc,90°,r=2.50 mm to	23.86	10.50		line to	2.46	17.26
line to	24.00	10.20		arc,180°,r=24.64 mm to	50.84	17.26
arc,90°,r=5.00 mm to	28.86	5.20		line to	51.74	15.00
line to	31.61	5.20		arc,90°,r=2.00 mm to	48.84	13.00
				line to	47.28	13.00
				arc,-90°,r=2.50 mm to	44.78	10.50
				line to	44.78	10.20
				arc,-90°,r=5.00 mm to	49.78	5.20
				line to	57.20	5.20

APPENDIX B

Publications and Presentations by Author

Publications:

[1] Y.C. Wang, S.Y. Hsu, C.S. Hwang, J.Y. Hwang, W.K. Lau, F.Y. Lin, T.T. Yang, **S. Rimjaem**. *Generation of Ultra-Short Electron Bunches for Light Source Research.* Accepted to be published in International Journal of Modern Physics B, 2006.

[2] C. Thongbai, V. Jinamoon, N. Kangrang, K. Kusoljariyakul, **S. Rimjaem**, J. Saisut, T. Vilaithong, M.W. Rhodes, P. Wichaisirimongkol, S. Chumphongphan. *Radiation Production Using Femtosecond Electron Bunches.* Solid State Phenomena, 107, 11-14 , 2005.

[3] **S. Rimjaem**, V. Jinamoon, N. Kangrang, K. Kusoljariyakul, J. Saisut, C. Thongbai, T. Vilaithong, M.W. Rhodes, P. Wichaisirimongkol, S. Chumphongphan. *Femtosecond Electron Pulses Production System.* Solid State Phenomena, 107, 15-20, 2005.

[4] **S. Rimjaem**, R. Farias, C. Thongbai, T. Vilaithong, H. Wiedemann. *Femtosecond Electron Bunches from an RF-gun.* Nucl. Instrum. Methods Phys. Res. A, 533, 258-269, 2004.

[5] R. Farias, **S. Rimjaem**, C. Settakorn, T. Vilaithong and H. Wiedemann. *Production and Use of Femtosecond Electron Bunches.* In Electron-Photon Interaction in Dense Media. Edited by H. Wiedemann. Kluwer Academic Publishers, Dordrecht, 321-329, 2002.

Presentations:

[1] **S. Rimjaem**, V. Jinamoon, N. Kangrang, K. Kusoljariyakul, J. Saisut, C. Thongbai, T. Vilaithong, M.W. Rhodes, P. Wichaisirimongkol, H. Wiedemann. *Beam Characterizations at Femtosecond Electron Beam Facility.* In Proceeding of the Particle Accelerator Conference (PAC2005), Knoxville, Tennessee, USA, May 16-20, 2005, pp. 3925-3927.

[2] C. Thongbai, V. Jinamoon, N. Kangrang, K. Kusoljariyakul, **S. Rimjaem**, J. Saisut, T. Vilaithong, M.W. Rhodes, P. Wichaisirimongkol, H. Wiedemann. *Generation of Femtosecond Electron and Photon Pulses.* In Proceeding of the Particle Accelerator Conference (PAC2005), Knoxville, Tennessee, USA, May 16-20, 2005, pp. 3946-3948.

[3] **S. Rimjaem**, V. Jinamoon, K. Kusoljariyakul, J. Saisut, C. Thongbai, T. Vilaithong, M.W. Rhodes, P. Wichaisirimongkol, S. Chumphongphan, H. Wiedemann. *Generation of Femtosecond Electron Pulses.* In Proceeding of the 9th European Particle Accelerator Conference (EPAC2004), Lucerne, Switzerland, July 5-9, 2004, pp. 431-433.

[4] **S. Rimjaem**, N. Chirapatpimol, M.W. Rhodes, J. Saisut, C. Settakorn, P. Wichaisirimongkol, T. Vilaithong. *Generation of Femtosecond Electron Bunches and FIR Radiation.* In Proceeding of the International Workshop on Particle Beam & Plasma Interaction on Materials (PIM2002), Chiang Mai, Thailand, January 31-February1, 2002, pp. 5-8.

[5] T. Vilaithong, N. Chirapatpimol, M.W. Rhodes, C. Settakorn, **S. Rimjaem**, J. Saisut, S. Amkaew, P. Wichaisirimongkol, H. Wiedemann. *SURIYA, a Source of Femto-second Electron and Photon Pulses.* In Proceeding of the 2001 Asian Particle Accelerator Conference, Beijing, China, September 17- 21, 2001, pp. 91-93.

[6] **S. Rimjaem**, N. Chirapatpimol, T. Vilaithong, H. Wiedemann, C. Settakorn. *Rf-Gun Optimization for Femto-Second Electron Bunches.* In Proceeding of the 2001 Asian Particle Accelerator Conference, Beijing, China, September 17- 21, 2001, pp. 523-525.

International Journal of Modern Physics B

World Scientific
www.worldscientific.com

GENERATION OF ULTRA-SHORT ELECTRON BUNCHES FOR LIGHT SOURCE RESEARCH

Y.C. Wang†, S.Y. Hsu, C.S. Hwang, J.Y. Hwang, W.K. Lau, F.Y. Lin, T.T. Yang

National Synchrotron Radiation Research Center, No. 101, Hsin-Ann Road, Hsinchu 30076, Taiwan
jackwang@nsrrc.org.tw

S. Rimjaem

Fast Neutron Research Facility (FNRF), Physics Department, Chiang Mai University, P.O. Box 217, Chiang Mai 50202, Thailand
neung@fnrf.science.cmu.th

Received 13th March 2006
Revised Day Month Year

An S-band thermionic 1.5-cell rf gun injector system is being built at NSRRC for Taiwan Photon Source (TPS) booster. At optimized field ratio, an electron beam with linear energy chirp can be generated by the rf gun. The beam is then compressed by an alpha magnet such that ultra-short electron bunches at femto-second bunch length can be obtained. Particle dynamics has been studied for an rf gun with nose cone at the cathode, simulation results show that 74 pC bunches at about 97 fs is achievable. Some of the critical components such as the rf gun and alpha magnet have been fabricated and being tested in house. Experiments for intense coherent THz radiations and tunable femto-second X-ray from ultra-short bunches are being proposed as future applications.

Keywords: rf gun; bunch compression.

1. Introduction

Ultra-short electron beam finds interesting applications such as generation of coherent radiations and tunable ultra-fast X-rays [1-2]. In contrast to electron bunch compression at higher beam energy by magnetic chicane, alpha magnet can be used to compress electron bunches that have lower kinetic energy. It was shown that electron bunches from a thermionic rf gun [3] can be compressed into bunches as short as 50 femto-seconds with the aid of an alpha-magnet [4]. An alpha-magnet is a half asymmetric quadrupole with a vertical mirror plate along the longitudinal axis. It has vertical magnetic field on the horizontal plane increases with increasing values of horizontal position. A properly designed alpha magnet can be an achromatic system with very large momentum range.

†Corresponding author

Another important property of the magnet is that as the beam enters the magnet through the vertical mirror plate at its center, at an angle of 40.71° from the normal of the mirror plate, it exits the magnet at the same point [5]. On the other hand, a beam with linear energy chirp can be generated from a thermionic rf gun at certain optimized field ratio.
A prototype rf gun injector system is being developed at NSRRC for the TPS (Taiwan Photon Source) booster. The system schematic is shown in (Figure 1). A 1.5-cell thermionic rf gun and an alpha magnet will be used in the injector system. As can be seen from the drawing, trajectory of an electron beam from a thermionic rf gun is bended by the alpha magnet and further accelerated to higher energy by rf linac. For this prototype system, the beam will be accelerated to 20-30 MeV in energy. The possibility of generating femto-second electron bunches for novel light source research with this injector system is being investigated in this work.

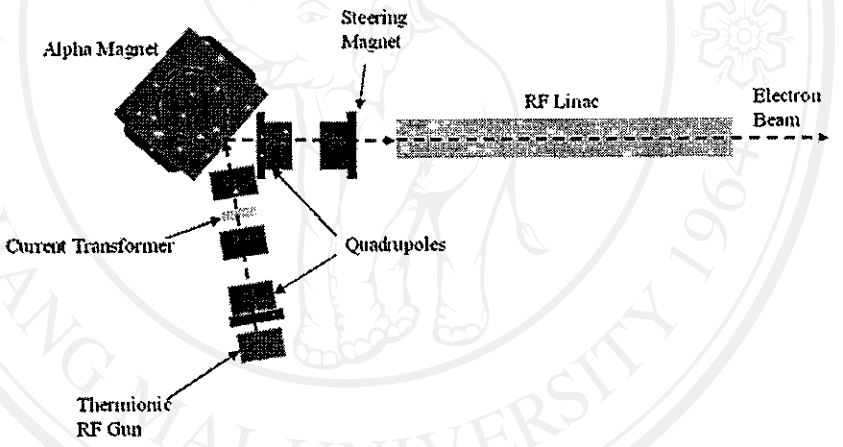

Figure 1: Setup for the S-band thermionic rf gun injector system.

This paper is organized as follows: In section 2, calculation results of electromagnetic field in the rf gun cavity and multi-particle dynamics of the electron beam in the thermionic rf gun as well as the particle dynamics during bunch compression with alpha magnet will be discussed. The progress experimental setup such as rf gun and alpha magnet construction and measurements are described in Section 3 and 4 respectively. Section 5 is the summary and discussion.

2. Particle Dynamics

To study the multi-particle dynamics in a 2856 MHz thermionic rf gun, a macro-particle tracking code, PARMELA [6], is being used. Electromagnetic fields of the rf gun cavity cells are calculated with SUPERFISH [7]. Output data files of SUPERFISH will be used for PARMELA calculations. For beam transport and bunch compression, beam dynamics

in the alpha magnet, beam transport system and rf linac has been simulated with a computer code called BCompress [8]. In PARMELA calculations, the effects of space charge and thermal emittance at the cathode have been neglected and will be included in further studies. In the BCompress calculations, transverse effects have been neglected for simplicity in these preliminary calculations.

2.1. *Calculation of Electromagnetic Fields in the RF Gun Cavity*

The rf gun cavity is a 1.5-cell structure with thermionic cathode assembly placed at the end-wall of the half cell. It is similar to the Stanford SSRL rf gun and has a nose cone for space charge beam focusing near the cathode [3]. The cathode assembly is a commercialized product provided by HeatWave Laboratory. High power microwave will be fed into the full cell through an S-band rectangular waveguide and will be coupled to the half cell via a side coupled cell. Therefore, it can be represented by three coupled resonators. For maximum energy transfer to the beam, the rf gun cavity will be operated in $\pi/2$-mode. That is, phase difference of electric field between half cell and full cell is 180°. It is essential to put the nose cone into the SUPERFISH model for electromagnetic field calculations. Electromagnetic fields of the half cell and full cell have been calculated separately by SUPERFISH. Phase of electric field in each cell will be adjusted in PARMELA calculated. Figure 2 shows the electron field line contours in the half cell with nose cone and the electric field lines in the full cell. Convergence test has been done to ensure mesh triangles are small enough for accurate field calculations.

Figure 2: Electric field line contours of the half cell (left) the full cell (right) as calculated by SUPERFISH.

2.2. *Generation of a Linear Energy Chirped Beam*

Particle distribution of a beam in longitudinal phase space will in general depends on the field amplitude ratio of the cavity cells. Particle distributions in longitudinal phase space at gun exit for different field ratios have been obtained from PARMELA output files. For field ratio of half cell to full cell equals to 1:2 and when average field gradients of full cell equals to 50 (MV/m), a nearly linear energy chirp can be produced. In these

calculations, 50,000 macro-particles have been used. During the acceleration in the rf gun cavity, due to improper injection phase angle at the cathode, more than 75% of the continuous electrons from the thermionic cathode have been lost. Figure 3 shows the particle distribution in the longitudinal phase space at field ratio of 1:2. The bars in the figure show the number of particles within a time bin of 5 ps. Undesired electrons can be filtered out with an energy slits inside the alpha magnet vacuum chamber. This linear energy chirped beam is considered as an ideal particle distribution in longitudinal phase space for bunch compression by alpha magnet.

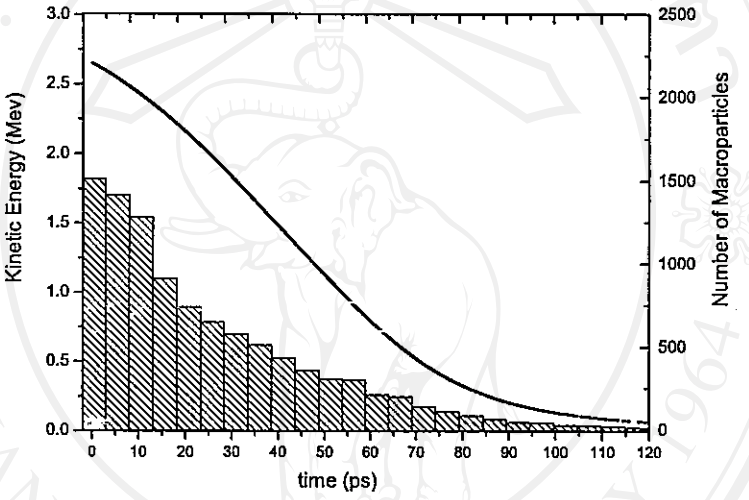

Figure 3: Particle distribution in the longitudinal phase space at rf gun exit as calculated by PARMELA at 1:2 field ratio.

2.3. *Bunch Compression by Alpha Magnet*

The electron beam from the rf gun is guided by magnetic focusing fields of a set of quadrupole magnets in the beam transport system located at the upstream of the alpha magnet (there is another set of beam transport system at downstream of the magnet) and enter the magnet through its vertical mirror plate at an angle of 40.71° from the normal of the plate. The alpha magnet will provide necessary energy dispersion for bunch compression. Data in the output file of PARMELA that represent particle distribution at rf gun exit is then imported into the BCompress code for optimizing the electron bunch length to femto-second order [8].

With rf linac operating at 8.8 MV/m in accelerating field gradient, the nominal magnetic field gradients of the alpha magnet has been scanned from 400 to 500 G/cm. Electron bunch compression to 97 fs feasible at 455 G/cm with 74 pC bunch charge. Calculated peak current can be as high as 760 A. However, in these calculations, the effects of space

charge and thermal emittance due to cathode temperature have been n eglected. These phenomena will be included in a more detailed study.

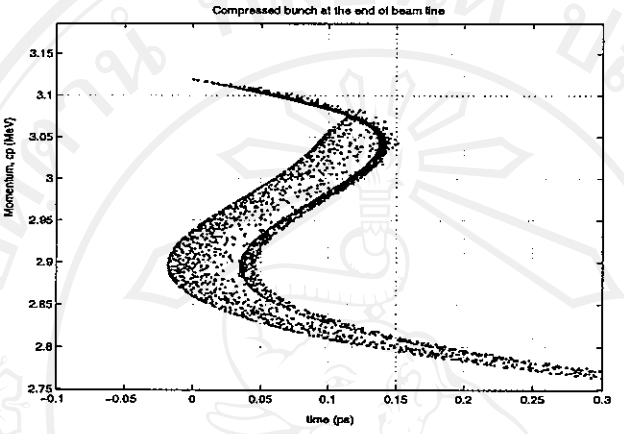

Figure 4: Particle distribution in longitudinal phase space after the linac.

3. The S-band Thermionic RF Gun

Fabrication of the S-band rf gun cavity has been completed. Since the rf gun cavity will be operated at $\pi/2$-mode, the full cell and half cell are coupled by a side coupled cell attached on the cavity. Field ratio of the rf gun cavity cells has been adjusted to 1:2 by tuning the frequency of this side coupled cell with a plunger. Measurement has been performed by network analyzer to identify the $\pi/2$-mode (operating cavity mode of the rf gun). By pulling a 3 mm metallic bead along the cavity axis, relative field amplitude has been deduced from the frequency shift due to the metallic bead at different longitudinal position [9].

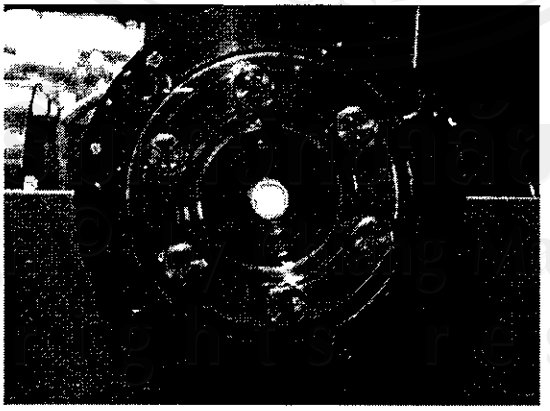

Figure 5: The S-band rf gun with thermionic cathode operating at 1100°C.

Cathode assembly has been installed in the cavity for heater test. Although the cathode temperature will be set at 950°C for normal operation, it has been heated successfully up to 1100°C as measured by a calibrated pyrometer and no thermal short has been found. Figure 5 shows the rf gun cavity with cathode surface temperature at 1100°C. A high power microwave system with the SLAC XK-5 klystron as the generator is being setup for high power microwave processing of the rf gun cavity.

4. The Alpha Magnet

A prototype alpha magnet has been fabricated also at NSRRC based to its original design at Stanford SUNSHINE facility. This magnet has been energized up to 110 A with a DC power supply and maximum gradient of 425 G/cm has been achieved (Figure 6). With adequate water cooling, no significant temperature rise has been observed during the measurement. This maximum value is not limited by the magnet itself but by the maximum available power of the power supply during the measurement. We believe higher field gradient can be achieved by further increasing the excitation current.

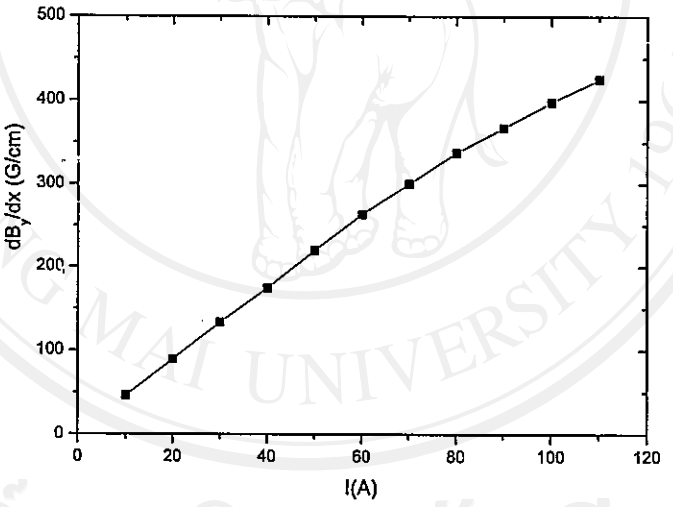

Figure 6: Measured magnetic field gradient versus DC currents.

At 110 A, vertical magnetic field gradient with respect to horizontal position has been measured along x-axis. Field gradient increases rapidly and saturates with increasing displacement from the mirror plate. Figure 7 depicts the magnetic field gradient (normalized to maximum gradient at the same current) versus horizontal position along x-axis. Since there must be a hole on the mirror plate for beam entrance and exit, stray fields near the beam entrance has to be considered. Preliminary measurement of magnetic field gradient near the beam entrance has been done to evaluate its effect on electron trajectory.

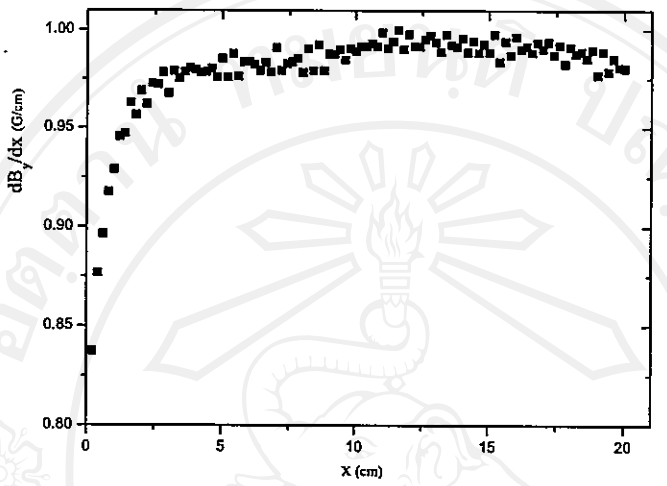

Figure 7: Measured magnetic field gradient (normalized) along horizontal axis at 110 A.

5. Summary and Discussions

A prototype S-band thermionic rf gun injector is being constructed at NSRRC for the booster synchrotron of the proposed 3 GeV Taiwan Photon Source. The possibility of generating femto-electron bunches with this injector system is being investigated. Experimental setup of the injector system is in progress, alpha magnet and other element for beam transport system has been fabricated. Field measurements are in progress. The rf gun cavity has been tuned to 1:2 in field ratio. Cathode heater test up to 1100°C has been done and we are preparing for a high power microwave test in the near future. Numerical multi-particle beam dynamics calculations showed that a beam with 74 pC bunch charge and about 97 fs bunch length is possible with the injector system. However, more investigation of beam dynamics with the inclusion of space charge and thermal emittance at the cathode are required. Applications of the ultra-short electron bunches on generation of coherent radiations are being considered.

Acknowledgments

The authors would like to thank Prof. Helmut Wiedemann for his enthusiasm to provide the technical details as well as his BCompress code. We appreciate very much for his patience to explain to us the interesting beam dynamics inside a thermionic rf gun and during bunch compression using alpha magnet.

References

1. C. Settakorn, M. Hernandez, K. Woods and H. Wiedemann, "Coherent Far-infrared Radiation from Electron Bunches", SLAC-PUB-7812, May 1998.
2. S. Rimjaem, R. Farias, C. Thongbai, T. Vilaithong, H. Wiedemann, "Femtosecond electron bunches from an RF-gun", Nucl. Instr. and Meth. A 533 (2004) 258-269
3. M. Borland, "A High-Brightness Thermionic Microwave Electron Gun", Stanford PhD Thesis, SLAC-R-0402, 1991.
4. P. Kung, H. Lihn H. Wiedemann and D. Bocek, "Generation and Measurement of 50-fs (rms) Electron Pulses", Phys. Rev. Lett., Vol. 73, p. 967-970, 1994.
5. H.A. Enge, "Achromatic Magnetic Mirror for Ion Beams', Review of Sci. Instr. 34(4), 1963.
6. L.M. Young, J.H. Billen, Los Alamos National Laboratory, Tech. Note LA-UR-96-1835, July 2004.
7. J.H. Billen, L.M. Young, Los Alamos National Laboratory, Tech. Note LA-UR-96-1834, July 2004.
8. BCompress is a beam optics code written by Professor Helmut Wiedemann at Stanford University.
9. W.K. Lau, B.J. Chan, L.H. Chang. C.W. Chen, H.Y. Chen, S.Y. Hsu, K.T. Hsu, J.Y. Hwang, K.K. Lin, Y.C. Wang, T.T. Yang,, "Characterization and Tuning of a Microwave Gun Cavity", PAC05, 2005.

Solid State Phenomena Vol. 107 (2005) pp. 11-14
online at http://www.scientific.net

Radiation Production Using Femtosecond Electron Bunches

C. Thongbai[1, a], V. Jinamoon[1], N. Kangrang[1], K Kusoljariyakul[1], S. Rimjaem[1], J. Saisut[1], T. Vilaithong[1], M.W. Rhodes[2], P. Wichaisirimongkol[2], and S. Chumphongphan[3]

[1]FNRF, Chiang Mai University, Chiang Mai, Thailand

[2]IST, Chiang Mai University, Chiang Mai, Thailand

[3]School of Science, Mae Fah Luang University, Chiang Rai, Thailand

[a]chlada@fnrf.science.cmu.ac.th

Keywords: femtosecond electron bunches, Far Infrared radiation, femtosecond X-ray

Abstract. Femtosecond electron bunches can be generated from a system consisting of an RF gun with a thermionic cathode, an alpha magnet, and a linear accelerator and can be used to produce femtosecond (fs) electromagnetic radiation pulses. At the Fast Neutron Research Facility (FNRF), Thailand, we are especially interested in production in Far-infrared (FIR) and x-radiation. In the far-infrared, radiation is emitted coherently for wavelengths which are longer than the electron bunch length, yielding intense radiation. Although, the x-rays emitted are incoherent, its femtosecond time scale is crucial for development of a femtosecond x-ray source.

Introduction

When accelerated, charged particles emit electromagnetic radiation. The radiation spectrum and characteristics are different depending on radiation production mechanisms. Successes in fs electron bunch generation [1-2], open up opportunities to develop fs electromagnetic radiation sources which are not widely available. Experimental and theoretical investigation on the generation of far-infrared radiation and x-rays from fs electron bunches will be described.

Femtosecond Electron Bunches

Femtosecond electron bunches can be generated from a system consisting of an RF gun with a thermionic cathode, an alpha magnet, and a linear accelerator [1-2]. The RF gun is designed such that the first particles in each S-band cycle are exposed to maximum acceleration while any later particles will accumulate less energy. By this condition, higher energy particles will emerge first from the rf-gun followed by lower energy particles, consequently generating a well-defined correlation between energy and time. Electron bunches of 20-30 ps at 2-3 MeV from the rf-gun are then compressed in an α–magnet, where the particle path length increases with energy. The lower energy particles emitted later in each bunch thus are able to catch up for effective bunch compression. At the end of this process, the bunches are compressed to less than one ps. After acceleration in a 3m single section S-band linac up to 30 MeV, the electrons are guided to experimental stations for radiation production.

Coherent Far-infrared Radiation

At a wavelength longer than the electron bunchlength, the radiation is emitted coherently with the intensity scaling like the square of the number of electron population [3]. Since there are 10^8 to 10^9 electrons in each bunch, the radiation intensity is enhanced by that same large factor over incoherent radiation and intense far-infrared (FIR) radiation can be derived from relativistic fs electron bunches [4]. The coherent spectrum depends greatly on the particle distribution in the bunch. The total radiated power from a mono-energetic bunch of N electrons can be written as

$P(\omega)=P_0(\omega)[N + N(N-1)f(\omega)]$, where $P_0(\omega)$ is the radiated power from a single electron. The *form factor*, $f(\omega)$, is the Fourier transform of the longitudinal bunch distribution. The second term in the square bracket describes the coherent radiation. The factor $Nf(\omega)$ will enhance the intensity of the incoherent radiation intensity emitted by any radiation production processes.

Transition Radiation TR is emitted when a charged particle passes through an interface between two media with different dielectric constants. A thin Al-foil is employed to serve as the radiator which represents the transition between vacuum and metal. A 45° tilted Al-foil can be used as the TR radiator to produce backward TR emitted at 90° with respect to the beam axis. The spectral-angular distribution of the emitted radiation energy can be described by

$$\frac{d^2W}{d\omega\, d\Omega} = \frac{r_c m_c^2 \sin^2\theta}{\pi^2 c (1-\beta \sin^2\theta)^2}, \qquad (1)$$

where θ is the emission angle with respect to the electron beam axis. The intensity increases from zero in the forward direction to a broad peak at an angle $\theta = 1/\gamma$. The single electron TR spectrum is uniform up to a very high frequency, but for coherent TR this uniform spectrum folds with the form factor of the electron bunch. Figure 1(a) shows a measured coherent TR spectrum obtained from approximately 120 fs of 26±4 MeV electron beams [4]. The radiation is broadband and its spectrum reaches from microwaves to 120 cm^{-1} wavenumber. The spatial distribution of TR was measured by moving a detector across the TR beam and is shown in Fig. 2. The radiation is hollow at the center of the radiation, reaching the maximum around the distance associated with $1/\gamma$ opening angle as indicated by equation (1). The horizontal and vertical polarization of the TR are observed using a wire grid polarizer and shown in Fig. 2 (b and c). The FIR radiation brightness of coherent TR estimated for 50 fs electron bunches, expected in the near future at FNRF [5], extending to over 300 cm^{-1} wavenumber greatly exceeds that of a black body as well as that of synchrotron radiation as shown in Fig.1(b).

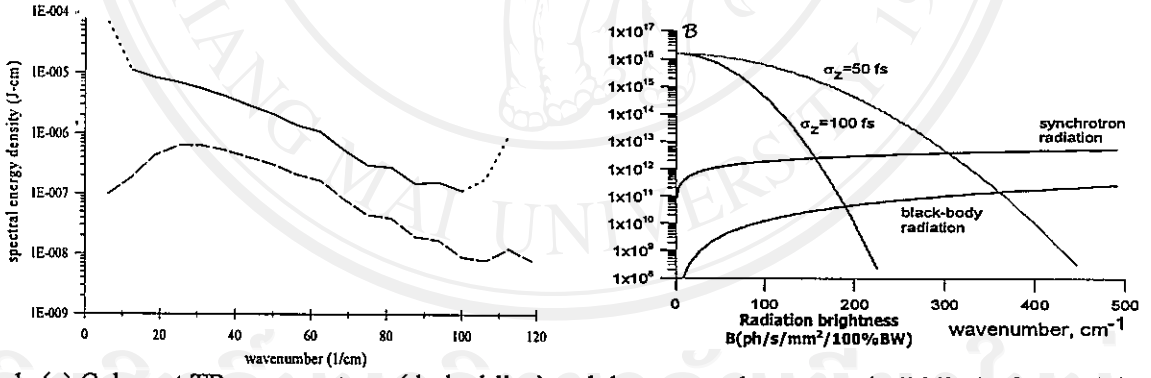

Fig.1: (a) Coherent TR raw-spectrum (dashed-line) and the corrected spectrum (solid line) after applying the correction for beam splitter (BS) efficiency. The dotted-section occupy region near singularities of the BS efficiency. (b) Radiation brightness B(Ph/s/mm²/100%BW) of Coherent TR, blackbody and synchrotron radiation.

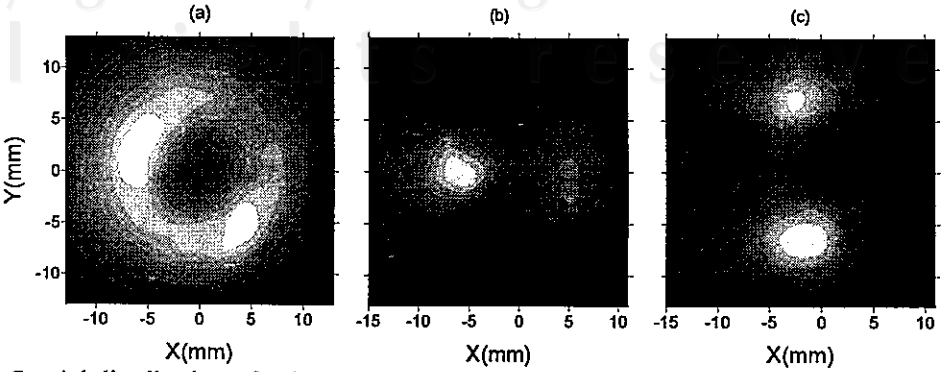

Fig.2: Spatial distribution of coherent TR (a) all- , (b) horizontal-, and (c) vertical-polarization.

Parametric X-rays

Different radiation production mechanisms can be used to convert the fs electron bunches to x-ray pulses as for example bremsstrahlung, synchrotron-, channeling-, transition-, Smith-Purcell-, and parametric x-radiation as well as Compton scattering. Among those, the parametric x radiation (PXR) is suitable for x-ray production using few tens MeV electron beams since the output photon energy is independent of the electron energy [6-9].

The name PXR is accepted in most experimental publications for the radiation from crystal in the X-ray band and can be understood as the diffraction of virtual photon on crystallographic planes while the electron beam passes through a crystal slab [7-9]. There are two schemes for PXR generation from relativistic electrons: Laue and Bragg geometry. For Laue geometry, the radiation production is associated with crystallographic planes perpendicular to the slab surface while Bragg geometry deals with crystallographic planes oriented parallel to the slab surface. PXR is generated under the Bragg condition $d \sin\phi = n\lambda$ allowing us to select the photon energy by adjusting the crystal rotation angle ϕ. The PXR production geometry can be described using Fig. 3 with a (100) Silicon wafer.

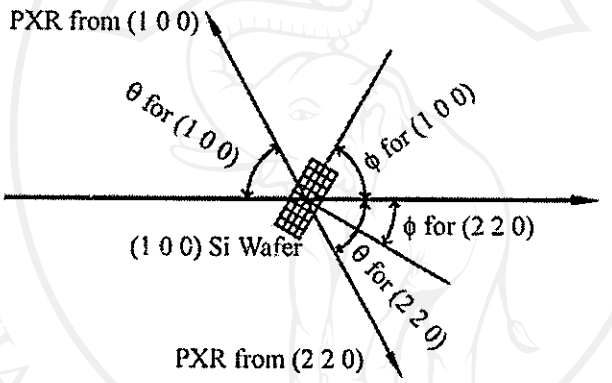

Fig. 3: Geometry for PXR generation from a (100) Silicon wafer.

The energy of PXR can be derived from [8-9]

$$E = \bar{h}\omega = \frac{c\bar{h}\left|\vec{g}\cdot\vec{V}\right|}{c-\sqrt{\varepsilon}\vec{V}\cdot\vec{\Omega}} \quad = \frac{\bar{h}\left|\vec{V}\right|\left|\vec{g}\right|\sin\phi}{1-\beta\cos\theta} \tag{2}$$

where E is the PXR energy, ω the PXR angular frequency, c the velocity of light in vacuum, $\vec{g}$ the reciprocal lattice vector, $\vec{V}$ the electron velocity, $\vec{\Omega}$ the direction of observation and ε dielectric constant of the crystal which becomes unity for x-rays. In the last step, we have used the geometry as shown in Fig. 3 with the crystal rotation angle ϕ and the observation angle θ.

The magnitude of the reciprocal lattice in the equation can be calculated from Miller indicies of the plane (hkl), and the lattice constant a as $|\vec{g}| = (2\pi/a)\sqrt{h^2+k^2+l^2}$. By comparing $|\vec{g}|$ for the (2 2 0)-plane and (1 0 0)-plane, one can see that radiation associated with the (2 2 0)-plane results in a higher energy based on the higher magnitude of reciprocal lattice vector. The estimated PXR energy associated with the (2 2 0)-plane as a function of crystal rotation angle at some fixed observation angles is shown in Fig. 4(a). The calculation indicates that generation of PXR energy as high as 130 keV is possible with crystal rotation angle of 45 degree and observation angle of 15 degree. However, the radiation cone will be concentrated around the Bragg direction determined by $\theta = 2\phi$. The PXR energy as a function of crystal rotation angle and observation angle keeping $\theta = 2\phi$ are shown in Fig.4(b)

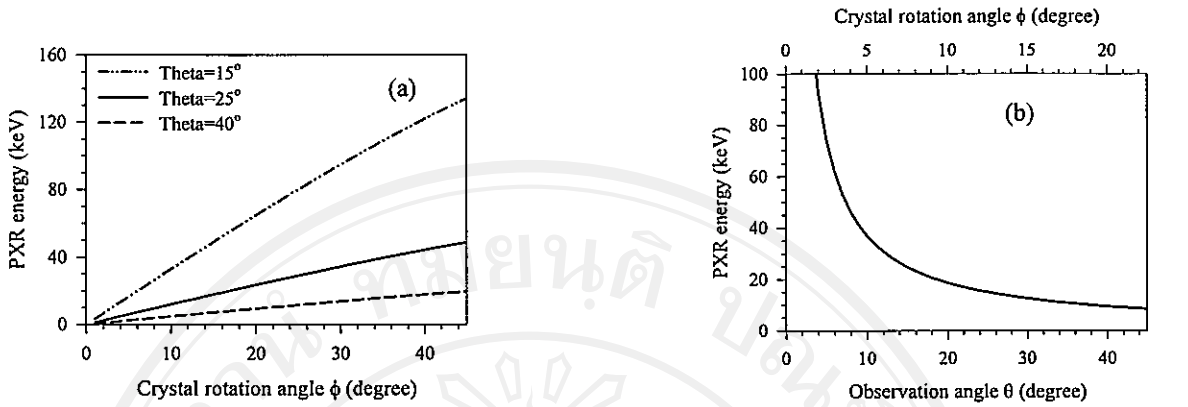

Fig. 4: PXR energy associated with the (2 2 0)-plane (a) as function of crystal rotation angle with some fixed observation angles (b) as function of observation angle θ and crystal rotation angle ϕ with $\theta = 2\phi$.

Although, at very small observation angles, the PXR energy can be as high as 100 keV, the radiation propagates in the direction close to the direction of the electron beams and makes it difficult to detect. We are looking for PXR in the range of 10-35 keV which can be obtained at more convenient observation angles of 10-45 degrees.

Conclusion

With the accessibility of fs electron bunches it is possible to generate high brightness, coherent, polarized, broadband FIR via transition radiation and generate tunable x-rays via parametric x radiation. The radiation pulses come in very short bursts of fs duration reflecting the electron bunch length and time structure. The high intensity fs FIR pulses can be applied for Dispersive Fourier Transform FIR Spectroscopy where the short pulses allow for direct determination of complex refractive index over the spectral range of the radiation [10]. The availability of fs X-rays will open up opportunities for time-resolved studies of ultrafast processes.

Acknowlegdements

We would like to acknowledge the support of the Thailand Research Fund (TGR4580055), the National Research Council of Thailand, the Thai Royal Golden Jubilee Scholarship Program, the US Department of Energy, the Hansen Experimental Physics laboratory (HEPL) of Stanford University, the Department of Physics, Faculty of Science, and Chiang Mai University.

References

[1] H. Wiedemann et. al., J. Nucl. Mat., Vol. 248 (1997), p.374.
[2] P. Kung et. al., Phys. Rev. Lett., Vol. 73 (1994), p.967.
[3] J. S. Nodvick and D. S. Saxon, H. Motz, Phys. Rev, Vol. 96 (1954), p.180.
[4] C. Settakorn, *Generation and Use of Coherent Transition Radiation from Short Electron Bunches,* Ph.D. thesis, Stanford University, California (2001).
[5] S. Rimjaem et. al., Nucl. Instr. And Meth. A Vol. 533 (2004), p.258.
[6] V. G. Baryshevsky and I. D. Feranchuk, NIM A, Vol. 228 (1985), p.490.
[7] M.L. Ter-Mikaelian, .*High Energy Electromagnetic Process in Condensed Media.* Wiley-Interscience, New York, 1972.
[8] A. V. Shchagin et.al., Phys. Lett. A Vol.148 (1990),p. 485.
[9] A. V. Schagin, in *Electron-Photon Interaction in Dense Media*, Edited by H. Wiedemann, Kluwer Academic Publishers, Netherlands (2001).
[10] K. Wood and H. Wiedemann, Chem. Phys. Lett., Vol. 393, No 1-3 (2004), p.159.

Solid State Phenomena Vol. 107 (2005) pp. 15-20
online at http://www.scientific.net

Femtosecond Electron Pulses Production System

S. Rimjaem[1, a], V. Jinamoon[1], N. Kangrang[1],
K. Kusoljariyakul[1], J. Saisut[1], C. Thongbai[1], T. Vilaithong[1],
M.W. Rhodes[2], P. Wichaisirimongkol[2] and S. Chumphongphan[3]

[1]FNRF, Chiang Mai University, Chiang Mai, Thailand

[2]IST, Chiang Mai University, Chiang Mai, Thailand

[3]School of Science, Mae Fah Luang University, Chiang Rai, Thailand

[a]neung@fnrf.science.cmu.ac.th

Keywords: femtosecond electron pulses, femtosecond electron production

Abstract The SURIYA project is designed to generate femtosecond (fs) electron pulses at the Fast Neutron Research Facility (FNRF), Thailand. The fs electron pulses production system consists mainly of a thermionic cathode RF-gun, a magnetic bunch compressor in form of an alpha magnet (α-magnet), a linear accelerator (linac), a beam transport line, and various electron beam diagnostic instruments. This system aims to produce a 20-25 MeV electron beam with micropulses of less than 100 fs in length. Theses pulses can be used either for direct experimentation or to produce fs pulses of intense coherent far infrared radiation (FIR) and/or x-ray. In this paper, an overview of the system and characteristics of its major components will be presented.

Electron Bunch Generation and Compression System

Production of fs electron pulses provides many opportunities for research to study extremely fast processes in chemical reaction, biological molecule and in time-resolved experiments [1, 2]. The SURIYA project at FNRF has been established since 2000 aiming to generate fs electron pulses [3]. The electron bunch generation and compression system at SURIYA consists of two major components: an electron gun and an α-magnet with energy filters. The electron gun consists of 1-1/2 standing wave RF cavities with a thermionic cathode operating at 2856 MHz and produces 2.4 MeV electrons bunches. Electrons in each bunch are distributed in the energy-time phase space with higher energy electrons located at early time at the head of the bunch and lower energy electrons at later time due to the time-varying RF-field. Then, electron bunches are steered into the α-magnet for compression.

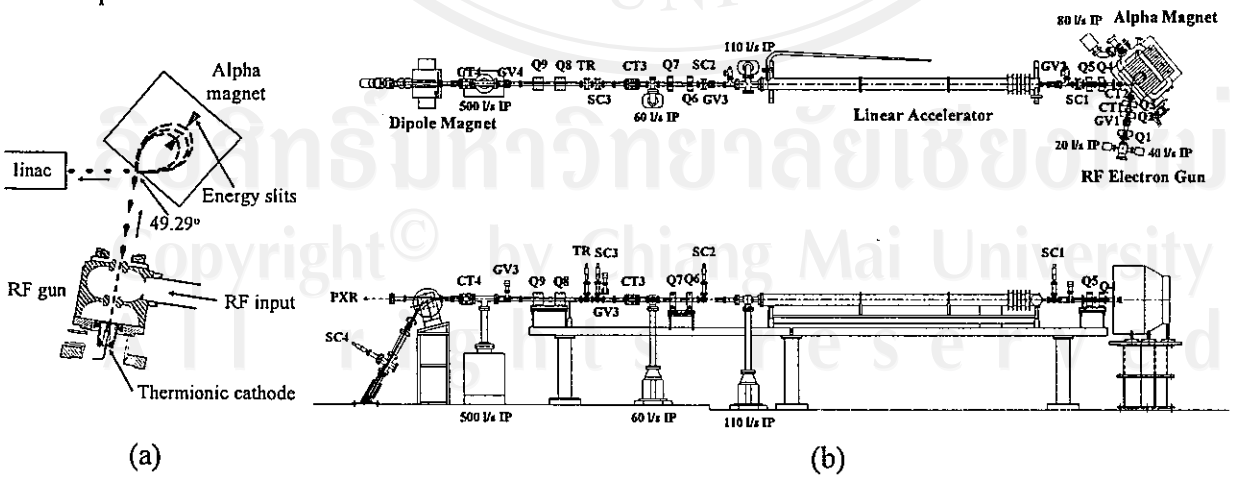

Fig.1: (a). Schematic diagram of the bunch generation and compression system, (b). schematic drawing of the top and the side view of SURIYA beamline.

As indicated in Fig.1(a), electrons follow a closed loop in the α-magnet similar to the letter α and exit the magnet exactly at the entrance point independence of the particle energy. Higher energy

electrons follow a longer path and spend longer time in the magnet than the lower energy ones. These features make the α-magnet a convenient and simple bunch compressor. One may change the magnet strength and thereby it is possible to compress part of electron bunch into sub-picosecond duration without changing the direction of the beam path outside the magnet. This optimized and compressed part of the electron bunch is then filtered by energy slits located in the α-magnet vacuum chamber and then transported through a 30 MeV SLAC type linac and a beam transport line to guide the electrons to beam diagnostic and experimental stations. At the end of the beam transport line a dipole magnet serves both as the beam dump and an energy spectrometer. Fig.1 (b) illustrates the schematic of the side and the top view of the beamline at SURIYA.

Beam Dynamics and RF Gun Simulations

RF characteristics of the RF-gun were studied and simulated using an electromagnetic field solver SUPERFISH [4]. The RF-gun geometry has been designed based on these numerical simulation results. Based on 2D-simulation, SUPERFISH cannot be used to investigate 3D-shape include coupling cavity, RF-input and vacuum pumping ports and can lead different between simulated and measured values. However, simulation results still give a close approximation of RF properties of the gun as well as helpful scaling concerning the RF-gun dimension and its resonant frequency (f_{rf}) while the final adjustments are made empirically.

A particle-in-cell computer code PARMELA [5] was used to study and investigate particle beam dynamics through the EM fields inside the gun. Results of the numerical simulation of the electron dynamics show that there is a high concentration of particles at the head of the bunch, consequently generating a small correlation between energy and time. The concentration of most particles within 10% of the maximum energy appears in the length of some 10-20 ps at the gun exit. While the electron bunches are traveling through an α-magnet the lower energy particles follow the shorter path and catch up with the higher one at the α-magnet exit resulting in bunch compression. The particle distribution at the experimental station after bunch compression and acceleration indicates a bunch length about 53 fs [6]. Some RF-gun and beam parameters are shown in Table 1.

Table 1: Some parameters for the optimized RF-gun and beam dynamic study results.

Parameters	Value	Parameters	Value
Max. beam energy, E [MeV]	2.4	Charge/bunch [pCb]	94
Avg./max. field in half-cell [MV/m]	23.9/29.9	Peak current [A]	707
Avg./max. field in full-cell [MV/m]	45.5/67.6	Bunch length, rms [fs]	52.8
Cathode emission current [A]	2.9	$\varepsilon_{n,rms}$ at rf-gun exit [mm-mrad]	3.8

RF-gun Fabrication and Testing

The RF-gun cavities have been fabricated based on SUPERFISH results out of Oxygen Free Copper blocks. During fabrication processes, modifications of the gun dimension based on SUPERFISH scaling law were performed together with the low power RF-measurements (cold tests). Cold test results show that the resonant frequency of the RF-gun is 2855 MHz at 30 °C in ambient air and the quality factor (Q-factor) is 12979. The resonant frequency can be adjusted precisely to 2856 MHz by adjusting the RF-gun operating temperature. Fig.2 shows the cross-section and 3D-view of the RF-gun and demonstrates the average longitudinal field mapping, which shows that the average electric field ratio of the full-cell to the half-cell measured via bead-pull measurement is 2.186 compared to the predicted value of 2.067 from PARMELA simulation. The cathode of the RF-gun is a BaO_2-Sr_2O_3 thermionic cathode, with a flat and circular emitting surface of 3 mm radius. It has been installed and tested via optical pyrometric measurement. The measurement result reveals that the cathode filament can be heated to exceed the cathode processing conditions and guarantee that

the cathode will emit electron with efficient amount in general operating temperature of about 950-1000 °C.

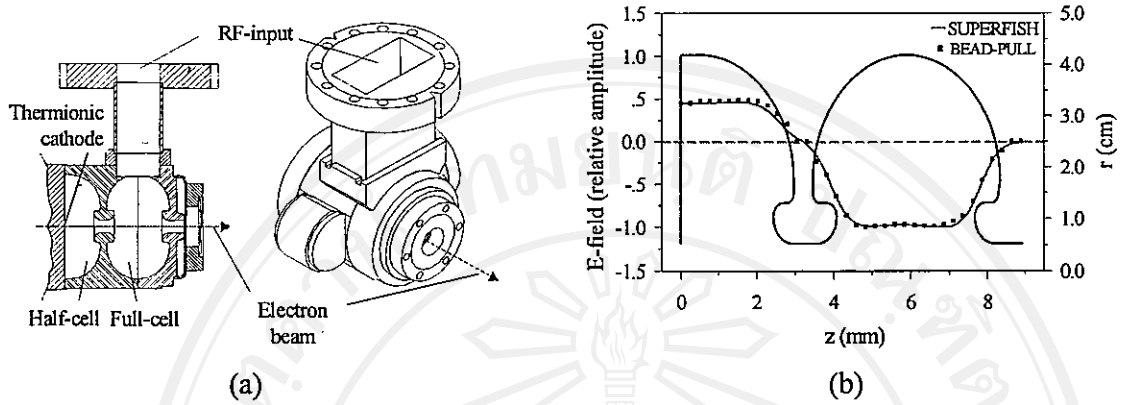

Fig.2: (a). Cross-section and 3D-view drawing of the RF-gun, (b). longitudinal electric field distribution on axial axis from SUPERFISH and Bead-Pull measurement.

Alpha Magnet Design and Construction

An α-magnet is half of a quadrupole magnet with two poles and a mirror plate replacing the other half. The alpha magnet is an achromat, while the lengths of the particle trajectory in the α-magnet exhibits a large dispersion and depends on the particle momentum cp and magnetic field gradient g scaling like $S \approx \sqrt{cp/g}$ [7]. Computer code POISSON [4] was used to design geometry and calculate magnetic field of the α-magnet. Simulations show that a gradient of 450 Gauss/cm, a current of 265 A is needed.

Low carbon iron was used to build the magnet poles because of its high permeability. Nine layers of thick iron sheet were used to construct the whole magnet. Double pancake technique was used for winding excitation coils. The excitation coil had 70 turn of hollow copper wire. Water cooling system was built for 3.7 kw power loss of the coils. Measurement of field distribution inside the magnet was performed using digital Hall Effect Teslameter and the results show that the measured magnetic fields agree well with the calculation.

RF System

Downstream of the α-magnet the beam is further accelerated in a SLAC type linac to 20-25 MeV limited by the available klystron RF-power. Both the RF-gun and the linac are powered from two separate RF sources consisting of a common RF oscillator driver and two 5 MW klystrons with their associated modulators. Fig.3 illustrate the schematic outline of the SURIYA RF system.

A low-level RF signal is generated by a resonant tank oscillator tuned to 2856 MHz. Then it is split into two signals by a 90° Hybrid directional coupler. One feeds the gun amplifier and the other the linac RF amplifier through an adjustable phase shifter. Both amplifiers produce an RF-output pulse of about 100W for 5-6 μsec. This RF-pulse is sent to the modulator grid of the klystrons. Each klystron consists of a klystron tube, focusing coil and pulse transformer with insulating oil. A high-current, high-voltage pulse drives the pulse transformer primary and the secondary drives the anode of the klystron. This pulse is then modulated at 2856 MHz by the klystron grid and then enters into a waveguide through a ceramic RF window. The klystron produces about 5 MW peak power in a flat-topped pulse 5-6 μs long with an average power of 250-300 W. The high power RF signal is transmitted to the RF-gun and linac through a rectangular waveguide system pressurized with SF6 to prevent electrical discharges. RF power is measured using directional couplers on the waveguides of the RF-gun and the linac.

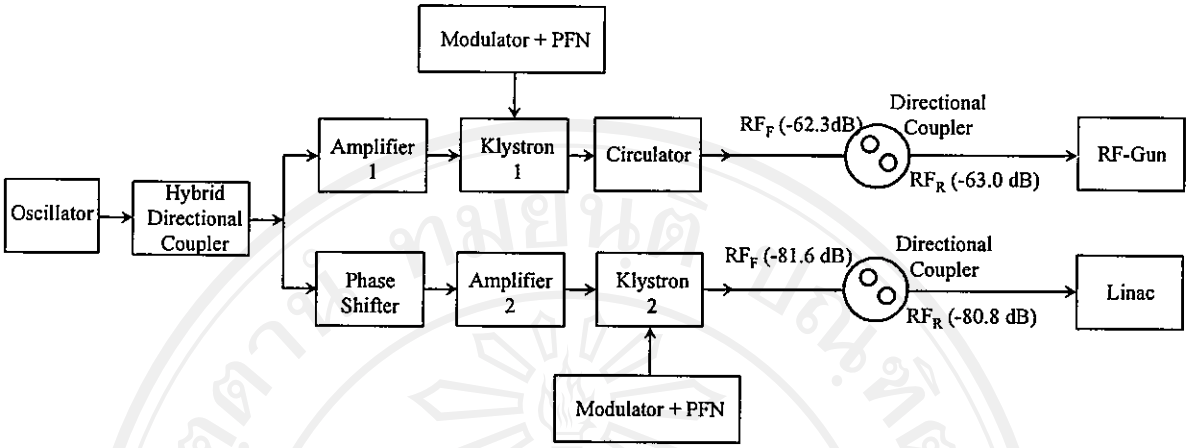

Fig.3: Schematic outline of SURIYA RF system.

Beam Diagnostics

So far SURIYA can produce an electron beam with a peak current of about 500 mA and a kinetic energy of 2.4 MeV at the exit of the RF-gun. The electron beam current is measured by a current monitor and an actual signal is shown in Fig.4(a). The electron beam energy is measured by using an energy filter inside the α-magnet. The 2.4 MeV electron beam is accelerated to reach higher kinetic energy when it is transported through the linac. Downstream of the linac several experimental stations are followed by a beam analysing station in form of a spectrometer. A 0.4 Tesla dipole magnet has been designed and constructed to deflect the electron beam into a Faraday cup. This combination allows us to use them as a spectrometer and charge monitor. The dipole pole profile has been designed and simulated using the RADIA [8] code. Figure 4(b) and (c) shows 3D-view of the magnet and demonstrates 3D magnetic field distribution from measurement.

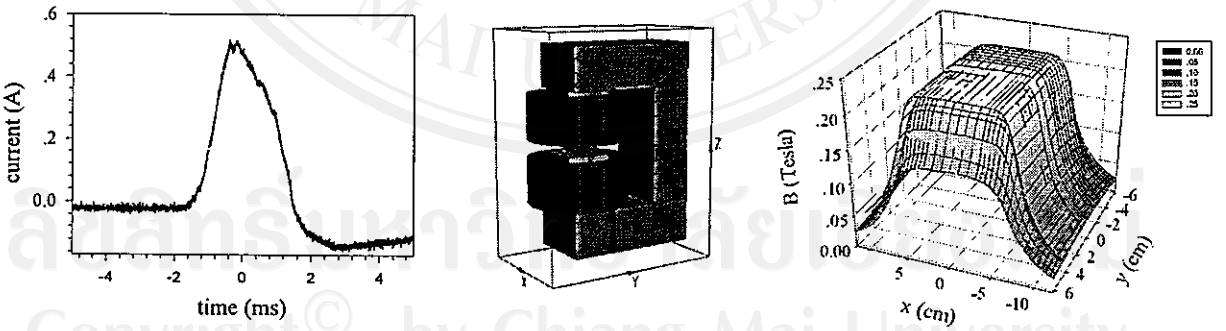

Fig.4: (a). 3D-view of dipole magnet, (b). magnetic field distribution from measurement, and (c). measured current pulse generating from the RF-gun.

Summary

Beam dynamics study results shows that about 2.4 MeV electron beam with normalized emittance of 3.8 mm-mrad with charge of 94 pCb can be generated from the RF-gun and the bunch length as short as 53 fs can be expected to produce at the experimental station. The main components and the beam transporting system of the fs electron pulses facility have been installed. The commissioning and electron beam diagnostics for characterizing the performance of the system and bunch length

measurement are in progress. At SURIYA, many applications are planed to be pursued such as generation of low energy fs electron pulses for direct application, production of intense coherent FIR and generation of fs x-ray pulses.

Acknowlegdements
We would like to acknowledge the support of the Thailand Research Fund, the National Research Council of Thailand, the Thai Royal Golden Jubilee Scholarship Program, the US Department of Energy, the Hansen Experimental Physics laboratory (HEPL) of Stanford University, Department of Physics and the Graduated School of Chiang Mai University.

References

[1] H. Ihee et. al., Science, Vol. 291 (2001), p. 458.
[2] M. Bauer et. al., Phys. Rev. Lett. Vol. 87 (2001) 025501-1.
[3] T. Vilaithong et. al., in Proc. APAC01, Beijing, China, 2001, p 91.
[4] L.M. Young, "POISSON/SUPERFISH," LANL Technical Note LA-UR-96-1834, 1999.
[5] L.M. Young, "PARMELA," LANL Technical Note LA-UR-96-1835, July 2002.
[6] S. Rimjaem et. al., Nucl. Instr. and Meth. A Vol. 533 (2004), p. 258.
[7] Enge, H.A. Achromatic Magnetic Mirror for Ion Beams, Rev. Sci. Instr., Vol. 34, (1963), p.385.
[8] www.esrf.fr/Accelerators/Groups/InsertionDevices/ Software/Radia

Available online at www.sciencedirect.com
SCIENCE DIRECT®
Nuclear Instruments and Methods in Physics Research A 533 (2004) 258–269
NUCLEAR INSTRUMENTS & METHODS IN PHYSICS RESEARCH Section A
www.elsevier.com/locate/nima

Femtosecond electron bunches from an RF-gun

Sakhorn Rimjaem[a,*], Ruy Farias[b], Chitrlada Thongbai[a], Thiraphat Vilaithong[a], Helmut Wiedemann[c]

[a] *Fast Neutron Research Facility, Physics Department, Chiang Mai University, P.O. Box 217, Chiang Mai 50202, Thailand*
[b] *Laboratorio National de Luz Sincrotron, LNLS, Campinas, Brazil*
[c] *Applied Physics and SSRL/SLAC Stanford University, Stanford, CA, USA*

Received 8 December 2003; received in revised form 3 May 2004; accepted 27 May 2004
Available online 29 July 2004

Abstract

Sub-picosecond electron pulses become a tool of increasing importance to study dynamics at an atomic level. Such electron pulses can be used directly or be converted into intense coherent far infrared radiation or equally short X-ray pulses. In principle, sub-picosecond electron pulses can be obtained in large, high-energy electron linear accelerator systems by repeatedly applying an energy slew and magnetic compression. Another process is the production of short electron pulses at low energies from an RF-gun with a thermionic cathode together with a bunch compressing α-magnet. In this paper, we present a systematic analysis of capabilities and limits of sub-picosecond electron pulses from such a source. We discuss particular parameter choices as well as the impact of geometric and electric specifications on the 6-dimensional phase space electron distribution. Numerical beam simulations with the computer code PARMELA are performed including effects and limitations due to space charge forces. While the production of femtosecond electron bunches is of primary concern, we also consider the preservation of such short bunches along a beam transport line.

PACS: 41.75.Lx; 29.27.Fh

Keywords: fs electron pulses; fs X-ray pulses; Far infrared radiation; Electron source; RF-gun

1. Introduction

Experimental opportunities based on particle beams are frequently determined by the particles' distribution in six dimensional phase space. Excellent progress has been made in the past 15 years to reduce the transverse phase space

*Corresponding author. Tel.: +66-53-943-379; fax: +66-53-222-776.
E-mail address: neung@fnrf.science.cmu.ac.th (S. Rimjaem).

0168-9002/$ - see front matter © 2004 Elsevier B.V. All rights reserved.
doi:10.1016/j.nima.2004.05.135

distribution of particle beams especially in the pursuit of high brightness third generation synchrotron light sources. Only recently has it become possible to significantly reduce the longitudinal phase space distribution and to produce intense electron pulses of very short duration without relying on high-energy accelerators and extensive bunch compression systems. Sub-picosecond electron pulses at low energies of a few tens of MeV are desired, for example, for direct applications in research of physical, chemical and biological materials [1–3]. Other applications are based on the transformation of the electron pulses into photon pulses by way of, for example, single pass free electron lasers (SASE) [4], Compton scattering [5], Parametric and other methods to produce femtosecond X-ray pulses [6], or for the generation of coherent far infrared radiation [7–9] with a photon brightness far exceeding that available from conventional and synchrotron radiation sources.

In large, high-energy linear accelerator systems, sub-picosecond electron pulses can be obtained by repeated application of RF beam-conditioning and bunch compression. At low energies, such bunches can be produced on a laboratory scale from an $1\frac{1}{2}$-cell RF-gun with a thermionic cathode and an α-magnet for bunch compression, albeit at lower charge intensities [10]. This type of electron source provides three essential features which allow efficient bunch compression. First, the high acceleration to near relativistic energies within a few centimeters minimizes detrimental space charge effects. Second, the energy-time phase space distribution of the electrons produced in a RF-gun is specially well suited for bunch compression as will be discussed in more detail. Third, a simple, reliable and easy to use thermionic cathode can emit a particle flux up to and beyond an intensity where space charge effects become uncontrollable at the low electron energies considered here. Utilizing such an RF-gun with a thermionic cathode at the Stanford SUNSHINE facility [9,11], it has been possible to produce electron pulses as short as 120 fs rms [9,12] and a bunch intensity of 100 pCb. Fig. 1 shows a schematic cross-section and a 3D-view of the electron source as installed at SUNSHINE.

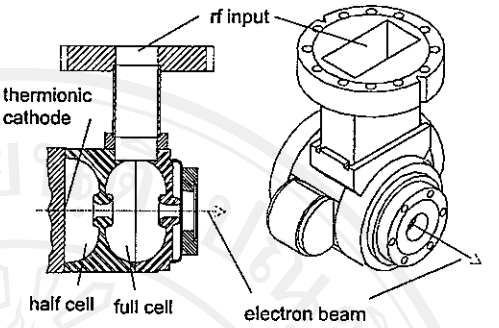

Fig. 1. RF-gun cross-section and 3D-view.

The SUNSHINE RF-gun, however, has been originally designed for a different application and was not optimized to generate femtosecond bunches. Specifically, the accelerating field was not optimized for bunch compression as will be discussed later. Furthermore, the geometry of the RF-gun produces transverse focusing forces which produce a convergent electron beam at the exit of the RF-gun. This and subsequent focusing generates a spread of total path length for individual particles and limit the shortest achievable bunch length at SUNSHINE to 120 fs rms. Specific optimization of the RF-gun to minimize this focusing and produce femtosecond electron bunches is therefore expected to result in shorter bunches. In this note, we report on the results of a systematic investigation and discussion of optimization procedures, choice of parameters and limitations in producing femtosecond bunches from an RF-gun. Specifically, we study the impact of particular geometric and electric parameter choices on beam performance including the influence of space charge. Following this optimization a new RF-gun has been built at Chiang Mai University for the SURIYA facility, soon to be commissioned [13].

2. Method

The electron source consists mainly of a $1\frac{1}{2}$-cell RF-cavity, operating at 2856 MHz with a thermionic cathode and followed by an α-magnet for

bunch compression. Electrons emerging from the cathode (Fig. 1) travel first through the half and then the full RF-cell reaching a kinetic energy of about 2.5 MeV. Later, we will discuss in more detail the optimum choice of the accelerating fields.

2.1. Numerical beam simulations

The dynamics of particle motion in the RF-gun has been simulated with the code PARMELA [14] to determine the dependence of expected beam characteristics on external parameters as well as on space charge forces. In this section, we show the final results of those studies followed by more detailed discussions in subsequent sections. These simulations exhibit a particle distribution at the RF-gun exit (Fig. 2) with a high correlation between momentum and time as is desired for effective bunch compression.

The distribution shown is that of a single S-band bunch repeating at 3 GHz. Adjacent bunches are separated by half a RF-period during which no particles can be accelerated. This temporal gap defines a definitive beginning (head) of the bunch when the microwave field at the cathode just starts to become accelerating. Although it is assumed that electrons are emitted in a uniform stream from the cathode, we notice an increased longitudinal particle density at the RF-gun exit as indicated in the histogram showing the number of macroparticles per picosecond. Unless otherwise noted, we use for this study a uniform cathode emission current of 2.9 A represented by 100,000 macroparticles per 2856 MHz RF-period. Each macroparticle represents a charge of 10.15 fCb or $n_e = 6.34 \times 10^4$ electrons. The uniform current of 2.9 A corresponds to 285.6 macroparticles per picosecond at the cathode, yet at the RF-gun exit, we observe a much higher particle density during the first few picoseconds at the head of each bunch (see Fig. 2). The dynamics of this concentration derives from the temporal variation of the microwave field. The first electrons accelerated encounter initially only a very small field which increases as the electrons travels through the $\frac{1}{2}$-cell. Particles emerging somewhat later from the cathode into the raising RF-field gain speed more quickly. They actually are able to partially catch up with earlier particles. This bunching of a CW beam from the cathode is due to the time variation of the RF-field yielding short pulses of about 10 ps duration. From now on, we concentrate therefore only on this part of each bunch.

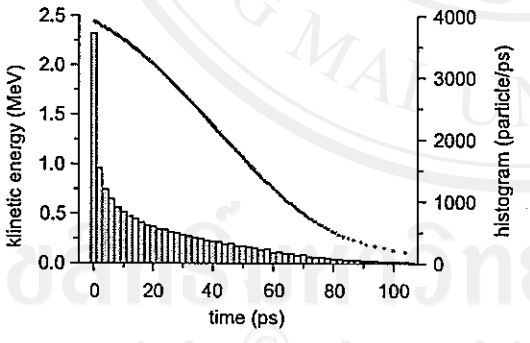

Fig. 2. Particle distribution in energy-time phase space for a single S-band bunch at the RF-gun exit with histogram. The units of the histogram are macroparticles (each representing 6.34×10^4 electrons) per picosecond.

2.2. Bunch compression

The concave shape of the phase space distribution in Fig. 2 matches especially well to bunch compression in an α-magnet [15] shown in Fig. 3.

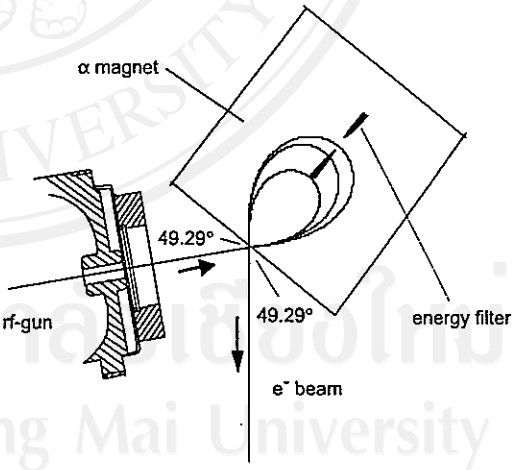

Fig. 3. Rf-gun and α-magnet layout (schematic).

This magnet is half a quadrupole with a mirror plate in the *yz*-plane to close the magnetic field lines. Generally, a beam would travel through a quadrupole along the *z*-axis, but in an α-magnet the electron beam enters the magnet in the *xz*-plane at an angle of 49.29° with respect to the magnet axis or *yz*-plane. As indicated in Fig. 3, particles follow a closed loop similar to the letter α and exit the magnet again exactly at the entrance point independent of the particle momentum, yet in a different direction. The α-magnet is therefore an achromat, while the path length s of the particle trajectory in the magnet exhibits a large dispersion, depending on the particle momentum cp and magnetic field gradient g like $s \propto \sqrt{cp/g}$ [16]. These features make the α-magnet a convenient and simple bunch-compressor for low-energy beams. One may change the magnet strength and thereby the compression without changing the direction of the beam path outside the α-magnet. It is interesting to note that the largest compression is obtained for a weak α-magnet strength because bunch compression of relativistic particles is mostly based on path length rather than velocity dispersion. The phase space distribution of Fig. 2 rotates clockwise as the beam travels through the α-magnet.

Although the electrons are generated as a CW beam from the thermionic cathode, they eventually emerge from the RF-gun in bunches with the periodicity of the RF frequency. No electrons are accelerated during half a RF-period, followed by a half-period of acceleration. From Fig. 2 we note that the highest energy electrons exit the RF-gun first and follow a longer path through the α-magnet than lower momentum electrons exiting the gun later. Even for moderately relativistic electrons, the velocity dispersion is small, although not negligible, and consequently lower momentum electrons following a shorter path can catch up to some degree leading to bunch compression. Still, to avoid excessive bunch lengthening due to velocity dispersion counteracting bunch compression, the beam energy should not be less than about 1 MeV and a short distance between RF-gun and α-magnet is desirable. An energy filter inside the α-magnet, where the momentum dispersion is large, is used to select the desired part of the beam.

Downstream of the α-magnet, there may be a linear accelerator and/or some transport line guiding the beam to an experimental station. To compensate for the velocity dispersion, the value of the α-magnet field-gradient must be chosen such as to generate the shortest bunches at the experimental station. Although we think of the α-magnet as being a bunch compressor, we have a short bunch within the α-magnet only for a very short time during the phase space rotation. To obtain the shortest bunch at the experimental station, we need to overcompress the bunch such that the lower momentum particles exit the α-magnet first and leaving higher energy particles behind. This phase space orientation together with the velocity dispersion due to the energy spread leads to the shortest bunch at the experimental station. This is a fortunate circumstance, since the bunch is most of the time long while the particle energy ahead of the linear accelerator is low and therefore space charge effects are negligible. Only for a very short time of a few ps does the bunch reach a very short length inside the α-magnet. Since the transverse beam dimensions are rather large due to the energy dispersion in the α-magnet, we only need to consider longitudinal space charge effects. Such space charge effects cannot be simulated with the PARMELA code (or any other code we know) in a beam line with an α-magnet and we must therefore use analytical methods to deal with this issue.

We calculated the energy gain a single particle would encounter being pushed from behind by all other particles. It was assumed that all particles are concentrated on a thin disk with the actual transverse radius as given by beam optics and the single particle ahead of this disk by half a bunch length or 15 μm. Such a particle would experience a relative energy gain of 7×10^{-5}, which translates into a velocity spread and hence into an increase in bunch length. Calculations show that an rms increase of 6 fs must be expected from this space charge acceleration, which is negligible for our conditions. The effect is even smaller noting that this increase in energy spread occurs just at the time when the bunch is the shortest and the (t, E) phase space distribution of the useful beam is spread along the energy coordinate. Due to the

energy change within the α-magnet a small transverse effect must be expected. The energy changing particle suffers a distortion of the α-type path leading to a transverse displacement of the particle trajectory at the α-magnet exit of some 2 μm or less than 0.1% of the beam size.

The numerically simulated particle distribution of Fig. 2 is shown in Fig. 4 after compression and acceleration in the linear accelerator to 26 MeV. Note that the temporal particle distribution is shown with respect to the initial momentum at the RF-gun exit. The particle distribution in phase space and the histogram exhibit some characteristics which we will discuss in more detail. Bunch lengthening due to path length dispersion caused by focusing in the beam transport line has been kept to a minimum in the particular design of the beam transport line (Fig. 5) and shows up as a small broadening of the Gaussian tails. Furthermore, the oscillatory temporal perturbation of the distribution is the result of an instability, the shock-wave instability, arising from the fast change of particle intensity at the front of each bunch [10] and is ultimately limiting the shortest achievable bunch length. This perturbation is established in the first half-cell persisting over a few oscillations. When space charge forces are ignored, this instability does not appear and the longitudinal phase space is determined only by cathode geometry, RF focusing and thermal energy distribution. The period of the perturbation

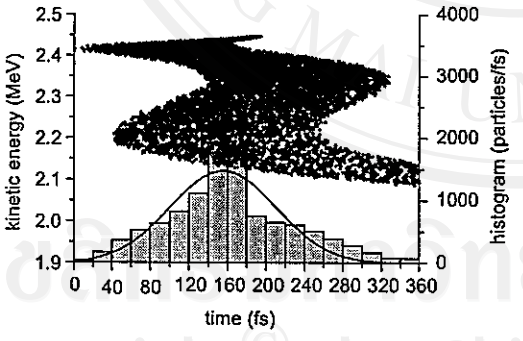

Fig. 4. Particle energy-time phase space distribution after bunch compression and transport to the experimental station with histogram. The histogram can be fitted by a Gaussian with a standard width of 52.8 fs and a charge of 94 pCb.

is varying in time from some 0.5 ps to about 7 ps after one period. This is much shorter than the RF-period, and the perturbation therefore cannot be caused by the 3 GHz RF-fields. Furthermore, the nonlinearity arising from bunch compression in the α-magnet causes only a slow monotonic variation of compression with particle momentum. The buildup of the perturbation, on the other hand, matches the rise time of the particle distribution while the perturbation amplitude increases with space charge. Indeed, in this study, the maximum beam charge is not limited by the cathode but rather by these oscillatory perturbations, which, at some level, prevent efficient bunch compression. The theory of this instability in [10] describes qualitatively the observations in beam simulations, but more quantitative studies are required and will be reported later.

In reality, we expect this shock wave instability to be somewhat reduced because the particle density in each bunch will rise less than assumed here due to the Langmuir–Child effect during the first few picoseconds. On the other hand, it is not quite clear how this effect manifests itself in a time varying field. According to the Langmuir–Child law no current should be emitted at zero field, but in our case there is no electron cloud yet in front of the cathode as theory assumes. Beam observation and measurements will hopefully shed more light on the beam construction in the presence of oscillating fields, space charge effects and shock wave instability.

The beam transport line used in this study is shown in Fig. 5 and has been designed for minimum bunch length broadening due to path length dispersion. While this is not the only solution possible, we use it as an example to demonstrate the dynamics of the electron beam. Focusing, being the source of path length dispersion, should be minimized as much as possible while still compensating the unavoidable strong focusing in the α-magnet.

The phase space distribution of Fig. 4 represents the result of an optimization study which we will use in this report as a reference for more detailed discussions. It shows the particle distribution at the end of the beamline which is the location of optimum bunch compression (Fig. 5). The most

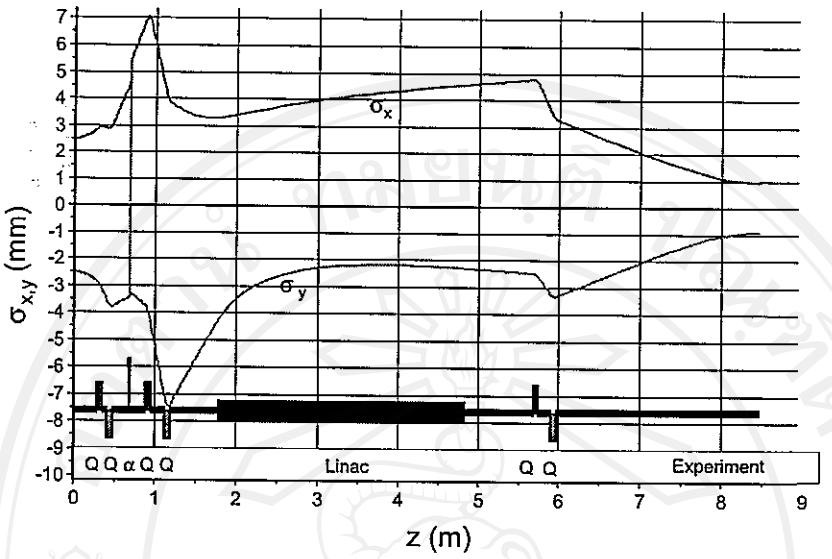

Fig. 5. Beam transport line from RF-gun to experimental station (QF1 - QD1 - QF2 - α-magnet - QF3 - QD2 - linac - QF4 - QD3). Note: α-magnet is shown as a thin element.

obvious feature of the distribution is the oscillatory variation in time. This oscillation is believed to be caused by an instability (shock wave instability [10]) caused by the sudden increase in the charge intensity at the head of each bunch. That leads to an oscillatory of energy due to space charge forces along the bunch which in turn gives rise to temporal oscillations after compression in the α-magnet. This effect is presently under intense quantitative study and is expected to ultimately limit the bunch compression of low-energy beams. From the temporal oscillations of about ±50 fs we derive a relative momentum ripple of $\pm 10^{-4}$. The expected bunch length, including transverse path length dispersion, is 53 fs rms at a total charge of 94 pCb. Some of the main beam characteristics from this optimized RF-gun are compiled in Table 1 with explanations given throughout this note. The geometric features of the RF-gun are compiled in Table 2 and described in a later section of this report.

Table 1
Optimized S-band RF-gun and beam parameters

Max.beam momentum, cp	2.91	MeV
Velocity, $\beta = v/c$	0.9851	
Avg./max. field in $\frac{1}{2}$-cell	23.9/29.9	MV/m
Avg./max. field in full-cell	45.0/67.6	MV/m
Cathode emission current	2.9	A
Cathode radius	3.0	mm
Charge/bunch	94	pCb
Peak current	707	A
Bunch length (rms)	52.8	fs
Norm.beam emittance, rms	3.8	mm mrad

2.3. RF-gun field

The choice of the electric accelerating field employed in each cell of the RF-gun greatly controls the efficacy of bunchcompression. In Fig. 6, we show the particle distribution in phase space at the RF-gun exit for different values of the accelerating fields in the half- and full-cell, respectively. The field ratio between half- and full-cell is kept constant to about 1:2 for this discussion.

In Fig. 6 we note that particles in the bunch head are virtually quasi-monoenergetic for electric fields of about 45 MV/m in the half-cell. This renders the beam unfit for bunch compression, yet exhibits a very desirable quasi-monochromatic

Table 2
Geometry of half (left) and full (right) cell for optimized RF-gun

Segment (units mm)	x	y	Segment (units mm)	x	y
Origin	0.00	0.00	Origin	0.00	5.20
Line to	0.00	41.90	Line to	4.35	5.20
Line to	5.00	41.90	arc,−90°, $r = 5.00$ mm to	9.35	10.20
arc,90°, $r = 24.64$ mm to	29.64	17.26	Line to	9.35	10.50
Line to	29.64	15.00	arc,−90°, $r = 2.50$ mm to	6.85	13.00
arc,90°, $r = 2.00$ mm to	27.64	13.00	Line to	4.46	13.00
Line to	26.50	13.00	arc,0°, $r = 2.00$ mm to	2.46	15.00
arc,90°, $r = 2.50$ mm to	24.00	10.50	Line to	2.46	17.26
Line to	24.00	10.20	arc,180°, $r = 24.64$ mm to	51.74	17.26
arc,90°, $r = 5.00$ mm to	29.00	5.20	Line to	51.74	15.00
Line to	32.10	5.20	arc,90°, $r = 2.00$ mm to	49.71	13.00
			Line to	47.35	13.00
			arc,−90°, $r = 2.50$ mm to	44.85	10.50
			Line to	44.85	10.20
			arc,−90°, $r = 5.00$ mm to	49.85	5.20
			Line to	58.00	5.20

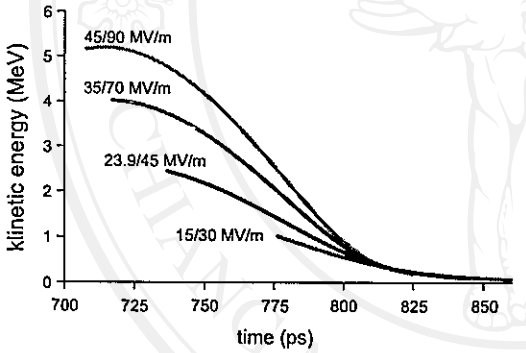

Fig. 6. Energy-time phase space distributions for different accelerating fields in the RF-gun. Parameters are averaged half/full-cell accelerating fields.

beam to drive, for example, a Free Electron Laser. In this high field case, particles pass through the half-cell in less than one half-RF-cycle and the integrated acceleration turns out to be about the same for particles emerging from the cathode during about the first 25 ps in the RF-cycle.

For lower fields, a monotonic correlation of particle energy with time appears as desired for bunch compression. In this situation, particles emerging at zero phase from the cathode will not quite reach the cavity exit before the field direction inverts and particles exiting the cathode at increasing RF-phases experience increasing negative acceleration before they reach the end of the half-cell. This becomes more true as the field is further reduced and is determined purely by the cavity dimensions, the RF-field amplitude and its temporal variation.

At this point, we need to get some guidance on the choice of the electric field strength for optimum bunch compression. With the knowledge of the beam line downstream of the RF-gun (for example Fig. 5), we may determine an ideally desired particle distribution at the gun exit.

2.4. Ideal phase space distribution

For a given beam transport line, an ideal electron phase space distribution at the RF-gun exit can be defined. The first particle to exit the RF-gun in each cycle at time $T_0 = 0$ is the reference particle, which also happens to be the particle with the highest momentum, will arrive at the experimental station at time T_{ref}. An electron with lower momentum travels to the experiment in a time ΔT and must therefore exit the RF-gun at a time δT compared to the reference particle such

that $\Delta T + \delta T = T_{ref}$ and in this case, both particles arrive at the experimental station at the same time. Calculating the ideal gun exit-times δT for all particle momenta, we obtain the ideally desired particle phase space distribution at the RF-gun exit as shown in Fig. 7 in comparison with an actual particle distribution.

For this particular simulation we used the beam transport line of Fig. 5 although another beam transport line could be used as well. The distribution within the bunch head of the ideal distribution has the same convex curvature as those we observe in Fig. 6. A proper choice of the electric field strength can therefore match the actual to the ideal distribution at least over a finite range of particle momenta. For too low-energy particles, both distributions diverge greatly because particles travel too slow to be able to catch up and, extremely, should have left the cathode when the accelerating field was still negative, which, of course, is nonphysical. The range of almost perfect match extends over about the first 10–15 ps of each bunch where most of the charge is concentrated. A similar, but much smaller dynamic effect occurs in the second, full-cell cavity and must therefore be included as a correction in the overall optimization procedure. For the RF-gun under discussion this optimization leads to a perfect match if the average accelerating field in the half-cell is 23.9 MeV and in the full-cell 45 MeV.

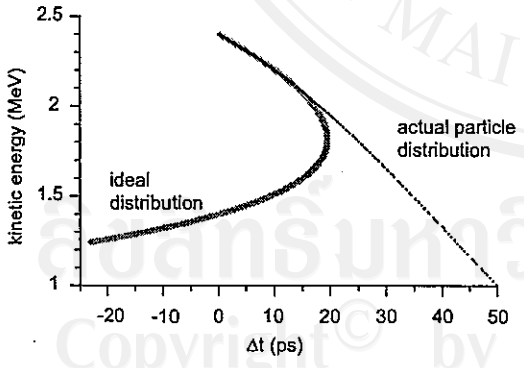

Fig. 7. Ideal and actual phase space distribution at the RF-gun exit.

3. RF-gun geometry

Internal geometric features of the RF-gun cavities determine greatly the final beam characteristics. In Fig. 8, the cross-section of both, the half-cell and the full-cell is shown together with the electric field profile.

The actual geometry of the optimized SURIYA RF-gun used for the simulations presented in this article is documented in Table 2 for both the half- and full-cell. The ratio in the full- to half-cell field can be chosen by practical considerations like RF-power availability and field break-down, while preserving optimum matching. Since the full-cell field affects the ideal particle distribution only little one might choose the highest practical field to minimize space charge effects. The electric field values along the cavity axis is shown in Fig. 9. The geometrical features can be separated into two groups; those which affect mainly RF-parameters and have little effect on beam parameters of interest and those which affect mostly the beam characteristics. Features further away from the axis (beam) like the wall defining the cavity diameter determine in particular the resonant frequency, which in our case should be 2856 MHz. The length of the effective cavity can be adjusted either by varying the dimension a or the iris length by varying dimensions c and e.

Close to ideal phase space distributions can be achieved if the accelerating field and length of the half-cell cavity is such that the reference particle can traverse its effective part within one half RF-period, the accelerating period.

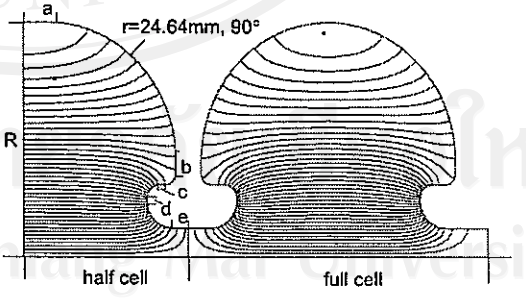

Fig. 8. Internal RF-gun geometry.

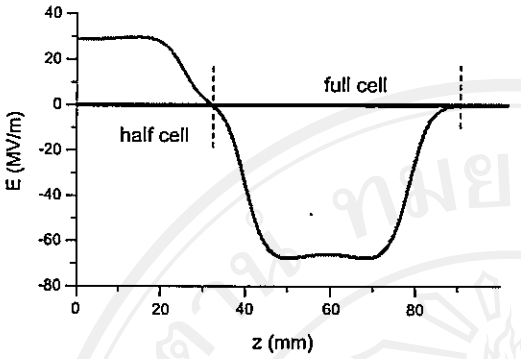

Fig. 9. Electric field profile along the cavity axis.

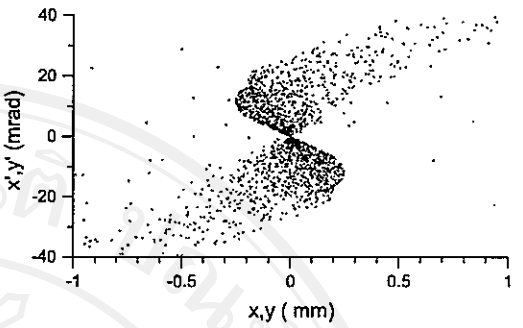

Fig. 10. Transverse phase space distribution at the exit of the SUNSHINE RF-gun.

As discussed earlier, internal features in the SUNSHINE RF-gun caused a significant beam convergence/divergence to seriously affect the achievable bunch length due to path length dispersion (Fig. 10). Specifically, a nose cone at the cathode plate introduced much of the focusing. In the new design this nose cone is eliminated and we use a flat cathode plate to minimize beam divergence. For the same reason the iris radii at the cell ends are increased sufficientiy to reduce the radial electric fields and it's effect on the beam divergence.

4. Transverse particle dynamics

Due to the natural divergence of the beam and under the forces of focusing elements, particles follow trajectories which are oscillatory about the ideal beam axis and therefore longer than on-axis trajectories leading to path length dispersion. The RF-gun used in the SUNSHINE facility creates a large beam convergence/divergence as shown in Fig. 10 which must be compensated with quadrupole focusing between RF-gun, α-magnet and experimental station. The slopes of particle trajectories being of the order of 10 mrad cause a significant spread of the pathlengths and thus limit the shortest bunch achievable to about $\sigma \approx 120$ fs [12].

In the optimized RF-gun design a flat cathode plate is used and the iris radii are increased to reduce the effect of radial RF-fields in their vicinity. Both changes result in a much reduced beam divergence as shown in Fig. 11 (left) compared to the case for the SUNSHINE RF-gun shown in Fig. 10. Ignoring space charge effects, a slightly convergent beam is desired (Fig. 11, left) which then becomes a parallel beam (Fig. 11, right) when repelling space charge forces are included.

Bunch lengthening depends quadratically on the beam divergence and is therefore greatly reduced for the optimized gun design with less than 1 mrad of divergence for the core of the beam. Unfortunately, the α-magnet introduces strong focusing which must be matched by some external quadrupole focusing causing an unavoidable finite amount of bunch lengthening. This has been included in the simulation of the particle distribution of Fig. 4 for the transport line in Fig. 5. The lattice parameters for this transport line are compiled in Table 3, where the parameters before and after the linac section are for an average beam momentum of $cp = 2.81$ MeV and $cp = 27.18$ MeV, respectively. Special care was taken in the design of this transport line to avoid any unnecessary focusing which could lead to path length dispersion. For the design of the beam line shown in Fig. 5 we were able to reduce these effects to a negligible level within the statistical fluctuations of bunch length due to the limited number of particles in the simulation.

To calculate the beam emittance, we take only the useful part of the beam with particle momenta

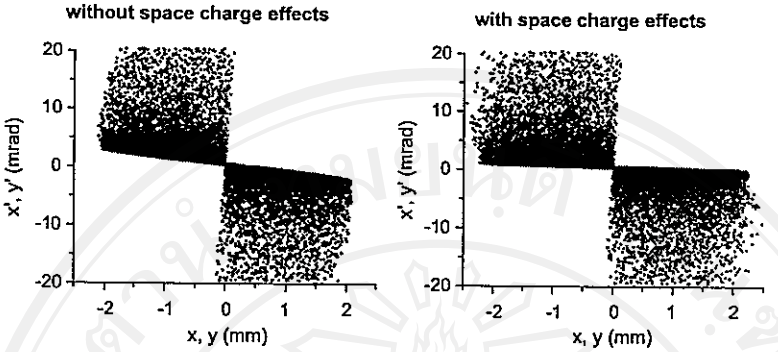

Fig. 11. Transverse phase space distribution of optimized RF-gun without (left) and with (right) space charge effects.

Table 3
Beam line lattice

#	Name	l (m)	Strength	Units
1	D1	0.283		m
2	QD1	0.073	18.750	$1/m^2$
3	D3	0.050		m
4	QF2	0.073	−34.440	$1/m^2$
5	D4	0.200		m
6	α-mag	n/a	399.00	G/cm
7	D5	0.189		m
8	QF3	0.073	43.300	$1/m^2$
9	D6	0.164		m
10	QD2	0.073	−39.717	$1/m^2$
11	D7	0.600		m
12	Linac	3.040	8.0	MeV/m
13	D8	0.853		m
14	QF4	0.073	19.664	$1/m^2$
15	D9	0.150		m
16	QD3	0.073	−21.623	$1/m^2$
17	D10	2.480		m

of $cp \geqslant 2.60$ MeV (Fig. 4). Using the definition $\varepsilon_{rms} = \sqrt{\langle x^2\rangle\langle x'^2\rangle - \langle xx'\rangle^2}$ the useful beam rms emittance is $\varepsilon_{rms} = 0.69$ mm mrad. For an average value of the kinetic energy of 2.35 MeV, $\beta\gamma = 5.51$ and the normalized beam emittance is $\varepsilon_{n,rms} = 3.8$ mm mrad. The normalized thermal cathode emittance (at $T \approx 1300$ K and a radius $r_{cath} = 3$ mm) of $\varepsilon_{n,therm} = 0.28$ mm mrad (page 102 of [17]) is still small, but has been included in the PARMELA simulations.

5. Effect of source size

The size of the cathode diameter can limit the shortest achievable bunch length. Particles emerging at the same time from different cathode radii will travel through regions containing different radial field components. As a consequence, the length of the trajectories for particles emerging from different parts of the cathode at the same time differ although the particle kinetic energies at the RF-gun exit are almost the same. Such particles cannot be distinguished energetically and therefore resist bunch compression, thus limiting the shortest achievable bunch length.

Reducing the cathode diameter, space charge effects become increasingly evident. An intense pencil beam, for example, does not remain thin during acceleration in the RF-gun if space charge forces are included. With decreasing cathode diameter and constant emission current, space charge forces from the bulk of the bunch accelerate particles in the head of the bunch to an undesirable degree. As a consequence, the bunch head follows a longer path in the α-magnet and the time distribution of the bunch head is tilted towards later times with respect to the rest of the bunch. Such a distribution cannot be compressed effectively. The choice of an emission current of 2.9 A from a 6 mm Ø cathode seems to be optimum while avoiding such problems.

5.1. Beam emittance and particle energy

The particle phase space distribution from RF-gun has the familiar "butterfly"-shape due to time-dependent focusing in the RF-field as evident from Fig. 11 [18]. If high bunch intensities are desired, a commensurate increase of the overall beam emittance must be accepted. Closer inspection of the particle phase space distribution in other dimensions reveals, however, a significant amount of correlation with particle energy. In Fig. 12 we show again the results of Fig. 11 (right) but this time including the finite effect of the thermal cathode emittance. Furthermore, we plot the transverse phase space distribution only for select energy bins of ±0.5% to show clearer the correlation. Since particles of different energies are also separated in time, this correlation provides an opportunity for emittance compensation. A cavity excited to produce radial fields (TM_{011}-mode cavity) seems suitable to eliminate, in first approximation, the emittance correlation and thereby significantly reduce the overall beam emittance.

The unnormalized slice-emittances for 95% of the beamlet intensities including (ignoring) thermal cathode emittance are $\varepsilon = 0.35(0.11)$, 0.42(0.21), and 0.45(0.34) mm mrad for the 2.44, 2.36 and 2.29 MeV beamlets, respectively, as shown in Fig. 12. A compensation of the apparent emittance increase due to the RF-field in the RF-gun seems very desirable and may be possible with the use of a TM_{011}-cavity. This possibility is presently under detailed study. In case of such a successful emittance compensation one could expect an overall normalized beam emittance of 2 mm mrad compared to 3.8 mm mrad without compensation.

6. Summary

Based on PARMELA simulations, we have systematically investigated the effect of geometric and electric features of an RF-gun with a thermionic cathode on electron beam parameters. Specifically, we were interested in the generation of femtosecond electron pulses. Beam characteristics are greatly influenced by RF-gun design and operational parameters. By proper design, the phase space distribution can be matched to an ideal distribution for the core of the beam, limited only by space charge forces. A compromise between cathode radius and space charge effects can be found which produces femtosecond electron bunches of significant intensity. These optimization methods have been applied to the design of an RF-gun specially optimized to produce femtosecond electron pulses. Such an electron source has been built at Chiang Mai University and will be being commissioned in 2003 [13]. Results from PARMELA simulations show, that for this S-band RF-gun, electron pulses with a bunch length of $\sigma = 52.8$ fs rms and a bunch charge of 94 pCb can be expected. This value does include effects of path length dispersion in the

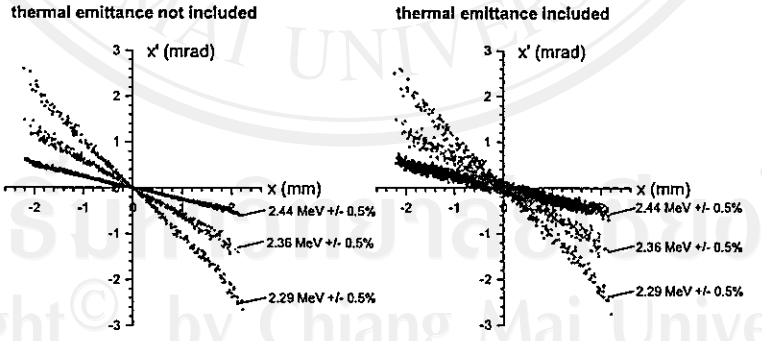

Fig. 12. Transverse phase space distribution for 1% energy slices of the full beam (Fig. 11). Thermal emittance ignored (left) and included (right). Parameter: kinetic particle energy.

beam transport line leading from the RF-gun to the experiment (Fig. 5).

A rms transverse beam emittance of $\varepsilon_{rms} = 0.69$ mm mrad at an average kinetic energy of $W = 2.35$ MeV or $\beta\gamma = 5.51$ can be achieved for the full intensity of 94 pCb per bunch. This corresponds to a normalized emittance of $\varepsilon_{n,rms} = 3.17$ mm mrad. The transverse phase space distribution is correlated with the particle energy or time opening a possibility for correction with the use of a TM_{011}-mode cavity.

Acknowledgements

We would like to acknowledge the financial support of the Thai Royal Golden Royal Jubilee Scholarship Program 3.F.CM/41/B.1 (Rimjaem); FAPESP, The State of Sao Paulo Research Foundation 97/7523-4 (Farias); the Thailand Research Fund (Thongbai, Vilaithong) and the US Department of Energy, BES DE-AC03-76SF00515 (Wiedemann).

References

[1] M. Bauer, C. Lei, K. Read, R. Tobey, J. Gland, M.M. Murnane, H.C. Kapteyn, Phys. Rev. Lett. 87 (2001) 025501-1.
[2] D.A. Reis, M.F. DeCamp, P.H. Bucksbaum, R. Clarke, E. Dufresne, M. Hertlein, R. Merlin, R. Falcone, H. Kapteyn, M.M. Murnane, J. Larsson, Th. Missalla, J.S. Wark, Phys. Rev. Lett. 86 (2001) 3072.
[3] H. Ihee, V.A. Lobastov, U.M. Gomez, B.M. Goodson, R. Srinivasan, C.Y. Ruan, A.H. Zewail, Science 291 (2001) 458.
[4] R. Bonifacio, C. Pellegrini, L.M. Narducci, Opt. Commun. 50 (6) (1985) 313.
[5] A.H. Chin, et al., Phys. Rev. Lett. 83 (1999) 336.
[6] H. Wiedemann (Ed.), Electron-Photon Interaction in Dense Media, Kluwer, Dortrecht, 2002.
[7] T. Nakazato, et al., Pattern Recogn. Lett. 63 (1989) 1245.
[8] E.B. Blum, U. Happek, A.J. Sievers, Nucl. Instr. and Meth. A 307 (1992) 568.
[9] P. Kung, D. Bocek, H.C. Lihn, H. Wiedemann, Phys. Rev. Lett. 73 (1994) 967.
[10] P.H. Kung, Generation and Characterization of Sub-Picosecond Electron Bunches, Ph.D. Thesis, Stanford University, 1996.
[11] H. Wiedemann, D. Bocek, M. Hernandez, C. Settakorn, J. Nucl. Mater. 248 (1997) 374.
[12] H. Lihn, P. Kung, C. Settakorn, H. Wiedemann, Phys. Rev. E 53 (1996) 6413.
[13] T. Vilaithong, N. Chirapatpimol, M.W. Rhodes, C. Settakorn, S. Rimjaem, J. Saisut, P. Wichaisirimongkol, H. Wiedemann, Proceedings of the Second Asian Particle Acceleration Conference APAC01, Beijing, China, 2001, p. 91.
[14] L.M. Young, J.H. Billen, Los Alamos National Laboratory, Tech Note LA-UR-96-1835, July 2002.
[15] H.A. Enge, Rev. Sci Instrum. 34 (1963) 385.
[16] M. Borland, A High-brightness Thermionic Microwave Electron Gun, Ph.D. Thesis, Stanford University, 1991.
[17] A.W. Chao, M. Tigner (Eds.), Handbook of Accelerator Physics and Engineering, World Scientific, Singapore, 2002.
[18] Kwang-Je Kim, Nucl. Instr. and Meth. A 275 (1989) 201.

PRODUCTION AND USE OF FEMTOSECOND ELECTRON BUNCHES

R. FARIAS†, S. RIMJAEM‡, C. SETTAKORN‡, T. VILAITHONG‡, H. WIEDEMANN§
†*Laboratorio National de Luz Sincrotron, LNLS, Campinas, Brazil*
‡*Fast Neutron Research Facility, FNRF, Physics Department, Chiang Mai University, Chiang Mai, Thailand*
§*Applied Physics Department and SSRL, Stanford University, Stanford, USA*

Abstract. Sub-picosecond electron pulses are desired in a variety of applications. Such bunches can, in principle, be obtained in large, high energy electron linear accelerator systems by repeatedly applying an energy slew and magnetic compression. Another process is the production of short electron pulses at low energies. An rf-gun with a thermionic cathode together with a bunch compressing α-magnet can serve as such a source. Although such sources have been constructed and are operating, a systematic analysis of capabilities and limits has not been performed yet. In this paper, we discuss the particular parameter choices to generate femto-second electron bunches from an rf-gun. The impact of geometric and electric specifications on the 6-dimensional phase space distribution of the electrons are investigated through numerical simulations with the particle-in-cell code PARMELA. Specifically, this includes effects and limitations due to space charge forces. While the production of femtosecond electron bunches is of primary concern, we also consider the preservation of such short bunches along a beam transport line.

1. Introduction

Experimental opportunities based on particle beams are often determined by the particles distribution in 6-dimensional phase space. Sub-picosecond electron pulses are desired, for example, for direct applications in materials research or in high energy physics for future linear colliders. Other applications are based on the transformation of short electron pulses into photon pulses by way of free electron lasers (FEL,SASE). Sub-picosecond x-ray pulses can be derived from these electron bunches by Compton scattering with an IR-laser beam or by interaction of electrons in dense media through the process of parametric x-rays, channeling- and transition radiation or other methods. So far, no existing x-ray source is able to produce sub-picosecond pulses. Synchrotron radiation sources are limited to pulse lengths of > 50 ps.

Sub-picosecond electron pulses can also fill the gap of useful radiation sources in the far infrared. Coherent far-infrared radiation with wavelength of 1 mm

H. Wiedemann (ed.), Electron-Photon Interaction in Dense Media, 321–329.

$\gtrsim \lambda \gtrsim 50\,\mu$m can be derived through any radiation process, be it transition radiation, Cherenkov radiation, synchrotron radiation etc. at a photon beam brightness which can be many orders of magnitude higher than black-body or synchrotron radiation. In Fig.1 the brightness of coherent transition radiation from $\sigma_\ell = 10$ and 30μm bunches are compared with 2000°K black-body radiation and synchrotron radiation from an 1 GeV, 500 mA storage ring. The very high efficiency of coherent fir-radiation from sub-picosecond electron bunches comes from the fact that the radiation intensity scales like the square of the number of electrons per bunch, $\sim N_e^2$, while synchrotron radiation is incoherent and therefore scales like $\sim N_e$. The high brightness of coherent fir-radiation together with sub-picosecond pulse duration opens new experimental possibilities including the use of room-temperature detectors.

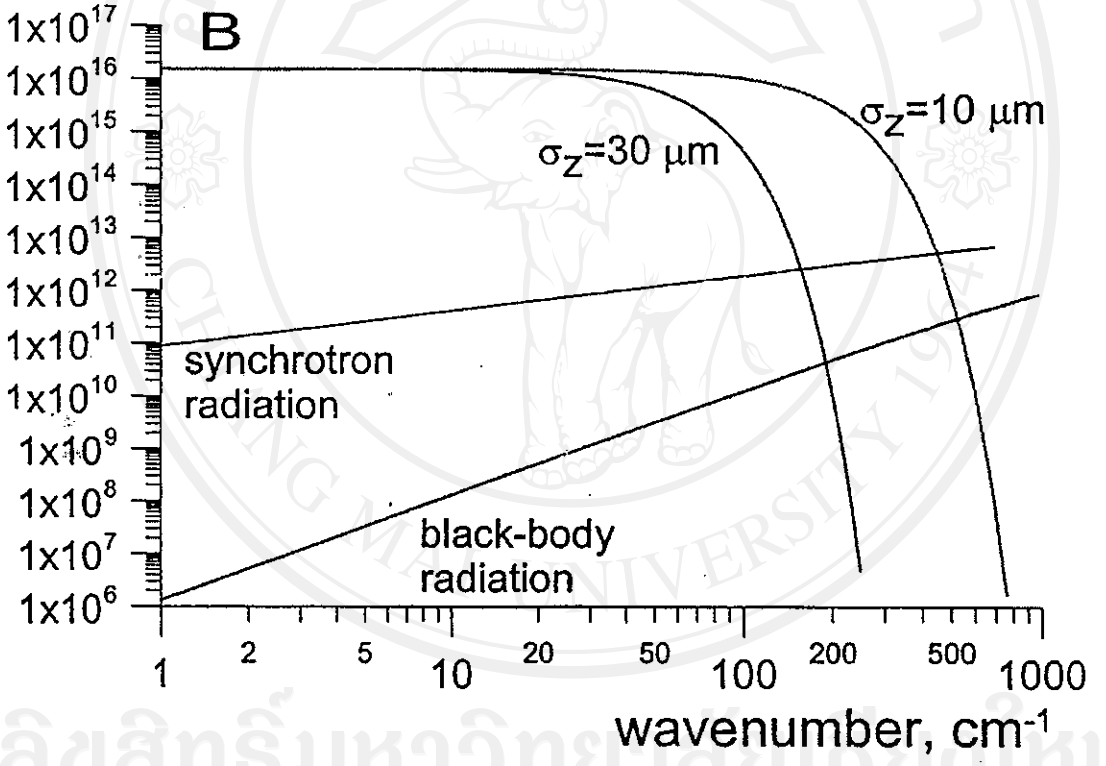

Figure 1. Photon beam brightness comparison between black-body radiation, synchrotron radiation and coherent radiation from sub-picosecond electron bunches. The brightness $\mathcal{B}$ is defined as the photon flux per unit source area (mm^2), angular acceptance ($mrad^2$) and band width.

The calculation of the brightness for coherent transition radiation is based on the actual electron beam performance of the SUNSHINE facility[1][2] with 1 μs long macro-pulses containing 3000 micro-bunches, each on average $\sigma_\ell = 30$ μm long, at a repetition rate of 10 Hz. The charge of each micro-bunch is 80 pC or $5 \cdot 10^8$ electrons per microbunch [3]. Of course, coherent radiation from short electron bunches occurs only at wavelength of the order of the bunch length and longer. The actual spectrum is determined by the form-factor which is the Fourier

transform of the particle distribution in the bunch and is for a Gaussian beam

$$f\ (\sigma_z, \lambda) = \exp\left(-\frac{4\pi^2\sigma_z^2}{\lambda^2}\right). \tag{1}$$

The expected coherent radiation power spectrum is determined by

$$P_{\mathrm{coh}}\ (\omega) = p(\omega)\left[N_{\mathrm{e}} + N_{\mathrm{e}}(N_{\mathrm{e}} - 1)\, f\ (\sigma_z, \lambda)\right], \tag{2}$$

where $p(\omega)$ is the power spectrum of a single electron for the radiation process under consideration and N_{e} the number of electrons per micro-bunch. For long wavelengths this form-factor is close to unity signifying a fully coherent photon beam scaling with the square of the number of electrons per microbunch. At wavelength comparable to and shorter than the bunch length, the form-factor vanishes exponentially leaving only the much weaker incoherent transition radiation. It is possible to create microbunches with $10^8 - 10^9$ electrons rendering the coherent radiation intensity higher by the same factor compared to incoherent radiation. This factor pushes the far-infrared photon brightness well beyond that available from other sources.

These possibilities stimulate efforts to promote the ability for sub-picosecond electron bunch generation. In this report we focus on such developments pursued at the SUNSHINE (Stanford University Short Intense Electron Source) facility, where we produce sub-picosecond electron bunches from a $1\frac{1}{2}$-cell rf-cavity (Fig. 2), operating at 3 GHz, with a thermionic cathode followed by an α-magnet for bunch compression (Fig. 3). The 6 mm $\emptyset$ thermionic dispenser cathode is mounted in the wall of the half cell and emits, for the cases discussed here, an electron current of 3.4 A corresponding to a modest current density of 12 A/cm^2.

Electrons emerging from the cathode travel first through the half and then the full rf-cell reaching a kinetic energy of 2 to 3 MeV. The use of a half-cell is necessary because the electrons from the cathode are very slow an cannot reach the end of a full cell even in a strongly accelerating field. The rf-gun is followed by some focusing elements and an α-magnet for bunch compression. After compression in the α-magnet the beam is further accelerated in a linear accelerator and transported to the experimental station.

1.1. NUMERICAL BEAM SIMULATIONS

The beam performance of the SUNSHINE rf-gun to produce sup-picosecond electron bunches was a fortunate side product since the gun was developed for another application. It is interesting therefore to investigate the bunch forming process in the rf-gun in more detail and optimize the rf-gun design for the generation of femtosecond electron bunches. Such a study has been performed based on numerical beam simulations with the program PARMELA [4]. Simulation results exhibit a special phase space distribution of the beam at the rf-gun exit as shown in Fig. 4 for one of many 3 GHz cycles, which makes efficient bunch compression possible. Considering the detailed particle dynamics in the half-cell we note that no electrons are emitted from the cathode during the decelerating half period of the electric

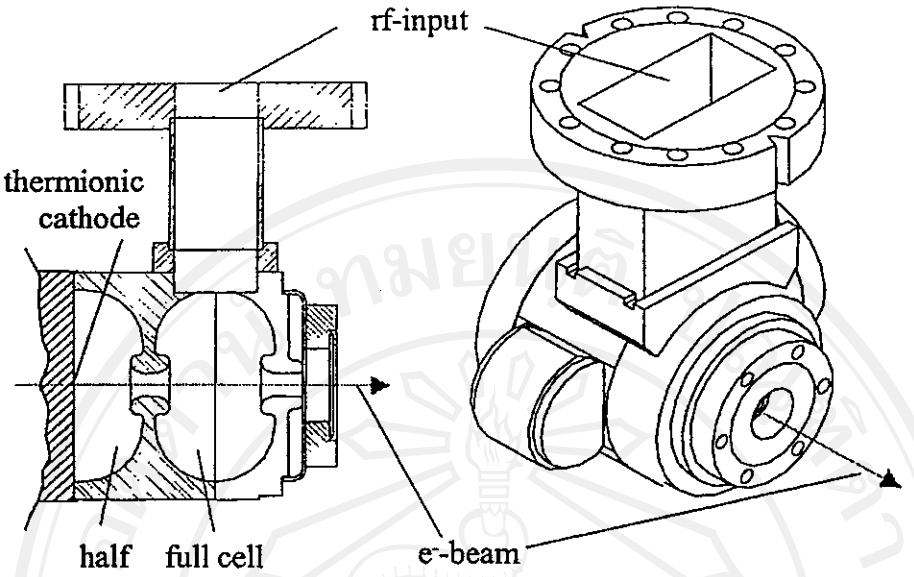

Figure 2. Cross section and 3D-view of a 1 $\frac{1}{2}$-cell rf-gun

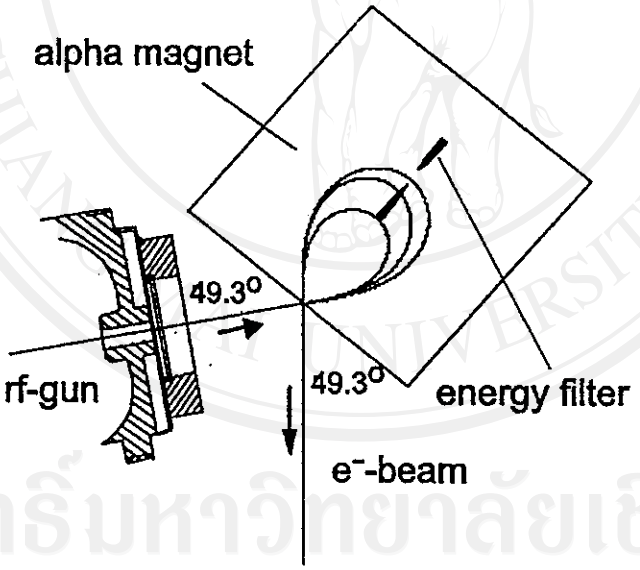

Figure 3. rf-gun with α-magnet for bunch compression

field. As soon as the field becomes accelerating, electrons emerge from the cathode forming a beam in the rf-gun.

The particle distribution shows electrons with the highest momenta exiting the rf-gun first followed by lower-momenta electrons. The path length in the α-magnet is momentum dependent such that electrons with higher momenta follow a longer path than lower-momenta electrons (Fig. 3). This feature leads to bunch

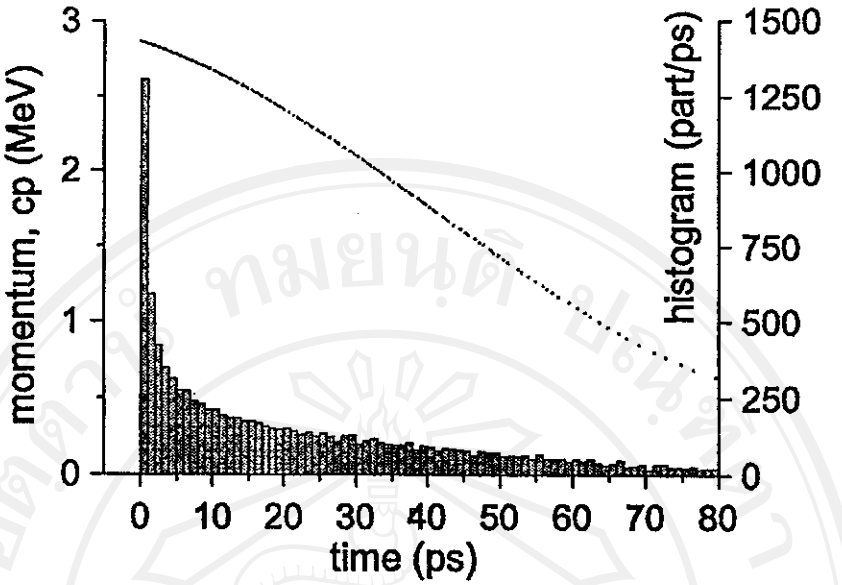

Figure 4. Particle distribution in phase-space at the rf-gun exit

compression. From the histogram in Fig. 4 we also note that most electrons are concentrated in the first 10-20 ps of the bunch. An electron source at the SUNSHINE based on these components is producing regularly micro-bunches of σ_ℓ =30 μm length at an intensity of about $4{\cdot}10^8$ electrons per micro-bunch.

A recently completed design study shows the possibility to reduce the micro-bunch length from about 30 μm at the SUNSHINE facility to 10 μm by optimizing the shape and operation of the rf-gun. PARMELA simulations indicate the feasibility of such short bunches at a bunch charge of 103 pC as will be discussed later in this article. A maximally compressed bunch resulting from PARMELA simulations is shown in Fig. 5 exhibiting two distinct features: a very narrow spike (σ_τ = 2.8 fs) and a broader base (σ_τ = 34 fs). The narrow spike is the result of constructive space-charge forces within the rf-gun, but is probably of no practical significance. Even a small transverse beam divergence can cause within only a short distance a spread in the bunch length of several fs. The bulk of the bunch has a width of σ =35 fs and contains $7 \cdot 10^8$ electrons or a charge of 103 pC. The wavy perturbation of the particle distribution is the result of a space charge induced instability which ultimately limits how short the electron bunches can be. In a practical application, one can adjust the momentum filter in the α-magnet such that only the desired part of the beam would pass (see Fig. 3).

The strength of the α-magnet, and thereby the compression is chosen such that the shortest bunch actually is reached not at the α-magnet exit but at the location of the experiment or of conversion into a photon beam. This procedure takes care of the velocity dispersion in the beam which transforms into a bunch-length variation between α-magnet and experiment. The particle distribution in Fig. 1 is therefore not reached at the α-magnet exit but rather at the location of

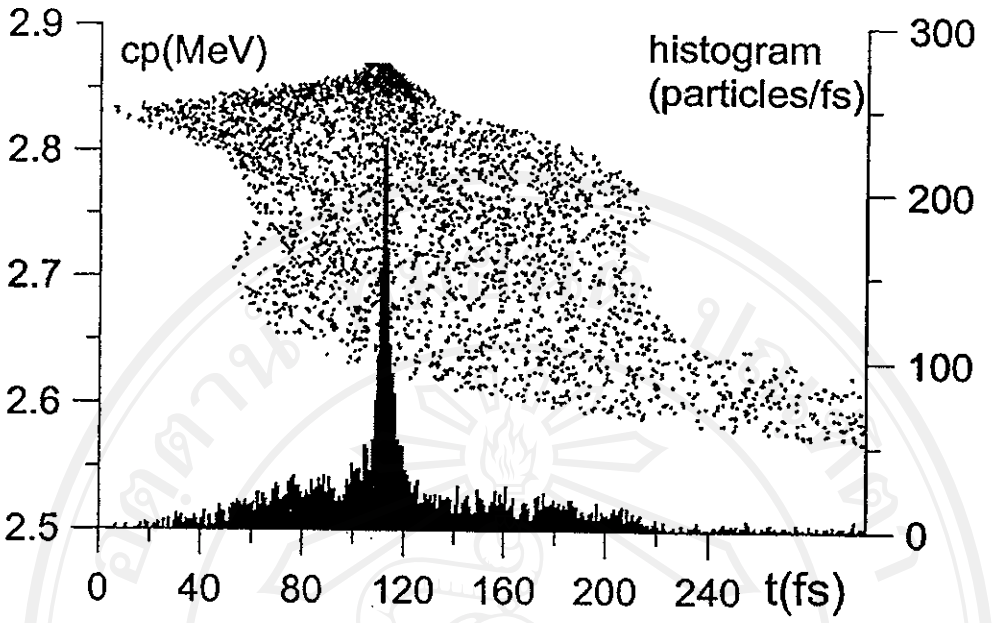

Figure 5. Particle distribution at the location where the bunch length is a minimum. The sharp spike and base have a width of 3 and 35 fs (rms) respectively. The charge contained in both parts is 35 and 105 pC.

the experiment.

2. Electron Beam Optimization

Optimization of the rf-gun design for the production of femtosecond electron bunches occurs in several areas. A detailed discussion of the optimization procedure can be found in [5]. As mentioned before, the choice of the rf-field in the half-cell greatly influences the ability to compress bunches. In Fig.6 electron phase-space distributions are shown for different accelerating fields in the half-cell. If the field is chosen to be too large, the phase-space distribution becomes quasi-monochromatic and unsuitable for bunch compression. This is the preferred mode of operation to drive a free electron laser.

For efficient bunch compression, the field must be reduced. The convex nature of the particle distribution in Fig. 4 during the first 10-15 ps matches well the dynamics of bunch compression in an α-magnet. By carefully selecting the accelerating fields in the half-cell of the rf-cavity, the degree of curvature in the phase space distribution can be shaped for virtually perfect compression. Only unavoidable space-charge forces limit the final bunch compression.

Further optimization procedures involve the geometry of the rf-gun. Here, we concentrate on geometric features close to the beam path which are responsible for radial field components. Such features must be adjusted to minimize the divergence of the beam at the rf-gun exit which becomes the cause of bunch spreading along the beam line. Specifically, we choose the radii of the irises between the cells

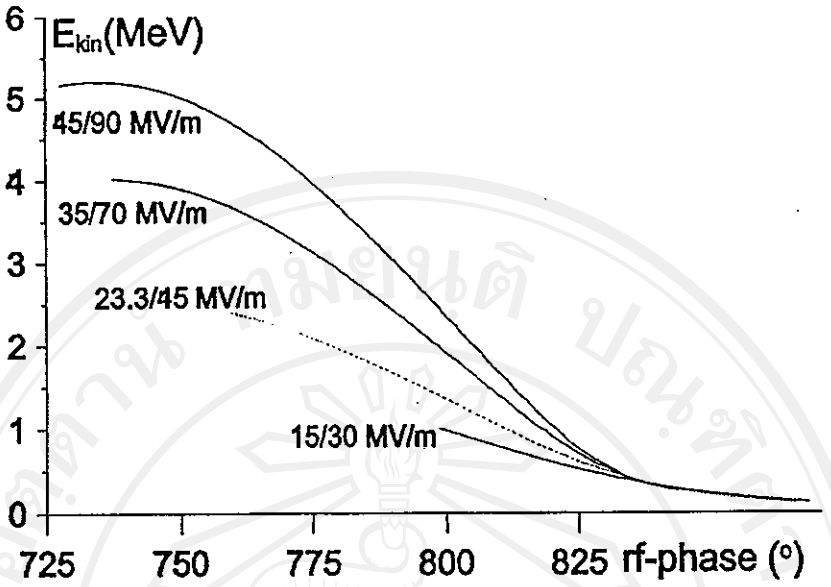

Figure 6. Phase-space distributions at the exit of the rf-gun for different electric fields in the half cell.

TABLE I. Optimized S-band Rf-gun and Beam Parameters

max. beam momentum, p	2.86	MeV/c
velocity, $\beta = v/c$	0.9845	
avg./max. axis-field in half cell	23.2 / 29.6	MV/m
avg./max. axis-field in full cell	45.0 / 67.6	MV/m
cathode emission current	3.4	A
cathode diameter	6.0	mm
peak/base bunch length, σ	3 / 34	fs
peak/base charge/bunch	34 / 103	pC
beam current, peak/base	4500 / 1190	A
beam emittance, slice/base	$\geq$ 0.046 / 0.63	mm mr

and at the rf-gun exit to minimize radial field components in the area of the electron beam. Geometric features of the rf-gun further away from the beam have little effect on the beam itself but influence mainly the rf-frequency and other microwave parameters. This optimization procedure leads to general rf-gun and beam parameters as compiled in Table 1.

The actual geometric shape of the inside contour in both cells is shown schematically in Fig. 7 and its geometric features are documented in Table 2, where all

TABLE II. Geometry for optimized S-band Rf-gun

segment	x	y	segment	x	y
origin	0.00	0.00	origin	0.00	5.20
straight to	0.00	41.90	straight to	4.35	5.20
straight to	5.00	41.90	arc -90°,r=5.00,	9.35	10.20
arc, 90°,r=24.64,	29.64	17.26	straight to	9.35	10.50
straight to	29.64	15.00	straight to	9.35	10.50
arc, 90°,r=2.00,	27.64	13.00	arc, -90°,r=2.50,	6.85	13.00
straight to	26.50	13.00	straight to	4.46	13.00
arc, -90°,r=2.50,	24.00	10.50	arc, 90°,r=2.00,	2.46	15.00
straight to	2.00	10.20	straight to	2.46	17.26
arc, -90°,r=5.00,	29.00	5.20	arc, 180°,r=26.64,	51.74	17.26
straight to	32.10	5.20	straight to	51.74	15.00
			arc, 90°,r=2.00,	49.74	13.00
			straight to	47.35	13.00
			arc, -90°,r=2.50,	44.85	10.50
			straight to	44.85	10.20
			arc, -90°,r=5.00,	49.85	5.20
			straight to	54.10	5.20

dimensions are in mm. . The shortest temporal width of the particle distribution or bunch length in Fig. 5 is limited by the 6 mm Ø cathode. Particles from different parts of the emitting cathode disk travel along more or less curved trajectories due to radial field components while gaining the same energy. Particles leaving the cathode at almost the same time travel along different paths resulting in a spread of the bunch length which cannot be compensated anymore because these particles have the same energy. Reduction of the cathode radius would reduce the path-length dispersion and thereby the resulting bunch lengths if it were not for space charge effects. For an emission current of 3.4 A the reduction in bunch length for cathode diameters less then 6 mm is compensated by space charge effects. In addition, the increase of charge density causes the appearance of an shock-wave instability preventing the shortening of the bunch [6]. Therefore, a compromise between cathode radius, electron beam current and bunch length must be made.

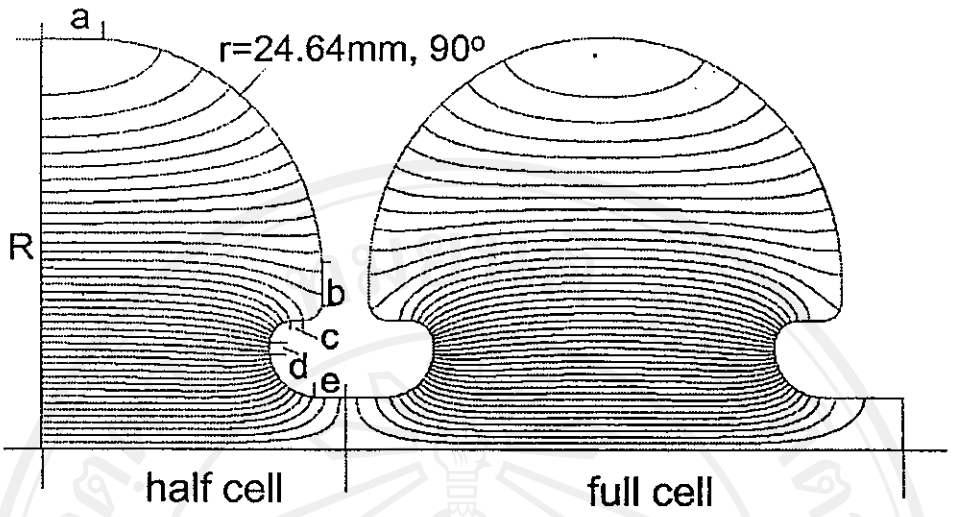

Figure 7. Rf-gun shape and field pattern

3. Summary

Sub-picosecond electron bunches provide the opportunity to perform experiments with sub-picosecond x-ray pulses as well as coherent far infrared radiation of very high brightness. Such photon beam characteristics presently cannot be obtained in any other way. We have described the optimization of an rf-gun to produce sub-picosecond electron bunches as short as $\sigma_\ell = 10\,\mu$m or $\sigma_\tau = 33$ fs. A prototype based on the design described has been machined and is under rf-evaluation. It is expected that the new rf-gun will be ready by the end of the year for beam testing. The shortest achievable bunch length is limited by space charge forces. Further improvements will be possible if these space charge forces can be compensated in some way. Beyond that the shock-wave instability and/or the unavoidable transverse divergence of the beam will put a more fundamental limit to the shortest bunches achievable. This limit, of course, assumes that a long bunch will be compressed to a short bunch limited only by the increasing charge density. An alternate way of generating short bunches, not considered here, is to provide coherent interaction with an electromagnetic wave like that of a free electron laser to break-up the long bunch into much shorter segments.

References

1. P. Kung, D. Bocek, H.C. Lihn, and H. Wiedemann, Phys. Rev. Lett. **73**, 967 (1994).
2. H. Wiedemann, D. Bocek, M. Hernandez, and C. Settakorn, J. Nucl. Mater. **248**, 374 (1997).
3. H.C. Lihn, D. Bocek, P. Kung, C. Settakorn, and H. Wiedemann, Phys. Rev. E **53**, 6413 (1996).
4. L.M. Young and J.H. Billen, Technical Report No. LA-UR-96-1835, Los Alamos National Laboratory (unpublished).
5. S. Rimjaem, R. Farias, C. Settakorn, T. Vilaithong, and H. Wiedemann, submitted to Phys.Rev. Spec.Topics-AB.
6. P. Kung, Ph.D. thesis, Stanford University, 1996.

BEAM CHARACTERIZATIONS AT FEMTOSECOND ELECTRON BEAM FACILITY

S. Rimjaem#, V. Jinamoon, N. Kangrang, K. Kusoljariyakul, J. Saisut, C. Thongbai, T. Vilaithong,
FNRF, Chiang Mai University, Chiang Mai, Thailand
M.W. Rhodes, P. Wichaisirimongkol, IST, Chiang Mai University, Chiang Mai, Thailand
H. Wiedemann, SLAC/SSRL, Menlo Park, California, USA

Abstract

The SURIYA project at the Fast Neutron Research Facility (FNRF) has been established and is being commissioning to generate femtosecond (fs) electron bunches. Theses short bunches are produced by a system consisting of an S-band thermionic cathode RF-gun, an alpha magnet (α-magnet) serving as a magnetic bunch compressor, and a SLAC-type linear accelerator (linac). The characteristics of its major components and the beam characterizations as well as the preliminary experimental results will be presented and discussed in this paper.

INTRODUCTION

The femtosecond electron facility was established and developed since 2000 at FNRF under SURIYA project [1] to study fs electron and photon pulses generation and applications. Femtosecond electron bunches generated from SURIYA set-up can be used for direct applications such as electron diffraction [2], or to produce either far-infrared (FIR) radiation or femtosecond X-ray pulses [3, 4]. The SURIYA project set-up is located at the basement of the FNRF building for radiation shielding reason. The basic components of SURIYA are a thermionic RF-gun, an α-magnet, a SLAC-type linear accelerator (linac), beam steering and focusing elements, beam diagnostic instruments, RF system, and control units. Figure 1 shows a schematic layout of SURIYA set-up and area.

Presently, commissioning and characterizations at SURIYA are underway. Preliminary beam characterizations reveal that up to 900 mA electron beams of 2.4 MeV can be produced from the RF-gun. Optimization for beam acceleration and beam guidance during post acceleration is currently in progress. The beam energy after acceleration is expected to be about 20-25 MeV. At experimental stations, FIR radiation will be produced in form of coherent transition radiation (TR) while fs X-ray pulses will be produced as Parametric X-ray (PXR). Electron bunch lengths will be measured by autocorrelation of the coherent TR via a FIR spectroscopy in a Michelson interferometer. More details regarding to the radiation productions are presented in reference [5].

GENERATION OF FEMTOSECOND ELECTRON BUNCHES

The SURIYA electron source and compression system, consists of a thermionic RF-gun and an α-magnet serving as a magnetic bunch compressor, of which the schematic layout is shown in Fig. 2. The RF-gun is 1-1/2 S-band standing wave cavities. It has a dispenser thermionic cathode with 6-mm diameter attached at the flat wall of the first half-cell. The cathode is heated by an AC power supply to produce an electron beam with thermal energy. Electrons are accelerated or decelerated depending on the phase of the supplied RF-oscillating fields. The RF-gun structure was designed to accelerate electrons such that the first electron gains maximum energy and get through the half-cell before the RF-fields become decelerating phase. The later ones feel less acceleration and therefore gain less energies. This results in energy-time distribution in which higher energy electrons locates at the head of the bunch followed by the lower energy electrons.

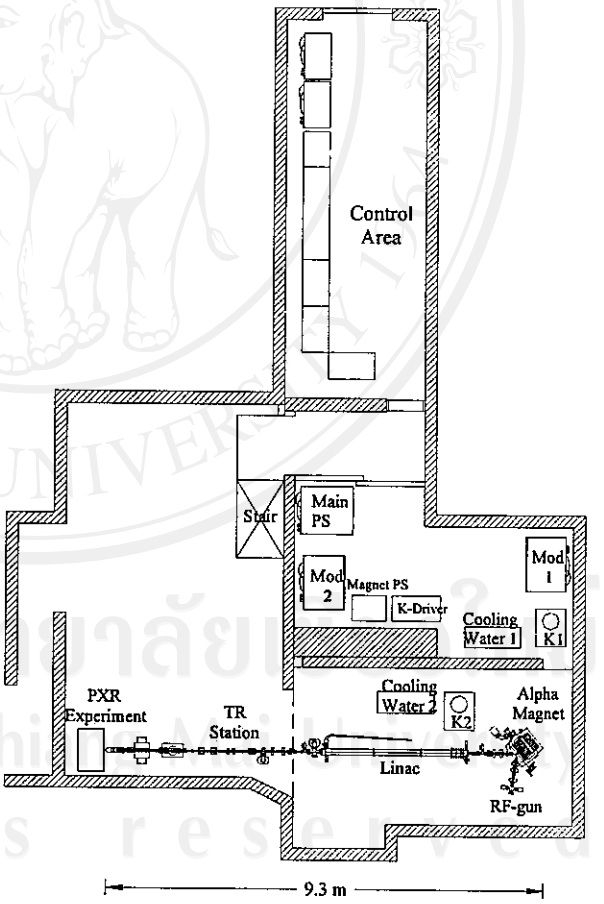

Figure 1: Schematic layout of SURIYA project at the Fast Neutron Research Facility (FNRF).

Bunch compression takes place in the α-magnet where higher energy electrons transverse longer closed path than

neung@fnrf.science.cmu.ac.th

0-7803-8859-3/05/$20.00

the lower ones. This method provides a simple yet effective electron bunch compression. Since the ultrashort bunch generation is the most concern for our applications, the RF-gun design and optimization of electron bunch compression have been studied to serve this purpose [6]. Inside a vacuum chamber of the α-magnet, two slits were installed as an energy filter. These energy slits is very helpful in the improvement of beam transmission through the linac without a big loss since we can select electrons with small energy spread. Results from measurements and testing of the RF-gun and α-magnet performance are listed in Table 1.

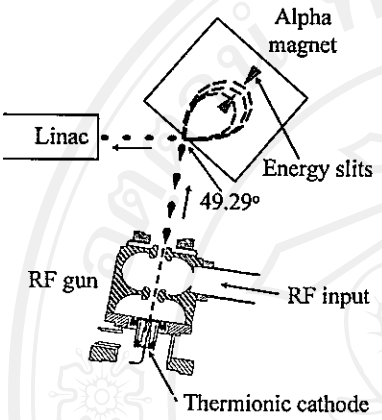

Figure 2: Schematic diagram of electron source and compression system.

Table 1: RF-gun and α-magnet Performance

Parameters	Value
f_{rf} of RF-gun from cold tests (GHz)	2.855
Q-factor of RF-gun from cold tests	12979
Average field ratio of HC:FC (bead-pull)	2.186
Max. beam energy from RF-gun (MeV)	2.4
α-magnet current (A)	265
α-magnet gradient (G/cm)	450

POST ACCELERATION AND BEAM TRANSPORT SYSTEM

Post Acceleration and RF System

To obtain higher beam energy and radiation collimation, the electron beam is further accelerated in a SLAC-type linac to reach about 20-25 MeV. The RF-gun and linac are powered by separately 5-MW klystrons with their associated modulators. At low RF-power, an RF oscillator tank generates 2.856 GHz signals. The RF signal is split into two parts by a 90° Hybrid directional coupler. One signal feeds the gun RF-amplifier and the other goes to the linac RF-amplifier via an adjustable phase shifter. The klystron can produce about 5 MW peak power with a maximum pulse width of 6 μs at 5-20 Hz repetition rates. The high power RF signals from klystron enter into waveguide section through a ceramic RF window and then are transmitted to the RF-gun and the linac through a rectangular waveguide system pressurized with SF6 to prevent electrical discharges. RF-power is measured using directional couplers installed at the waveguide section for the RF-gun and the linac. At the end of the waveguides, there are ceramics windows to separate the SF6 pressurized waveguides from the rest of the beam transport line.

Beam Transport System

To minimize the transverse dimension of electron beam, some beam focusing and steering elements are needed. There are several quadrupole and steering magnets placing along the beam transport line. The air-coil small dipoles are used as beam steering elements. The quadrupoles magnets are used mainly for beam focusing and can also be used for beam emittance measurement. The beam emittance measurement will be performed by quadrupole scan technique.

Combination of a 0.4 Tesla electromagnetic dipole magnet and a Faraday cup are placed at the end of the beam transport line serving as an energy spectrometer and a charge collector. The spectrometer had been designed and simulated by using the computer code RADIA [7]. The field distribution measurement was performed to verify the simulation results and to be used for beam energy measurement.

BEAM CHARACTERIZATIONS

In this section some of preliminary beam diagnostics at SURIYA, especially the beam characteristics from the RF-gun will be presented and discussed. At the initial stage of beam commissioning, we fed 3.5 MW RF-power pulses of 5-6 μs long to the RF-gun. Electron peak currents of about 1A with sharp rising edge were observed. There are evidences indicating significant the cathode self-heating from back-bombardment. To reduce the effect of the electron back-bombardment due to high average RF-power, we reduce the RF-pulses to 3-5 μs for the RF-gun operation. This results in lower beam currents, shorter current pulses with slower rise times. Measured signals of incident and reflected RF-power as well as the beam current signals are illustrated in Fig. 3. The pulse length of the incident RF signal is 4 μs (FWHM) with about 4 MW peak power.

Beam Current and Charge

Beam current of the electron macropulse is measured by a current monitor that installed at several locations along the beam transport line. The current monitor is a pulse transformer with a ferromagnetic core. The winding coil around the core works as the secondary while electron beam acts as a primary coil. The electron beam pulse signals from the RF-gun and after the α-magnet are shown in Fig. 3. The RF-gun produces electron macropulses with the pulse length of about 1.5 μs and 100 ms apart at a repetition rate of 10 Hz. Each macropulse

consists of about 4000 electron microbunches which are spaced at 350 ps. About half of the electrons can get through the α-magnet before guiding to further acceleration in the linac.

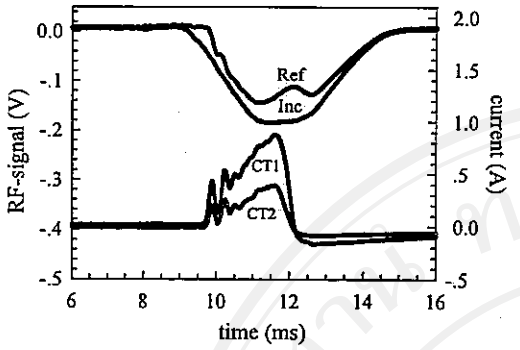

Figure 3: Measured waveforms for the incident RF-power (Inc) and the reflected RF-power (Ref) at the RF-gun, the current monitor after the gun exit (CT1), and after α-magnet (CT2).

The amount of electrons generated from the RF-gun depends significantly on the cathode temperature. The study of cathode temperature effects on electron density to determine the range of cathode temperature was performed and the results are presented in Fig. 4 for three different RF-power levels. The results reveal that the cathode has to be heated to reach temperature threshold where electrons can be emitted. At a temperature lower than the limit no electron will be emitted. On the contrary, heating to a temperature above the limit will lead in current saturation. The study results are also show that the higher RF-power employed to the RF-gun, the lower heating is needed to be supplied to the cathode. At the operation with the peak power of RF about 3.0-4.5 MW, the RF-gun can produce the electron beam with a pulse current of about 700-900 mA depending on the cathode temperature and the RF-power.

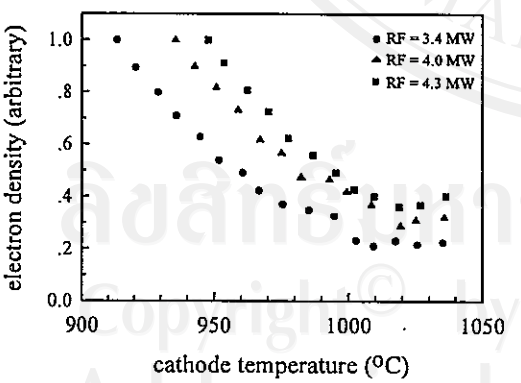

Figure 4: Electron density from the RF-gun as function of cathode temperature.

Beam Energy and Image

The electron beam energy is measured by using energy slits inside the α-magnet. Preliminary experimental results show that we can generate the electron beams with kinetic energy of about 2.4 MeV at the exit of the gun. Electron energy after acceleration by the linac measured via a small air-coil dipole magnet is about 15-17 MeV. Energy spectrometer is needed for more precise measurement results. We plan to measure the electron energy as a function of the linac temperature and phase of the RF-power.

The electron beam transfer line was commissioned to the end of the beam line in April 2005. The image of the first beam on the fluorescent screen at the end of the beamline is shown in Fig. 5.

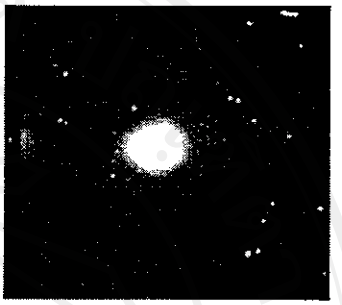

Figure 5: Image of the first beam at the end of the beamline.

SUMMARY

The description of the accelerator set-up at the SURIYA project is presented as well as the status of the commissioning and beam tests. Preliminary measurement results show that the electrons beam of energy about 2.4 MeV with current of 700-900 mA can be generated from the RF-gun while the cathode is heated at temperature of 900-1040°C. More beam diagnostics are needed to characterize the beam properties after the linac acceleration as well as at the experimental station which planed to be station for FIR radiation and PXR.

ACKNOWLEDGEMENTS

We would like to acknowledge the support of the Thailand Research Fund, the National Research Council of Thailand, the Thai Royal Golden Jubilee Scholarship Program, the US Department of Energy, the Hansen Experimental Physics laboratory (HEPL) of Stanford University, and the Physics Department of Chiang Mai University.

REFERENCES

[1] T. Vilaithong et al., "SURIYA, a Source of Femto-second Electron and Photon Pulses," Proc. APAC01, Beijing, China, September 2001, p 91.
[2] H. Ihee et al., Science 291 (2001) 458.
[3] C. Settakorn, Generation and Use of Coherent Transition Radiation from Short Electron Bunches, PhD Thesis, Stanford University, August 2001.
[4] A.V. Schchagin et al., Phys. Lett. A 148 (1990) 485.
[5] C. Thongbai et al., "Generation of Femtosecond Electron and Photon Pulses," in this proceeding.
[6] S. Rimjaem et al., NIM A 533 (2004) 258.
[7] www.esrf.fr/Accelerators/Groups/InsertionDevices/Software/Radia

0-7803-8859-3/05/$20.00 ©2005 IEEE

GENERATION OF FEMTOSECOND ELECTRON AND PHOTON PULSES

C. Thongbai *, V. Jinamoon, N. Kangrang, K. Kusoljariyakul, S. Rimjaem, J. Saisut, T. Vilaithong,
FNRF, Chiang Mai University, Chiangmai Thailand
M. W. Rhodes, P. Wichaisirimongkol, IST, Chiang Mai University, Chiangmai Thailand
H. Wiedemann, SLAC/SSRL, Menlo Park, California, USA

Abstract

Femtosecond (fs) electron and photon pulses become a tool of increasing importance to study dynamics in ultrafast processes. Such short electron pulses can be generated from a system consisting of a thermionic-cathode RF-gun and a magnetic bunch compressor. The fs electron pulses can be used directly or used as a source to produce equally short electromagnetic radiation pulses via certain kind of radiation production processes. At the Fast Neutron Research Facility (FNRF), Thailand, we are especially interested in production of radiation in Far-infrared and X-ray regime. In the far-infrared wavelengths, the radiation emitted from fs electron pulses is emitted coherently resulting high intensity radiation. In the X-ray regime, development of fs X-ray sources is crucial for application in ultrafast sciene.

INTRODUCTION

Ultrashort electron and photon pulses, especially in the femtosecond (fs) time scale, have become important tools for study dynamics in ultrafast processes. Accesibility of such short pulses made it possible to monitor dynamics of chemical reactions, biomolecular processes and in time-resolved experiments with fs resolving power [1, 2]. The SURIYA project, to develop fs electron and photon sources, has been established at the Fast Neutron Research Facility (FNRF), Thailand, and is now under commissioning. A schematic layout of SURIYA set-up is shown in Fig. 1 consisting of an RF-gun with a thermionic cathode, an α-magnet, a linear accelerator and beam transport components. The electron bunches of ultrashort duration, even at the low energy level without further acceleration, can be used directly for time-resolved analysis applications [1]. Furthermore, the electron bunches can be used to generate fs electro magnetic radiation pulses.

When accelerated, charged particles emit electro magnetic radiation and the radiation characteristics are different depending on radiation production mechanisms. Utilizing fs electron bunches to produce radiation with proper radiation production processes makes it possible to generate fs electromagnetic radiation pulses. Under SURIYA project, we are especially interested in production of far-infrared (FIR) radiation and X-ray. High intensity FIR radiation can be produced via coherent transition radiation (TR) while the X-ray can be produced by way of parametric x- radiation (PXR).

GENERATION OF FEMTOSECOND ELECTRON BUNCHES

As shown in Fig. 1, fs electron bunches are generated from a thermionic-cathode and an α-magnet serving as a magnetic bunch compressor. The specially-design RF-gun was studied and constructed [3]. It was designed such that the first particle in each S-band cycle will be exposed to maximum acceleration while any later particles will accumulate less energy. By this condition, higher energy particles will emerge first from the RF-gun followed by lower energy particles, consequently generating a well-defined correlation between energy and time. Electron bunches of 20-30 ps at 2-3 MeV from the RF-gun are then

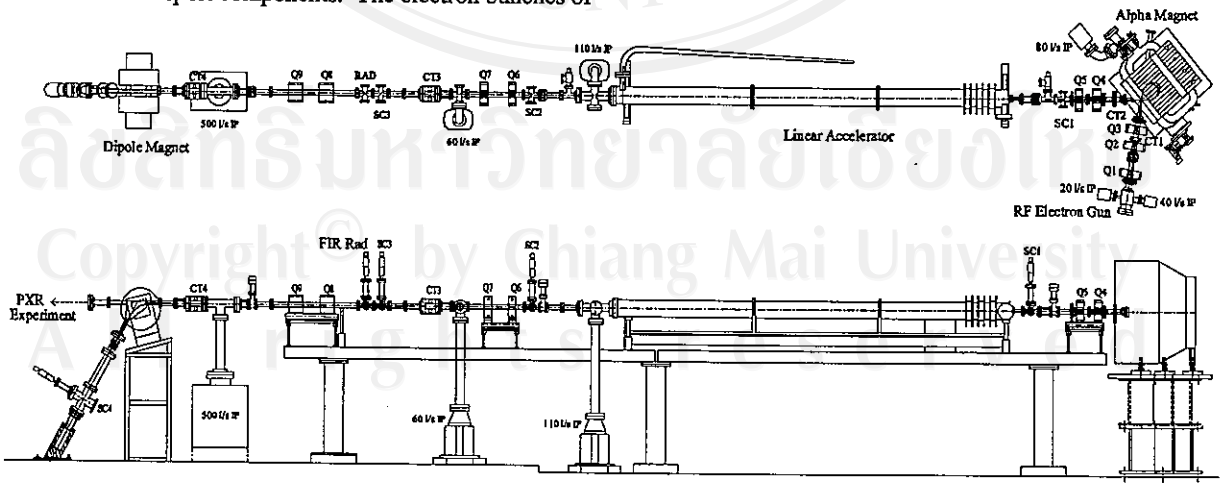

Figure 1: Schematic layout of the system at SURIYA of the Fast Neutron Research Facility.

*chlada@fnrf.science.cmu.ac.th

compressed in an α-magnet, where the particle path length increases with energy. This allows the lower energy particles, emitted later in each bunch, to catch up with the front for effective bunch compression. At the end of this process, the bunches are compressed to less than 1 ps. After acceleration in a single section S-band linear accelerator up to 20 MeV, the electrons are guided to experimental stations for radiation production.

GENERATION OF COHERENT FAR-INFRARED RADIATION

At a wavelength longer than the electron bunch length, the radiation is emitted coherently with the intensity scaling like N^2. With a typical number of electrons N around 10^8 to 10^9 electrons in each bunch, the radiation intensity will be enhanced by the large factor. Intense FIR radiation can therefore be derived from relativistic fs electron bunches [4]. The total radiated power from a mono-energetic bunch can be written as $P(\omega)=P_0(\omega)[N + N(N\text{-}1)f(\omega)]$, where $P_0(\omega)$ is the radiated power from a single electron. The *form factor*, $f(\omega)$, is the Fourier transform of the bunch distribution and the second term in the square bracket describes the coherent radiation. The factor $Nf(\omega)$ will enhance the incoherent radiation intensity emitted by any radiation production processe.

Transition Radiation (TR) is emitted when a charged particle passes through an interface between two media with different dielectric constants. A thin Al-foil is employed to serve as the TR radiator which represents the transition between vacuum and conductor. A 45°-tilted Al-foil can be used as the TR radiator to produce backward TR emitted at 90° with respect to the beam axis, as shown in Fig. 2.

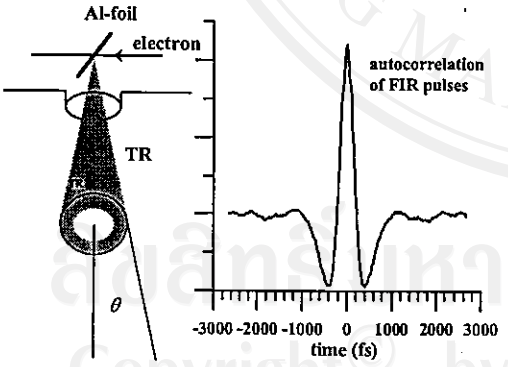

Figure 2: Coherent TR in the FIR from electron bunches.

The spectral-angular distribution of the emitted TR energy can be described by

$$\frac{d^2W}{d\omega\, d\Omega} = \frac{r_e m_e{}^2 \sin^2\theta}{\pi^2 c(1-\beta\sin^2\theta)^2}, \qquad (1)$$

where θ is the emission angle with respect to the electron beam axis. The intensity increases from zero in the forward direction to a broad peak at an angle $\theta = 1/\gamma$. Figure 2 also shows an autocorrelation of FIR pulses generated by approximately 120 fs of 26 MeV electron beams from a similar system [4]. The autocorrelation pattern, which can be used to determine the radiation and electron pulse lengths, was taken by using a Michelson interferometer. As described by Eq. 1, the single electron TR spectrum is uniform up to a very high frequency, however, for coherent TR this uniform spectrum folds with the form factor of the electron bunch. Figure 3 shows a measured coherent TR spectrum obtained from the same measurement shown in Fig. 2. The radiation is broadband and its detectable spectrum reaches from microwaves to 120 cm^{-1} wavenumber. The FIR radiation brightness of coherent TR estimated for 50 fs electron bunches, expected in the near future at FNRF [3], extending to over 300 cm^{-1} wavenumber greatly exceeds that of a black body as well as that of synchrotron radiation as shown in Fig. 4.

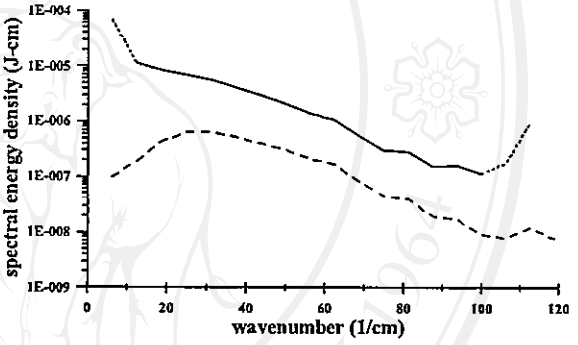

Figure 3: Coherent TR raw-spectrum (dashed-line) and the corrected spectrum (solid line) after applying the correction for beam splitter (BS) efficiency. The dotted-section occupy region near singularities of the BS efficiency.

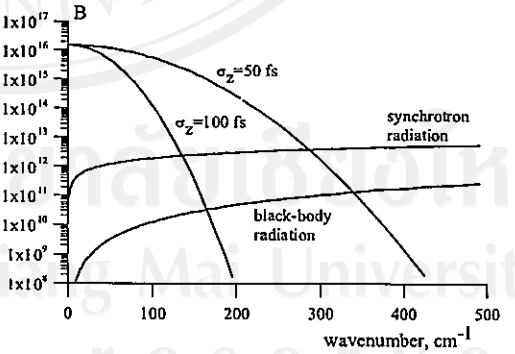

Figure 4: Radiation brightness B (Ph/s/mm^2/100%BW) of Coherent TR, blackbody and synchrotron radiation.

GENERATION OF X-RAY PULSES

Variety of radiation production mechanisms can be used to convert the fs electron bunches to x-ray pulses as for example bremsstrahlung, synchrotron-, channeling-,

0-7803-8859-3/05/$20.00 ©2005 IEEE

transition-, Smith-Purcell-, and parametric x-radiation as well as Compton scattering. Among those, the parametric x-radiation (PXR) is suitable for X-ray production using few tens MeV electron beams since the photon energy being produced is independent of the electron energy. The name PXR is accepted in most experimental publications for the X-ray emitted when a charged particle passing through a crystal [5-7]. There are two schemes for PXR generation from relativistic electrons: Laue and Bragg geometry. For Laue geometry, the radiation production is associated with crystallographic planes perpendicular to the slab surface while Bragg geometry deals with crystallographic planes oriented parallel to the slab surface. PXR is generated under the Bragg condition $d\sin\phi = n\lambda$ allowing us to select the photon energy by adjusting the crystal rotation angle ϕ. The PXR production geometry can be described using Fig. 5 with a (100) silicon wafer at observation angle θ.

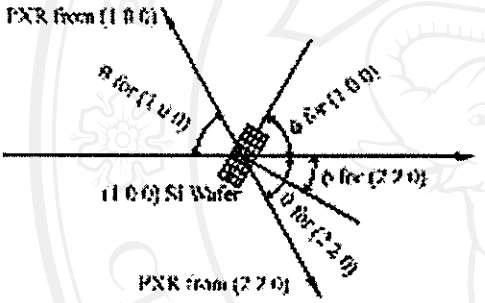

Figure 5: Geometry for PXR generation from a (100) silicon wafer.

The energy of PXR can be derived from [7]

$$E = \bar{h}\omega = \frac{c\bar{h}\left|\vec{g}\cdot\vec{V}\right|}{c - \sqrt{\varepsilon}\vec{V}\cdot\vec{\Omega}} = \frac{\bar{h}\left|\vec{V}\right|\left|\vec{g}\right|\sin\phi}{1-\beta\cos\theta} \qquad (2)$$

where E = PXR energy, ω = PXR angular frequency, c = velocity of light in vacuum, $\vec{g}$ = the reciprocal lattice vector, $\vec{V}$ = electron velocity, $\vec{\Omega}$ = direction of observation and ε = dielectric constant of the crystal which becomes unity for X-rays. The reciprocal lattice magnitude in Eq. 2 can be calculated from Miller indicies of the plane (hkl), and the lattice constant a as $|\vec{g}| = (2\pi/a)\sqrt{h^2+k^2+l^2}$. By comparing $|\vec{g}|$ for the (220)-plane and (100)-plane, one can see that the radiation associated with the (220)-plane results in a higher energy based on the higher magnitude of reciprocal lattice vector. Estimated PXR energy associated with the (220)-plane as a function of crystal rotation angle ϕ and observation angle θ by keeping $\theta = 2\phi$, as indicated by Bragg direction, are shown in Fig. 6.

Although, at very small observation angles, the PXR energy can be as high as 100 keV, the radiation is emitted in the direction close to the direction of the electron beams and makes it difficult to detect. PXR in 10-35 keV

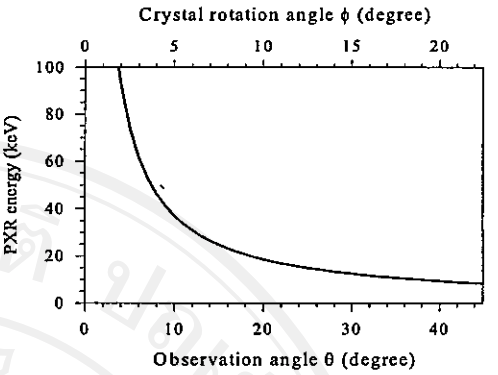

Figure 6: PXR energy from Si(220)-plane as function of observation angle θ and crystal rotation angle ϕ.

range can be obtained at more convenient observation angles of 10-45 degrees and thus become our main interest for X-ray pulses production.

CONCLUSION

With accessibility of fs electron bunches it is possible to generate high brightness, coherent, broadband FIR via TR and generate tunable x-rays via PXR. The radiation pulses come in very short bursts of fs duration reflecting the electron bunch length and time structure. The high intensity fs FIR pulses can be applied for FIR spectroscopy allowing direct determination of complex refractive index [8]. The availability of fs X-rays will open up opportunities for time-resolved studies of ultrafast processes.

ACKNOWLEDGEMENTS

We would like to acknowledge the support of the Thailand Research Fund (TGR4580055), the National Research Council of Thailand, the Thai Royal Golden Jubilee Scholarship Program, the US Department of Energy, the HEPL of Stanford University, the Department of Physics, Faculty of Science, and Chiang Mai University.

REFERENCES

[1] H. Ihee et. al., Science, **291** (2001) 458.
[2] M. Bauer et. al., Phys. Rev. Lett., **87** (2001) 025501-1.
[3] S. Rimjaem et. al., NIM A, **533** (2004) 258.
[4] C. Settakorn, *Generation and Use of Coherent Transition Radiation from Short Electron Bunches*, Ph.D. thesis, Stanford University, California (2001).
[5] V. G. Baryshevsky and I. D. Feranchuk, NIM A, **228** (1985) 490.
[6] M.L. Ter-Mikaelian, *High Energy Electromagnetic Process in Condensed Media.* Wiley-Interscience, New York, 1972.
[7] A. V. Shchagin et. al., Phys. Lett. A, **148** (1990) 485.
[8] K. Wood et. al., Chem. Phys. Lett., **393** (2004) 159.

GENERATION OF FEMTOSECOND ELECTRON PULSES

S. Rimjaem*, V. Jinamoon, K. Kusoljariyakul, J. Saisut, C. Thongbai, T. Vilaithong,
FNRF, Chiang Mai University, Chiang Mai, Thailand
M.W. Rhodes, P. Wichaisirimongkol, IST, Chiang Mai University, Chiang Mai, Thailand
S. Chumphongphan, School of Science, Mae Fah Luang University, Chiang Rai, Thailand
H. Wiedemann, SLAC/SSRL, Menlo Park, California, USA

Abstract

At the Fast Neutron Research Facility (FNRF), Chiang Mai University (Thailand), the SURIYA project has been established aiming to produce femtosecond electron pulses utilizing a combination of an S-band thermionic rf-gun and a magnetic bunch compressor (α-magnet). A specially designed rf-gun has been constructed to obtain optimum beam characteristics for the best bunch compression. Simulation results show that bunch lengths as short as about 50 fs rms can be expected at the experimental station. The electron bunch lengths will be determined using autocorrelation of coherent transition radiation (TR) through a Michelson interferometer. The paper discusses beam dynamics studies, design, fabrication and cold tests of the rf-gun as well as presents the project current status and forth-coming experiments.

INTRODUCTION

Femtosecond electron and photon pulses have become interesting tools for basic and applied applications, especially in time-resolved experiments [1,2,3]. Such short electron pulses can be used to generate intense coherent far-infrared (FIR) radiation, ultrashort X-ray pulses, and free electron laser (FEL). Although, photocathode rf-gun is a promising source to generate a high brightness ultra short electron pulses [4], it involves a complex laser injector and requires high financial cost. On the contrary, a thermionic cathode rf-gun with suitable compression system can play similar role to produce intense electron beam with pulses duration in order of femtosecond [5].

At SURIYA, femtosecond electron bunches will be produced from a combination of an S-band rf-gun with thermionic cathode and a magnetic bunch compressor in the form of an α-magnet [6]. The schematic layout of SURIYA beamline is presented in Fig. 1.

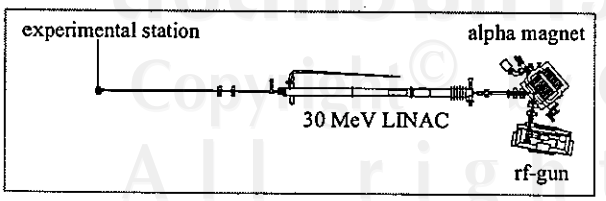

Figure 1: Schematic layout of SURIYA set up at FNRF.

The rf-gun generates 2-3 MeV electron beams, which are then traveling through the α-magnet for bunch compression. A 30 MeV linac is used to achieve higher energy as well as more confine beams. At experimental stations, coherent FIR radiation will be generated as coherent TR either for beam diagnostics or other experimental uses.

RF-GUN AND RF SIMULATIONS

Fig. 2 is illustrated the SURIYA rf-gun cross section and 3D-view showing the thermionic cathode attached at the end wall of the half-cell (HC) and electron beam exits out at the end of the full-cell (FC). The field in the two cells is coupled through an external coupling cavity.

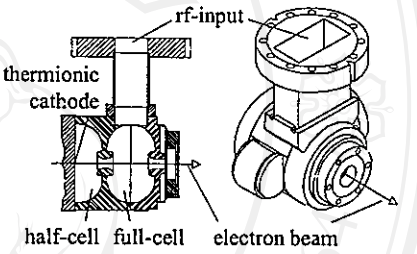

Figure 2: Rf-gun cross-section and 3D-view.

Numerical simulations for rf characteristics of the SURIYA rf-gun were performed using the EM field solver code SUPERFISH [7]. Based on 2D-simulation, SUPERFISH cannot be used to investigate 3D-shape include coupling cavity, rf-input and vacuum pumping ports. This leads to a deviation of the simulated results from the measured values. SUPERFISH results, however, give fair ideas regarding to the rf-gun electrical properties as well as the helpful scaling law concerning the rf-gun dimension and its resonant frequency (f_{rf}). During fabrication processes, modifications of the rf-gun dimension based on SUPERFISH scaling law were performed together with the rf-measurements.

BEAM DYNAMICS STUDY

A particle-in-cell computer code PARMELA was used to simulate and investigate particle dynamics through the EM fields inside the rf-cavities [8]. In the studies the 6-mm diameter thermionic cathode is set to emit a 2.9 A uniform distribution electron beam which is represented by 100,000 macroparticles per 2856 MHz rf-period with space-charge effects.

Longitudinal Particle Dynamics

Due to a sinusoidal time-varying field inside the cavities a very concentration of particles are accumulated

*neung@fnrfscience.cmu.ac.th

in the head (defining as the field becomes acceleration) of the bunch leading to a small correlated particle distribution between energy and time as shown in Fig. 3. Ten percent of high-energy particles concentrate at the head of the bunch appears in the length of some 10-20 ps.

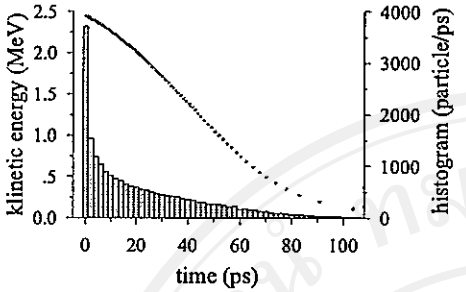

Figure 3: particle distribution in energy-time phase space for a single S-band electron bunch at the rf-gun exit.

The concave shape of the particle distribution at the rf-gun exit in Fig. 3 matches well to bunch compression in the α-magnet. It will rotate clockwise as the beam travels through the α-magnet with α loop paths of the length (S) depending on the particle momentum (cp) and the magnetic gradient (g) as $S \approx [cp/g]^{1/2}$. Thus, lower momentum particles follow shorter path than the higher one, leading to simply magnetic bunch compression. The value of the α-magnet field gradient is chosen to compensate velocity dispersion so that the shortest bunches are generated at the desired experimental station.

A computer code Bcompress is used to simulate particles dynamics from the gun exit to the experimental station. Locations of the experimental station where the shortest bunch length can be achieved as well as other parameters can be determined using the code. Among those, the choice of the electric accelerating field employed in each cell of the rf-gun highly affects the bunch compression. The simulation results suggested that the field ratio between HC and FC should be 1:2 for optimum bunch compression [9]. The temporal particle distribution after compression and acceleration with respect to the initial momentum at the rf-gun exit is presented in Fig. 4. The expected bunch length, including transverse path length dispersion, at an optimum experimental location is 53 fs rms with a total charge of 94 pCb.

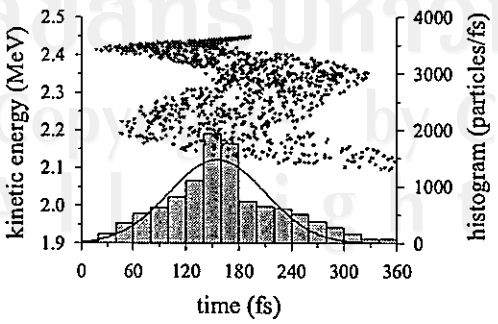

Figure 4: Particle distribution in energy-time phase space after bunch compression and transport to the experimental station.

Transverse Particle Dynamics

Since bunch lengthening depends quadratically on beam divergence, reducing the beam divergence facilitates ultrashort bunch generation. For this reason, the SURIYA rf-gun was therefore designed with a flat cathode plate and optimised the iris radii to reduce the radial rf-field effects. PARMELA calculation including the finite effect of the thermal cathode emittance was performed to simulate the transverse beam dynamics. The simulation results reveal that a normalized emittance of 3.8 mm-mrad can be achieved at the rf-gun exit [9]. Some of the beam parameters from PARMELA and Bcompress simulations are listed in Table 1.

Table 1: Some parameters for the optimised rf-gun.

Parameters	**Value**
Max. beam momentum, cp (MeV)	2.91
Avg./max. field in half-cell (MV/m)	23.9/29.9
Avg./max. field in full-cell (MV/m)	45.5/67.6
Cathode emission current (A)	2.9
Charge/bunch (pCb)	94
Peak current (A)	707
Bunch length, rms (fs)	52.8
$\varepsilon_{n,rms}$ at rf-gun exit (mm-mrad)	3.8

FABRICATION AND COLD TESTS

The HC and the FC of the rf-gun have been fabricated precisely, based on the SUPERFISH results, out of OFE copper cylindrical blocks, at the Thai-German Institute (Thailand). The cavities were first machined to resonate at a slightly different frequency from the target frequency (2856 MHz) to leave some rooms for fine modification. Preliminary cold tests of the rf-gun cavities before brazing have been preformed using Network Analyser at the Stanford Synchrotron Research Laboratory (SSRL/ SLAC), USA, and at the National Synchrotron Research Centre (NSRC), Thailand. Cold test results of the rf-cavities ready for brazing show that the f_{rf} of the rf-gun is very close to 2856 MHz at the operating temperature of 45°. The rf-gun was then brazed at the National Synchrotron Radiation Centre (SSRC), Taiwan, in an O_2-free high temperature furnace.

The rf-cold tests of the rf-gun were performed again after brazing at SSRL to measure the f_{rf} of individual rf-cells and determine the coupling between the two cells by adjusting the tuning rod of the coupling cavity while measuring longitudinal field profile. The measurement is done by Bead-Pull technique, which is performed by introducing a 2.36 mm diameter dielectric sphere bead at each position in the rf-gun. This results in a resonant frequency shift that reflects directly the longitudinal electric field magnitude at that location. Fig. 5 illustrates the consistency between normalized axial longitudinal

fields from SUPERFISH and the bead-pull measurement. The ratio of the maximum field amplitude in the FC to the HC from SUPERFISH calculation and Bead-Pull measurement is 2.186 and 2.067, respectively.

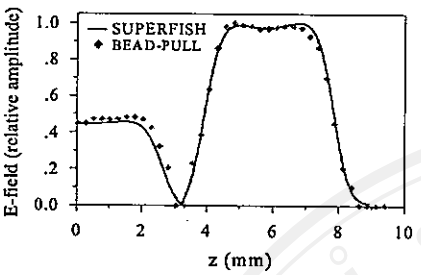

Figure 5: Longitudinal electric field distribution on axial axis from SUPERFISH and Bead-Pull measurement.

The coupled-cell resonant frequency and Q-factor were measured at the Rajamangala Institute of Technology (RIT), Thailand. Table 2 shows a comparison of the predicted rf-parameters obtained from SUPERFISH to those measured values in the rf-cold tests.

Table 2: Rf-parameters of the rf-gun calculated using SUPERFISH comparing to the cold test results.

Parameter		SUPERFISH	Cold Tests
f_{rf}	HC/FC	2881/2862	2855/2858
	Coupled-cell	2862	2855
Q factor	HC/ FC	15334/12980	-
	Coupled-cell	13037	12979

PRESENT STATUS OF SURIYA

The optimised rf-gun, the α-magnet and the 30 MeV SLAC type linac including 5 MW S-band klystrons for the rf-gun and the linac as well as the beam transport line have been installed and the system is now being commissioned The picture of SURIYA system is illustrated in Fig. 6.

Figure 6: Beamline set up at SURIYA project.

At an experimental station, coherent TR radiated at wavelength longer than the bunch length will be generated by introducing the Al-foil at 45° with respect to the electron path. The backward TR emitted at 90° can be used for bunch length measurements or FIR spectroscopy. For the electron bunch as short as we expected, the bunch length measurement by autocorrelation of coherent TR should be done in vacuum to avoid pulse spacing in the ambient air [10]. An in-vacuum Michelson interferometer as shown in Fig. 7 is ready to be installed for the measurement.

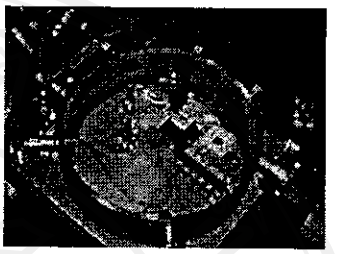

Figure 7: In-vacuum Michelson interferometer set up.

ACKNOWLEDGEMENTS

Authors are grateful to M. Nalls at SSRL for cathode installation and testing. We thank SSRL, NSRC and RIT for the use of Vector network Analyzer as well as SSRC for brazing process. We would like to acknowledge the support of the Thailand Research Fund, the National Research Council of Thailand, the Thai Royal Golden Jubilee Scholarship Program, the US Department of Energy, the Hansen Experimental Physics laboratory (HEPL) of Stanford University, the Faculty of Science, and the Graduated School of Chiang Mai University.

REFERENCES

[1] H. Ihee et. al., "Direct Imaging of Transient Molecular Structures with Ultra Fast Diffraction," Science, **291**(2001)458.

[2] M. Bauer et. al., "Direct Observation of Surface Chemistry Using Ultra Fast Soft-X-Ray Pulses," PRL **87**(2001)025501-1.

[3] D.A. Reis et al., "Probing Impulsive Strain Propagation with X-Ray Pulses," PRL 86(2001)3072.

[4] R. Sheffield et. al., "High-Brightness Electron Injectors: A Review," Proc. 1989 Part. Accel. Conf., IEEE Catalog No. 89CH2669-0(1989)1089.

[5] P. Kung et. al., "Generation and Measurement of 50-fs (rms) Electron Pulses," PRL, **73**(1994)967.

[6] T. Vilaithong et. al., "SURIYA, a Source of Femto-second Electron and Photon Pulses," Proc. APAC01, Beijing, China, September 2001, p 91.

[7] L.M. Young, "POISSON/SUPERFISH," LANL Technical Note LA-UR-96-1834, 1999.

[8] L.M. Young, "PARMELA," LANL Technical Note LA-UR-96-1835, July 2002.

[9] S. Rimjaem et. al., "Femto-second Electron Bunches from an Rf-gun," accepted for publish in NIMA.

[10] C. Settakorn, "Generation and Use of Coherent Transition Radiation from Short Electron Bunches," PhD Thesis, Stanford University, August 2001.

GENERATION OF FEMTO-SECOND ELECTRON BUNCHES AND FIR RADIATION

S. Rimjaem[*], *N. Chirapatpimol, M.W. Rhodes, J. Saisut, C. Settakorn, P. Wichaisirimongkol, and T. Vilaithong*

Fast Neutron Research Facility, Department of Physics, Faculty of Science, Chiang Mai University, 50200 Thailand

H. Wiedemann

Applied Physics Department, Stanford University, USA

Abstract

This research aims to produce electron bunches which are shorter than 100 fs. These short bunches can generate intense coherent FIR radiation in the wavelength range of 10 μm to 1000 μm. The FIR radiation which is created from these short electron bunches have higher intensities than black body radiation and synchrotron radiation. Femto-second electron bunches can be produced by a combination of a S-band rf-gun with a thermionic cathode and an α-magnet serving as the bunch compressor. The bunch compression of electrons can be simulated by the particle-in-cell code PARMELA. The optimum geometry and beam characterizations as a function of the rf-parameters of the rf-gun have been studied. The simulation results show that an electron bunch length as short as few fs can be expected. Coherent FIR radiation will be generated at the experimental station as the transition radiation, which is the radiation, emitted when electrons pass through an interface between an Al-foil and vacuum. To achieve higher intensity of FIR radiation the electron bunches will be accelerated to reach kinetic energies of about 20-30 MeV.

1 INTRODUCTION

The far infrared (FIR) radiation can be used for basic and applied research in many fields e.g. material science, phonon physics, surface physics, metrology standard, studies of high temperature material, dynamics and structure of polymer and large biomolecule. However, this FIR radiation regime is not covered by any source except blackbody radiation, synchrotron radiation, and FEL's. Thus, it is interesting to develop the new source to cover this spectrum range.

According to the fact that at wavelength much longer than the bunch length, radiation field add up coherently and the shorter bunch length provides the broader spectrum. The coherent radiation from a bunch containing N electrons proportional to the number of electrons square and typically the number of electrons up to 10^8 to 10^9 provides very high intensity of coherent radiation. Therefore, to generate the coherent FIR radiation of wavelength equal or longer than 10 μm, the bunch length in order of femto-second is required.

The SURIYA facility, which is under way at the Fast Neutron Research Facility (FNRF), Chiang Mai University, aims to generate femto-second electron pulses which have the bunch length shorter than 100 fs. As the result of this short bunch, it can be used to produce coherent, polarized FIR radiation in the wavelength range of about 10-1000 μm with the intensity much higher than the conventional sources. The source under construction at the SURIYA facility is a novel development from the SUNSHINE facility at Stanford University which electron bunches as short as 100 fs (rms) with the microbunch intensities of the order of 100 pC can be produced [1-4].

2 GENERATION OF FEMTO-SECOND ELECTRON BUNCHES

Femto-second electron bunches can be generated by the combination of an rf-gun with thermionic cathode as the electron source and a magnetic bunch compressor in the form of α-magnet. Following the α-magnet is a linear accelerator, which accelerates electron beam to achieve higher energy as the result of more confine of electron beam. At the experimental station of SURIYA facility coherent FIR radiation will be produced first as the transition radiation. A schematic outline of the proposed SURIYA facility planed at the FNRF is shown in Fig.1.

2.1 Electron Source

The electron source consists mainly of a 1-1/2 S-band rf-cavity with a side coupling cavity, which are fed by a 2856 MHz rf-input from klystron. The thermionic cathode is attached to one wall of the first half-cell, exposing emerging electrons to a high accelerating rf-

[*] Proceedings of the International Workshop on Particle Beam & Plasma Interaction on Materials, Chiang Mai, Thailand, 2002

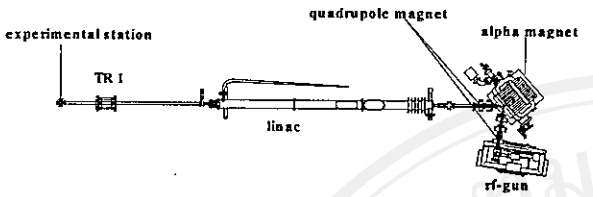

Figure 1: Layout of the proposed FIR radiation source (SURIYA) at the FNRF, Chiang Mai University.

field. Electrons emerge from the cathode travel pass through the first half-cell and then the full-cell, which the field in the half-cell is about one half of the full-cell. Theelectron beam reaches a kinetic energy of about 2-3 MeV for typical accelerating fields. In this paper the discussion will be concentrate on the numerical simulation design including of specific feature to optimize the ability to produce femto-second electron bunches, the fabrication, and the rf-measurement of the rf-gun. The cross section and 3D-view of the rf-gun is shown in Fig.2.

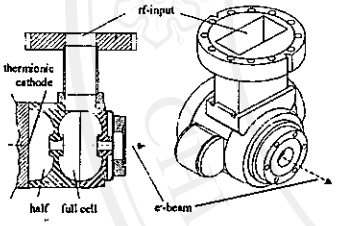

Figure 2: Cross section and 3D-view of the rf-gun.

2.2 Magnetic Bunch Compressor

Following the rf-gun is an α-magnet serving as the bunch compressor. The α-magnet has the shape of the half-quadrupole with the poles and a mirror plate to terminate the field across the vertical midplane. The electron beam exits the rf-gun and enters the α-magnet in the xy-plane at an angle of 49.30° with respect to the magnet axis or yz-plane as indicated in Fig.3 and exits at

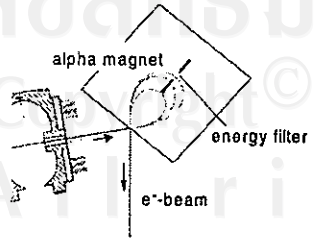

Figure 3: Layout of the rf-gun and the α-magnet.

the same of the entrance point. The path length (S) of the particle in the α-magnet is the closed loop similar to the alphabet α and depends on the particle momentum (cp) and magnetic gradient (g) follows the relation $S \approx [cp/g]^{1/2}$. Consequently, lower momentum particles follow shorter path than the higher one. This feature makes the α-magnet a convenient and simple magnetic bunch compressor. We may change only the magnetic gradient to change the compression without changing the direction of the beam path outside theα- magnet.

3 GENERATION OF FIR RADIATION

Coherent FIR radiation will be generated at the experimental station as the transition radiation (TR) which is emitted when electron pass through an interface between two media with different dielectric constant. In our case, we shall use an Al-foil for the radiator, which represents as the transition between vacuum and metal. Placing the foil by 45° with respect to the electron path deflects the backward TR emitted at 90° with respect to the beam exits through a polyethylene window into open air as indicated in Fig.4. This polarized coherent FIR radiation will be measure with the Michealson Interferometer and a room temperature bolometer.

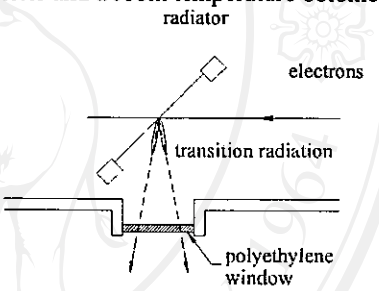

Figure 4: Transition radiation at the experimental station.

In principle, coherent FIR radiation can be generated from the electron short bunch after the compression. However, transition radiation has maximum intensity at angle (θ) equal one over gamma (γ) [$\theta_{max}=1/\gamma$].

For 20 MeV electron beam, θ_{max} is equal 1.4°, which is more confine than that from 2.5 MeV electron bunch with θ_{max} is equal 11.5°. Thus, adding of 20 MeV linac, which accelerates electrons to reach kinetic energies of about 20-3- MeV, after compression is a reasonable way to generate the more confine beam of FIR radiation at the experimental station.

4 NUMERICAL SIMULATIONS TO OPTIMIZE RF-GUN

The main purpose of the rf-gun design is to optimize the rf-gun geometric shape and the rf-parameters, i.e. resonant frequency and field ratio of the electric field inside the half-cell and the full-cell, for the ability to produce femto-second electron bunches.

The dynamics of the particles inside the rf-gun is very complicate because the field in each cell is time-varying field. So it is important to use computer code to calculate and simulate the particle dynamics through the field. In our study, we use two programs together to simulate and optimize the rf-gun. Both codes developed by the Los

Alamos National Laboratory (LANL). The first code is SUPERFISH, which calculates EM field by solves Maxwell's equation in certain boundary conditions of the rf-cavity. Another code is the particle-in-cell code PARMELA which tracks particles through the field obtained by the SUPERFISH. PARMELA can calculate including of the space charge effect and shows the results in both longitudinal and transverse particle distributions.

In our numerical simulation, we assumed that the thermionic cathode of the rf-gun produces a uniform stream of particles. The particles will emerge from the cathode and enter the rf-cavity while the electric field becomes accelerating phase. The first particle with the maximum kinetic energy feels a very small field at the beginning, which will increase as this particle travels through the cavities. Particles, which emerge from the cathode later, feel immediately a higher field and gain speed more quickly. Some of them are closely catch up with the first particle. The rest of the particles, which emerge too late from the cathode, feel the non-accelerating field inside the cavities and some of them may turn back to the cathode causing of the backbombardment effect. BY this dynamics, there is a very concentration of particles in the head of the bunch, consequently generating a small correlated particle distribution between energy and time as shown in Fig.5. The concentration of 10 % of high-energy particles at the head of the bunch appears in the length of some 10-20 ps.

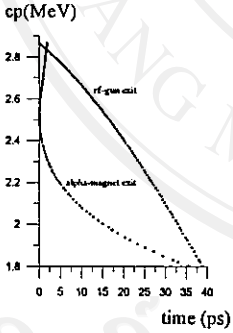

Figure 5: Particle distribution in energy-time phase space at the rf-gun and the alpha-magnet exit.

The concave shape of the particle distribution at the rf-gun exit matches well to bunch compression in the α-magnet. This particle distribution will rotate clockwise as the beam travels through the α-magnet because lower momentum particles follow shorter path and catch up the higher one leading to bunch compression. Because after the alpha-magnet there are 20 MeV linac and some beam transport line and the effect of the finite velocity dispersion, the value of the α-magnet gradient must be chosen such to generate the shortest bunches at the experimental station. Therefore, some overcompression of the particle distribution at the α-magnet exit is required (as shown in Fig.5).

The particle distribution after bunch compression and acceleration with respect to the initial kinetic energies (at the rf-gun exit) at the experimental station indicated in Fig.7. It represents the expected bunch length about 34 fs in time or 10μm (rms), which is much shorter than the initial distribution at the rf-gun exit.

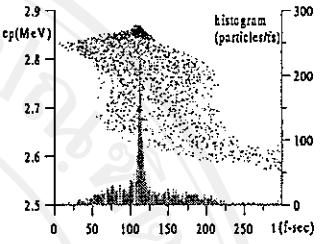

Figure 6: Particle distribution in energy-time phase space at the experimental station.

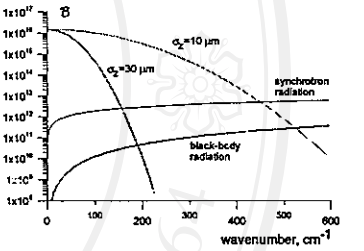

Figure 7: Radiation brightness (B) vs. wave number (k) of FIR spectrum.

The radiation brightness (B) vs. wave number (k) of FIR spectrum shows that the femto-second electron bunches can provide broad band radiation in FIR regime with intensity much higher than black body radiation and synchrotron radiation and shorter bunch provide broader spectrum. Comparison of the electron bunch length about 100 fs (30 μm) of the SUNSHINE source and the expected bunch length about 30 fs (10μm) of the SURIYA source also indicated in the figure. It shows that the shorter bunch of about a factor of three of the SURIYA bunch provides the three times of broader spectrum than the SUNSHINE bunch.

5 FABRICATION AND RF-MEASUREMENT OF RF-GUN

All major parts of the optimum rf-gun base on the numerical simulations have been designed and machined in Thailand. The assembly drawing ant the machined parts of the rf-gun are shown in Fig.8.

The coupling cavity between the half-cell and the full-cell was not included in the simulations because the SUPERFISH is 2D code. Thus, we have to design and machine the first fabrication of the rf-gun in case that we can adjust the geometric shape later. From this limitation, it is important to do rf-measurement and fine tuning of the rf-gun geometric shape several times to obtain the rf-

parameters close to the expectation values. The rf-measurement set up is shown in Fig.9.

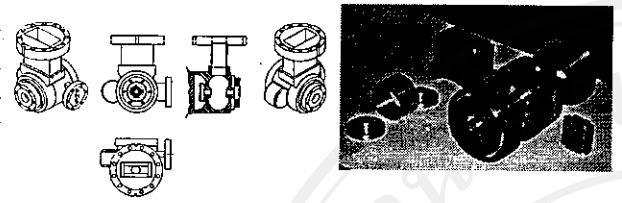

Figure 8: Assembly drawing ant the machined parts of the rf-gun.

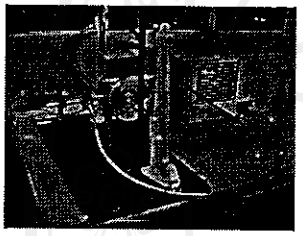

Figure 9: Rf-measurement set up with the network analyzer.

Results of the final rf-measurement before brazing show that the resonant frequency of the rf-gun is about 2856 MHz at the operating temperature (45°). In addition, the bead-pull measurement has been done to adjust the ratio of the field inside the half-cell and the full-cell. As the results, the ratio of those fields is 2:1 (Fig.10) which is exactly the same as the expected value from the simulations.

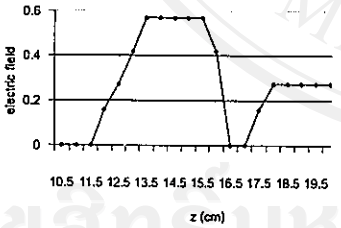

Figure 10: Field ratio of the field inside the half-cell and the full-cell.

6 STATUS OF SURIYA PROJECT

Presently, the rf-gun has finished the rf-measurement and under the process of the brazing. This rf-gun will be installed during year 2002. A 2856 MHz klystron and modulator is under installation as the rf-source for this rf-gun.

Computer design bases on the rf-gun requirement and construction of the α-magnet have been completed. Presently, it is under the experiment of the high-current testing. The full system of this α-magnet will be completed at the early of year 2002.

The FNRF has obtained a 20 MeV s-band linac from the Chiang Mai Hospital. This system includes all related components to accelerate an electron beam. The linac including of its sub-system has been installed. The rf-gun, the α-magnet, and the linac at the SURIYA facility shown in Fig.11.

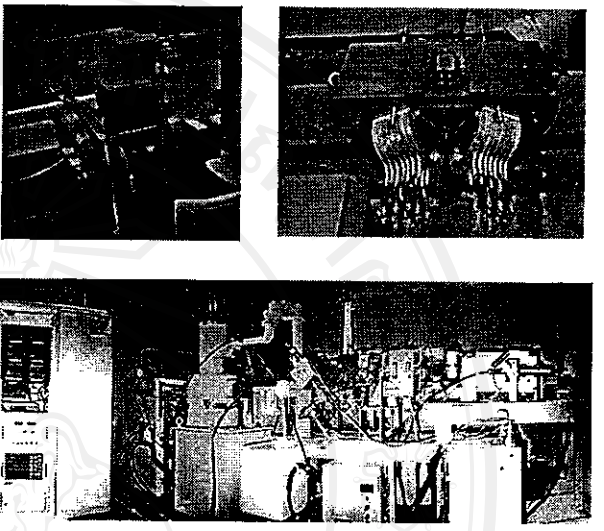

Figure 11: Rf-gun, α-magnet, and linac at SURIYA.

7 ACKNOWLEDGEMENTS

This work has been supported by the Thailand Research Fund, the Royal Golden Jubilee Scholarship, and under collaboration with Stanford University, USA.

REFERENCES

[1] H. Wiedemann et. al., " Femto-Second Electron Pulses from a Linear Accelerator", J. Nucl. Mat. 248 (1997) 374.
[2] P. Kung et al. "Generation and Measurement of 50 fs(rms) Electron Pulses", Phys. Rev. Lett. 73 (1994) 967.
[3] C. Settakorn et.al.,"Coherent Far-Infrared Radiation From Electron Bunches", Proc. of the First Asian Particle Accelerator Conference (APAC98) Tsukuba, Japan, 1998
[4] C. Settakorn, "Generation and Use of Coherent Transition Radiation from Short Electron Bunches", PhD Thesis, Stanford University, 2001
[5] L.M. Young and J.H. Billen, "Technical Report No. LA-UR -96-1835: PARMELA", Los Alamos National Laboratory
[6] T. Vilaithong et. Al., " SURIYA, a Source of Femto-Second Electron and Photon Pulses ",Proc. of the Second Asian Particle Accelerator Conference (APAC01) Beijing, China, 2001
[7] S. Rimjaem et. al., " An RF-Gun Optimized for Femto-Second Electron Bunches ",Proc. of the Second Asian Particle Accelerator Conference (APAC01) Beijing, China, 2001
[8] S. Rimjaem, R. Farias, C. Settakorn, T. Vilaithong, H. Wiedemann, "Femto-Second Electron Bunches from an Rf-Gun", (submitted to Phys. Rev. ST-AB)
[9] M. Borland, "A High-Brightness Thermionic Microwave Electron Gun", Ph.D. Thesis, Stanford University 1991.

SURIYA, A SOURCE OF FEMTO-SECOND ELECTRON AND PHOTON PULSES

T. Vilaithong, N. Chirapatpimol, M.W. Rhodes, C. Settakorn, S. Rimjaem, J. Saisut, P. Wichaisirimongkol, Fast Neutron Research Facility (FNRF), Chiang Mai University, Thailand,
H. Wiedemann, Applied Physics and SSRL, Stanford University, USA

Abstract

A new facility, SURIYA, is being constructed at the Fast Neutron Research Facility (FNRF), Chiang Mai University (Thailand), to generate femto-second electron bunches. These bunches can be used either directly, or to create coherent far infrared radiation or femto-second X-ray pulses. A 20 MeV linear accelerator has been installed and is presently equipped with a conventional electron source. A newly designed rf-gun is under rf-testing and is expected to be installed in 2002. Layout and status of the SURIYA project will be presented.

1 INTRODUCTION

Construction and installation is underway at the Fast Neutron Research Facility, Chiang Mai University, of the SURIYA facility to produce intense, coherent, polarized far infra-red radiation in the wavelength range from 50 μm to a few 1000 μm. This source will provide high intensity, broad band radiation in this wavelength regime far in excess to that available from black body radiators or synchrotron light sources. In Fig. 1 the expected radiation brightness of coherent transition radiation (CTR) from a 30 μm (rms) electron bunch is compared with that available from a synchrotron light source (SR) and a black body radiator.

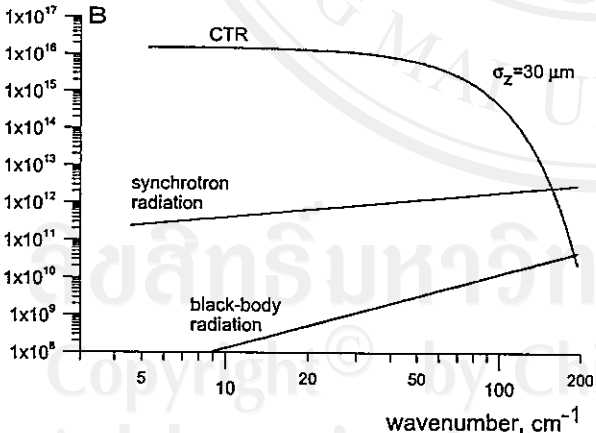

Figure 1: Radiation brightness B(ph/s/mm^2/100%BW) vs. wave number for CTR, SR and black body radiation.

Because the radiation is broadband and comes in ultra-short pulses (< 100 f-sec, rms), this source also provides characteristics, which are not available from FEL's in this wavelength regime. This radiation can be used for basic and applied research in many fields including material science, studies of high-Tc materials, polymer dynamics and structure, biological molecules, phonon and surface physics, metrology standards etc [1,2,3]. A 1994 report by a subcommittee of the American Academy of Science suggests that a "compelling" reason for the establishment of a new national facility to produce radiation can be made only for the wavelength range from 10 μm to 1000 μm [4].

The source under construction at the FNRF is similar to that at the SUNSHINE facility at Stanford University [5-8] producing coherent FIR radiation with intensities far exceeding those from black body radiators. At SUNSHINE, electron bunches as short as 120 f-sec (rms) are produced routinely at microbunch intensities of the order of 100 pC [8]. Such high intensities together with coherence and ultrashort pulse lengths provide new research opportunities, which cannot be pursued with conventional sources. In addition to the research potential of such a source, its components provide a broad training ground for the education and training of graduate students toward master and Ph.D. theses. This is due to the application of many basic physical principles from a variety of fields like mechanics, optics, electronics, component controls, data acquisition, ultra high vacuum technology, magnetics, beam dynamics, and computer simulation.

Specifically, studies can be expanded into radiation production in the form of undulator-, transition-, stimulated transition-, Cherenkov-, Smith-Purcell or diffraction radiation. If desired, a Free Electron Lasers, or a single pass FEL can be added in this wavelength range. By head-on collision of a laser beam with the electron beam ultrashort, quasi- monochromatic soft or hard x-ray pulses can be produced by the process of Thompson backscattering. Through the interaction of the electron beam with crystals ultra short pulses of x-rays can be generated as channelling radiation, as parametric x-rays or resonant transition radiation to name just a few. The research and educational potential associated with such a source fits well the objectives of the Fast Neutron Research Facility at Chiang Mai University.

2 METHOD TO PRODUCE FEMTO SECOND ELECTRON BUNCHES

The particular design of the rf-gun (Fig. 2) exhibits a small correlated particle distribution in phase space as derived from numerical PARMELA [9] simulations and

shown in Fig. 3 with most of the particles concentrated in the first 10 psec. A more detailed discussion of the rf-gun design is given in another contribution to this conference [10]. The thin phase space distribution allows for efficient bunch compression in an α-magnet (Fig. 2). An energy filter within the α-magnet allows to select the useful part of the beam.

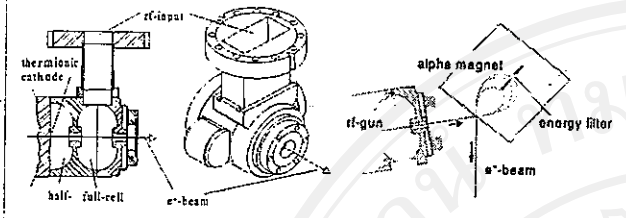

Figure 2: Rf-gun (left) and α-magnet with energy filter (right) [5].

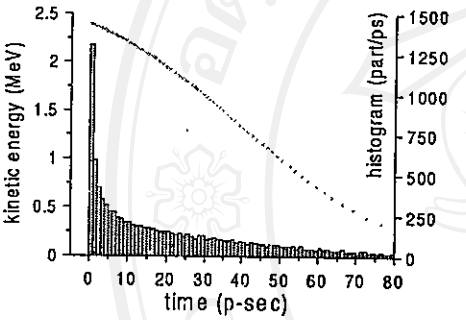

Figure 3: Particle distribution (PARMELA) in energy-time phase space at the rf-gun exit with histogram [11].

High-energy particles, emerging first from the rf-gun will travel a longer path through the α-magnet than lower energy particles, thus leading to bunch compression. After further acceleration in a linac the beam is guided to the experimental stations.

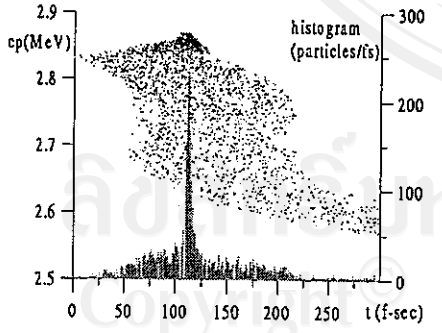

Figure 4: Particle distribution at the experimental station after optimum compression (PARMELA simulation)[11].

From this electron source we expect to obtain bunches as short as 34 fs or 10 μm (rms), which is shorter by at least a factor of 3 compared to the SUNSHINE source [6,12]. As a consequence, the coherent far infrared spectrum available is extended by a factor x3 and thereby covers the wavelength regime from about 30 μm to several mm, or in terms of wave numbers from 10 to 300 cm^{-1} and beyond as shown in Fig. 5.

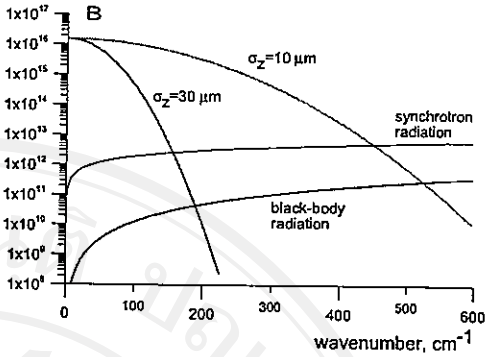

Figure 5: Expected coherent radiation spectrum from the new rf-gun.

3 INSTALLATION STATUS OF SURIYA

The FNRF has obtained a 20 MeV RF linear accelerator from the Chiang Mai Hospital. This system includes all related components to accelerate an electron beam. The installation of the linac including all of its sub-systems and conventional electron source has been completed (Fig. 6). All features related to medical-radiation therapy treatment and not used at SURIYA have been removed. The control electronics has been fully updated to remove therapy related interlocks and replace them with a system guided by research requirements.

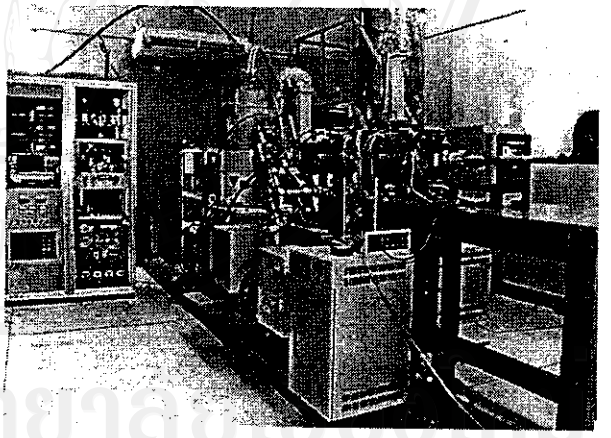

Figure 6: Rf-linac installed at the SURIYA project.

At the SURIYA project laboratory, all personnel and machine protection systems have been installed and tested. An international standard security and safety protocol has been incorporated into the operation of the machine, which includes access door interlocks and panic buttons for automatic beam shut-off in case of personnel access to a restricted area. Beam-on warning lights, high voltage signs and audible sirens are implemented and

appropriate locations to notify of machine operating status and radiation hazards. Operator and user training programs are being developed for operational and radiation safety.

In a collaboration with Stanford/SLAC (USA) and LNLS (Brazil) a new rf-gun has been developed [10,11] through numerical studies with PARMELA [10]. This new gun has been optimized for most efficient bunch compression reaching bunch lengths of 34 fs or 10μm (rms), which is three time shorter than those obtained at the SUNSHINE facility. All major parts of the newly designed rf-gun have been machined in Thailand and are presently under rf-evaluation and fine-tuning. This rf-gun will be installed in 2002. A second klystron and modulator is ready for installation as the rf-source for the rf-gun.

Design of an α-magnet can be separated into two main parts: poles and coils design. To match rf-gun requirements, the α-magnet is designed for a maximum field gradient of 450 G/cm. Computer designs of α-magnet and coil have been completed (Fig. 7) and are under construction. We plan to complete the full system of the α-magnet by the end of 2001.

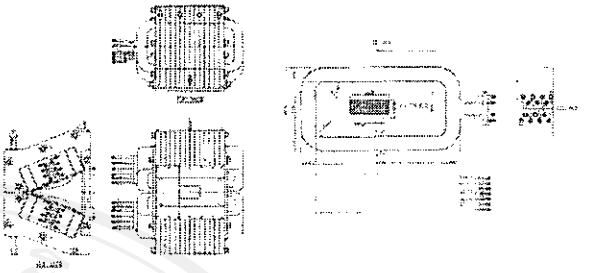

Figure 7: Assembly drawing and coils of the α-magnet

The whole facility is installed in a below ground well shielded enclosure which became available from an earlier neutron beam activity. The final floor plan of the SURIYA facility is shown in Fig. 8 with rf-gun, α-magnet, 20 MeV linac, beam line, radiation station and beam dump.

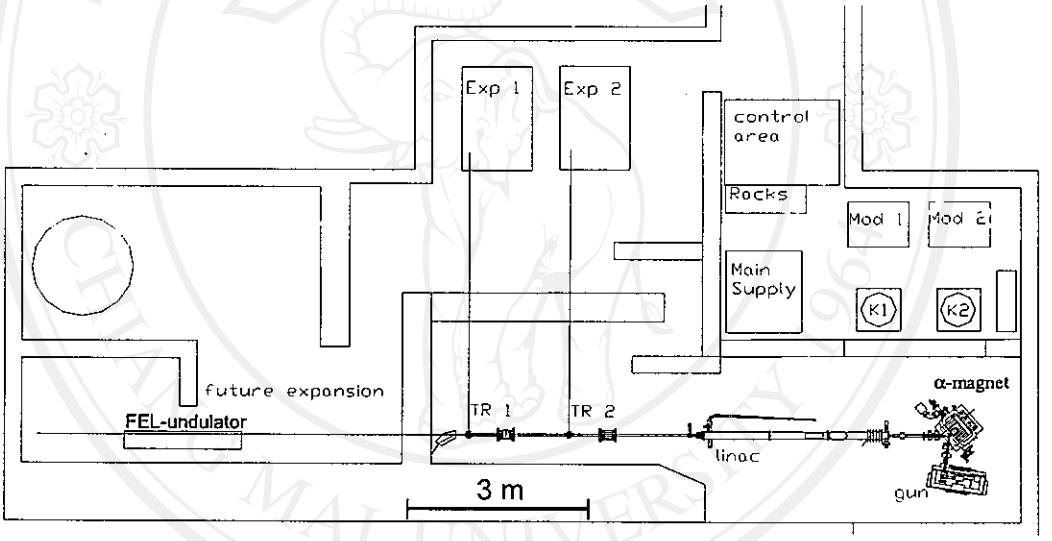

Figure 8. Floor plan of the SURIYA facility with accelerator, experimental stations, equipment and control area and space for future expansion to add, for example, a FEL undulator.

4 ACKNOWLEDGEMENTS

This work has been supported by the Thailand Research Fund.

5 REFERENCES

[1] L. Thrane et. al., "THz Reflection Spectroscopy of Liquid Water", Chem. Phys. Lett. 240 (1995) 330.
[2] J.R. Birch et. al., "An Improved Experimental Method for Reflection Dispersive Fourier Transform Spectrometry of Very Heavily Absorbing Liquids", Infrared Physics 21 (1981) 229.
[3] W.F. Passchier et. al. " A New Method for the Determination of Complex Refractive Index Spectra of Transparent Solid in the Far-Infrared Spectral Region", J. Phys. D: Appl.. Phys. 10 (1997) 509.
[4] "Free Electron Lasers and Other Advanced Sources of Light", Committee on free electron lasers and other advanced coherent light sources, Nat. Res. Council, National Academy Press, Washington, D.C. 1994
[5] H. Wiedemann et. al., " Femto-Second Electron Pulses from a Linear Accelerator", J. Nucl. Mat. 248 (1997) 374.
[6] P. Kung et al. "Generation and Measurement of 50 fs(rms) Electron Pulses", Phys. Rev. Lett. 73 (1994) 967.
[7] C. Settakorn et.al.,"Coherent Far-Infrared Radiation From Electron Bunches", Proc. Of the First Asian Particle Accelerator Conference (APAC98) Tsukuba, Japan, 1998
[8] C. Settakorn, "Generation and Use of Coherent Transition Radiation from Short Electron Bunches", PhD Thesis, Stanford University, 2001
[9] L.M. Young and J.H. Billen, "Technical Report No. LA-UR - 96-1835: PARMELA", Los Alamos National Laboratory
[10] S. Rimjaem et. al., these proceedings
[11] S. Rimjaem, R. Farias, C. Settakorn, T. Vilaithong, H. Wiedemann, "Femto-Second Electron Bunches from an Rf-Gun", (submitted to Phys. Rev. ST-AB)
[12] M. Borland, "A High-Brightness Thermionic Microwave Electron Gun", Ph.D. Thesis, Stanford University 1991.

RF-GUN OPTIMIZATION FOR FEMTO-SECOND ELECTRON BUNCHES

S. Rimjaem, N. Chirapatpimol, T. Vilaithong, FNRF, Chiang Mai University, Thailand
R. Farias, LNSL, Campinas, Brazil
H. Wiedemann, C. Settakorn, Applied Physics and SSRL, Stanford University, USA

Abstract

The aim of this study is to optimize and construct an rf-gun to be a source of femto-second electron bunches to produce coherent far infrared (FIR) radiation or femto-second x-ray pulses. To produce ultra-short bunches we use an rf-gun with a magnetic bunch compression in the form of α-magnet. In this study we concentrate on the specific optimization of an rf-gun to produce femto-second electron bunches. The optimum geometric and electric rf-gun specifications have been investigated through numerical simulation with the particle-in-cell code PARMELA. The numerical simulation show that the electron bunches from this optimum rf-gun as short as a few fs rms can be expected.

1 INTRODUCTION

This study is part of the research and development for the project SURIYA which is presently under construction at the Fast Neutron Research Facility (FNRF) at the Chiang Mai University, Thailand. SURIYA is a facility that has the purpose to produce intense, coherent, polarized FIR radiation in the wavelength range of 10 μm to 1000 μm or femto-second x-ray pulses to be used for basic and applied research. An electron source and a beam transport system under construction at the SURIYA is similar to SUNSHINE facility at Stanford University [1,2,3], which can produce electron pulses as short as 100 fs rms. SURIYA will consist mainly of an rf-gun with a thermionic cathode, an α-magnet for bunch compression, post linear accelerator (linac) to accelerate electron beam to 25-30 MeV, and beamlines guiding the electron beam to experimental stations where intense FIR or femto-second X-ray pulses are generated. The details about the SURIYA project are discussed in another contribution to this conference [4]. A schematic outline of the SURIYA facility planed at the FNRF is shown in Fig. 1.

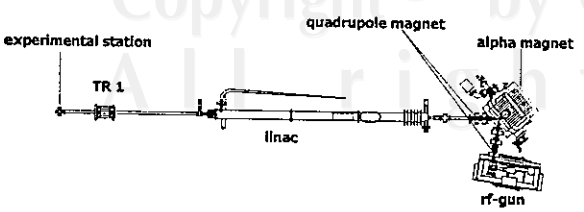

Figure 1: Layout of the proposed SURIYA source at FNRF, Chiang Mai University.

2 RF-GUN CHARACTERISTICS AND NUMERICAL SIMULATIONS

2.1 General Characteristics of Rf-Gun

A microwave or rf-gun is an electron source consisting of a cathode serving as an electron emitter, which emits electrons into the rf- fields inside a metal-walled cavity. Depending on the type of the cathode we distinguish between a thermionic cathode and a photocathode rf-gun. In our electron source, we use a thermionic cathode, which produces an electron beam by thermal emission of electrons from a material with a low workfunction [5]. The main advantages of an rf-gun are the higher current, lower emittance, and higher momentum electron beams compared to a conventional DC-gun. In addition, the rf-gun with thermionic cathode exhibits essential features for efficient bunch compression. First, high acceleration to near relativistic energy (2-3 MeV) within a short distance allow space charge effects little time to dilute the beam emittance. Second, the momentum-time phase space of the particle distribution is very well suited for a simple and efficient bunch compression in an α-magnet. Finally, the particle flux obtainable from a thermionic cathode can be increased to values at which space charge effects cannot be controlled anymore.

The rf-gun consists of one and a half standing wave structure rf-cavities with a thermionic cathode attached to the wall of the half-cell. All rf-cavity cells operate at 2856 MHz and are energized by a klystron through an rf-input rectangular waveguide port in the full-cell. The half-cell is coupled to the full cell by an external-coupling cavity as shown in Fig. 2.

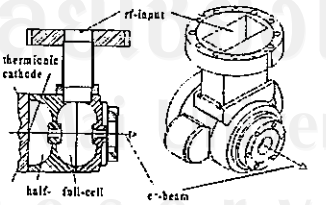

Figure 2: Cross section and 3D-view of the rf-gun [6].

The half-cell, full-cell, and side-coupling cavity, allow for three possible structure modes and operate in the π/2 mode. That means, there is a phase-shift of 90° between the first half-cell and the side-coupling cell, and between the side coupling cell and the full-cell. Thus the rf-fields are 180° out of phase between the half- and full-cell.

Electrons emerge from the cathode with thermal velocities, then travel through the half and full cell during the accelerating phase. The electron beam reaches a kinetic energy of about 2-3 MeV at the gun exit

2.2 Numerical Simulations

The electron dynamics inside the rf-gun is very complicated and must take space charge effects into account. Therefore, it is necessary to use a numerical computer program to simulate the details of the gun operation and evaluated the optimum geometric and electric rf-gun parameters.

In this study we use mainly PARMELA and SUPERFISH to simulate and optimize the specific parameters of the rf-gun. SUPERFISH is a well-established code from Los Alamos National Laboratory (LANL) that calculates the frequency and the electromagnetic field distribution for TM modes for resonant cavities in two dimensions. This code lets us to simulate rf-cavity shapes to the desired frequency. PARMELA is a particle-in-cell code, also developed by LANL, which can track many particles through the fields obtained from SUPERFISH. PARMELA' s results show both longitudinal and transverse particle phase space distributions at selected points along the beam line. This code includes space charge effects. In PARMELA simulations, we assume that the cathode emits a uniform stream of macroparticles comprising a cathode current of 3.4 A composed of 50,000 macroparticles per 2856 MHz rf-period. Therefore, the cathode emits 142.8 macroparticles per ps, and each macroparticle simulates 1.48×10^5 electrons.

3 RF-GUN OPTIMIZATION

3.1 Longitudinal Particle Distributions

Electrons emerge from the cathode during the rf-period phase from 180°-540°. During the accelerating half wave of the rf-fields these electrons gain almost relativistic energies in a very short distance. For the optimum field, the particles emerging from the cathode as the field turns accelerating reach the exit of the half-cell just when the field becomes decelerating again. Particles emerging from the cathode later will see some decelerating field at the exit of the half-cell and therefore gain less energy. The rf-fields inside the second rf-cell continue to accelerate the electrons to travel through the second rf-cell during the accelerating phase reaching velocities near the velocity of light ($v \approx 0.98$ c). By this dynamics the phase space distribution of the beam at the rf-gun exit is shown in Fig.3 for each 2856 MHz cycle.

We observe a thin monotonic distribution of particles and the histogram tells us that most particles are concentrated in the head of the bunch. It is this thin distribution that allows efficient bunch compression.

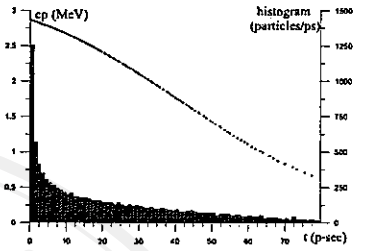

Figure 3: Momentum-time phase space distribution at the rf-gun exit with histogram.

As long as the rf power from the klystron is supplied to the rf-gun, this cycle is repeated every rf-period, resulting in a train of bunches separated by 350 ps at the 2856 MHz rf-period.

3.2 RF-Gun Fields and Ideal Phase Space Distribution

A critical parameter determining the limiting bunch is the electric accelerating field in the half-cell. The particle phase space distribution at the gun-exit shows a varying curvature for different electric fields as shown in Fig. 4.

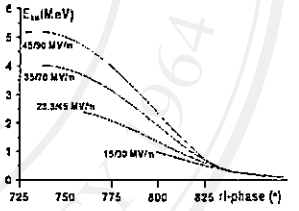

Figure 4: Energy-time phase space distributions for different accelerating fields in the rf-gun [6].

At very high fields, particles reach almost the same fields during a finite time interval in each bunch. Such a distribution cannot be compressed for lack of a monotonic energy-time correlation. The required monotonic energy-time variation of the particle distribution appears only for lower electric fields. Knowing the bunch compression system and the beam line to be used we may calculate an ideal phase space distribution that would result in a zero bunch length at a selected point downstream in the beam line.

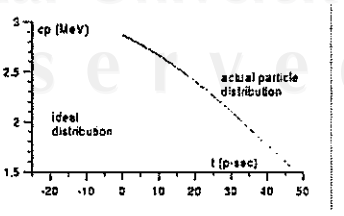

Figure 5: Ideal and actual phase space distribution at the rf-gun [6].

Such an ideal distribution is shown in Fig. 5 and we may adjust now the electric field in the rf-gun cells such that the actual particle distribution matches the ideal distribution. This is possible at least over the range of 10-20 ps where most of the particles are concentrated anyway.

3.3 Bunch Compression

To produce femto-second electron bunches we use an α-magnet [7]. The α-magnet has the shape of half a quadrupole magnet with two poles and a mirror plate to terminate the field across the vertical midplane (yz-plane). The electron beam enters an α-magnet in the xz-plane at an angle of 49.3° with respect to the magnet axis. Particles travel along a closed loop similar to the letter α inside the α-magnet and exit again exactly at the entrance point but at a different angle (as indicated in the Fig. 6).

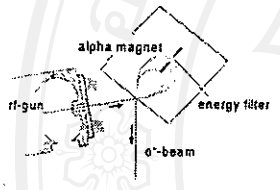

Figure 6: rf-gun and α-magnet layout.

The path length of the particle trajectory in the α-magnet depends on the particle momentum and magnetic field gradient scaling like $s \approx (cp/g)^{1/2}$ [5]. For a relativistic electron beam the effect of velocity dispersion is very small compared to the path length dispersion. Therefore, by adjusting the gradient of the α-magnet the bunch compression can be optimized. Since we perform experiments downstream from the α-magnet we must adjust the compression such that the shortest bunch length is obtained there and not at the α-magnet exit. Consequently, we overcompress the bunches such that lower energy particles exit α-magnet first followed by higher energy particles. While the particles travel through the beam transport line including linac, higher energy and faster particles will catch up with slower particles forming the shortest bunch at the experimental station.

The momentum-time phase space distribution after bunch compression and acceleration with respect to the initial distribution at the rf-gun exit (Fig. 3) is shown in Fig. 7 (left). It shows an extremely short spike of only about 2.8 fs-rms on top of a broader base of some 34 fs-rms. While it would be interesting to contemplate 2.8 fs bunches, at this time we cannot offer an efficient way to preserve such a short bunch length and we must therefore ignore this spike for the time being. However, the length of the base at 34 fs-rms together with a charge of 0.1 nC constitutes a peak current of 3 kA and is about three times shorter than the bunch lengths obtained at the SUNSHINE facility which can produce electron pulses as short as 100 fs rms (Fig. 7 right).

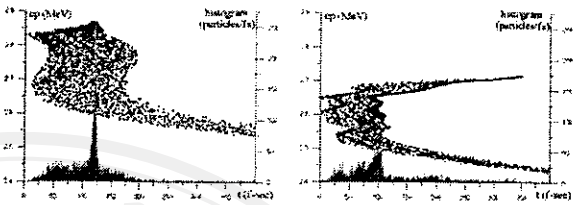

Figure 7: Momentum-time phase space distribution after bunch compression and acceleration with histogram of SURIYA (left) and SUNSHINE (right).

3.4 Transverse Particle Distributions

Ultra short bunches can be diluted again along the beam transport line by excessive focusing of beam divergence. This effect limits the bunches at SUNSHINE to about 100 fs-rms. The SURIYA rf-gun has been designed for much smaller beam divergence compared to the SUNSHINE gun as shown in Fig.8. Bunch lengthening due to a quadratic effect and is greatly reduced for the SURIYA rf-gun with only about 1 mrad of divergence beam [6].

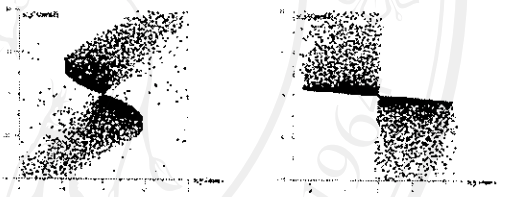

Figure 8: Transverse phase space distributions show 10 mrad divergence beam at the SUNSHINE gun-exit (left) and 1mrad divergence beam at the SURIYA gun-exit (right).

4 ACKNOWLEDGEMENTS

This work has been supported from the Golden Royal Jubilee Scholarship Program, Thailand Research Fund and the Faculty of Science (Chiang Mai University)

5 REFERENCES

[1] H. Wiedemann, P. Kung and H.C. Lihn, Nim, A 319, 1 (1992)
[2] P. Kung, D. Bocek, H.C. Lihn and H. Wiedemann, " High-intensity coherent FIR radiation from Sub Pico-Second Electron Bunches", SPIE. Proc. 2118, 191 (1994)
[3] P. Kung et.al. "Generation and Measurement of 50 fs (rms) Electron Pulses" , Phys Rev. Lett. 73 (1994) 967
[4] T. Vilaithong et al., these proceedings
[5] M. Borland, Ph.D. Thesis, Stanford University, 1991
[6] S. Rimjaem, R. Farias, C.Settakorn, T. Vilaithong, H. Wiedemann, "Femto-Second Electron Bunches from an Rf-Gun", (submitted to Phys. Rev. ST-AB)
[7] H.A. Enge, "Achromatic Magnetic Mirror for Ion Beams", Rev.Sci.Instr. 34 (1963) 4

CURRICULUM VITAE

Name	Sakhorn Rimjaem	
Date of birth	9 September 1975	
Education	1998	B.S. (Physics), Chiang Mai University
Scholarship	1998-2003	Royal Golden Jubilee Scholarship (RGJ)
Training	2002	US-CERN-JAPAN-RUSSIA Joint Accelerator School Long Beach, California, USA
	Subject:	Linear Accelerator Physics and Technology
	2000	US Particle Accelerator School State University of New York, Stony Brook, New York, USA
	Subject:	Computational Methods in Electromagnetism